SYNTHESIS, CHARACTERIZATION AND CATALYTIC ACTIVITY OF NANOCRYSTALLINE CERIA MODIFIED WITH ZIRCONIA

Thesis submitted to

Cochin University of Science and Technology

in partial fulfillment of the requirements for the degree of

Doctor of Philosophy

in

Chemistry

Under the Faculty of Science

By

CIMI A. DANIEL

Under the Supervision of

Dr. S. SUGUNAN

DEPARTMENT OF APPLIED CHEMISTRY
COCHIN UNIVERSITY OF SCIENCE AND TECHNOLOGY
COCHIN-682 022, KERALA, INDIA

January 2014

Synthesis, Characterization and Catalytic Activity of Nanocrystalline Ceria Modified With Zirconia

Ph.D. Thesis under the Faculty of Science

Author:

Cimi A. Daniel

Research Fellow,

Department of Applied Chemistry,

Cochin University of Science and Technology,

Cochin – 682 022, Kerala, India.

Email: danielcimi@gmail.com

Supervisor:

Dr. S. Sugunan

Emeritus Professor,

Department of Applied Chemistry,

Cochin University of Science and Technology,

Cochin – 682 022, Kerala, India.

Email: ssg@cusat.ac.in

January 2014

Department of Applied Chemistry
Cochin University of Science and Technology
Kochi - 682 022, India.

Dr. S. Sugunan
Emeritus Professor

Date: *23-01-2014*

Certificate

Certified that the thesis work entitled "**Synthesis, Characterization and Catalytic Activity of Nanocrystalline Ceria Modified with Zirconia**" submitted by Ms. Cimi A. Daniel is an authentic record of research work carried out by her under my supervision at the Department of Applied Chemistry in partial fulfillment of the requirements for the degree of Doctor of Philosophy in Chemistry of Cochin University of Science and Technology and has not been included in any other thesis previously for the award of any other degree. All the relevant corrections and modifications suggested by the audience and recommended by the doctoral committee of the candidate during the presynopsis seminar have been incorporated in the thesis.

Dr. S. Sugunan
(Supervising Guide)

Declaration

I hereby declare that the work presented in the thesis entitled **"Synthesis, Characterization and Catalytic Activity of Nanocrystalline Ceria Modified with Zirconia"** is my own unaided work under the supervision of **Dr. S. Sugunan**, Emeritus Professor in Department of Applied Chemistry, Cochin University of Science and Technology, Kochi-22, and not included in any other thesis submitted previously for the award of any other degree.

Kochi-22 **Cimi A. Daniel**
23 -01-2014

“The fear of the LORD is the beginning of wisdom: a good understanding have all they that do his commandments”: (Psalms: 111:10).

Dedicated to my family…

Acknowledgement

"Thy word is a lamp unto my feet and a light unto my path": Psalms (119:105)

First and foremost, praises and thanks to the God, the Almighty, for His showers of blessings, for forgiving my mistakes, for leading me in the right path. I thank Lord Jesus Christ for the wisdom and perseverance that has been bestowed upon me during this research work, and indeed, throughout my life.

There are many people who have played important roles in my journey to complete this thesis. I take this opportunity to express my deepest sense of gratitude and reverence towards my research supervisor, Dr. S. Sugunan for guiding me in the right direction throughout the course of this work. His constant inspiration and invaluable guidance helped a lot to focus my views in proper perspective. I salute his supporting attitude that has always led me to think and work independently.

My honest thanks go to Dr. N. Manoj, Head of the Department for providing me the opportunity to accomplish my research work in this department. I would like to express my profound gratitude to Prof. K. Sreekumar and Prof. K. Girishkumar, former Heads of the department for their support and for providing me all the facilities required for my research work. I express my gratitude to Dr. S. Prathapan for being my doctoral committee member. My heart full thanks are due to all teaching and non-teaching staffs of the department for their help and wishes.

I am deeply obliged to Dr. Shibu Eapen (STIC-CUSAT) for his timely help and support. I would like to express my gratitude to Dr. M.R. Anantharaman, DOP, CUSAT and Dr. Salim Al- Harthi, SQ University, Muscat for XPS analysis, Dr. M. K. Jayaraj, DOP, for SXRD and Raman analysis, SAIF-Mumbai, Mr. Narayanan (IIT Chennai) for various analyses. A special note of thanks to Dr. Mohanan (Kerala University) and Mrs. Preethy for their help and contribution. I owe my special thanks

to Madhu Sir (Scientist, RRII) for his help and suggestions during my research work. My honest thanks go to Dr. Aby, Hasna, Leena, Rekha, Sunil and Mr. Adarsh for their help in various analyses. I would also like to thank Mr. Vishnu (Alfa Chemicals), Mr. Jamal, Mr. Suresh (Chemito) for their help in various junctures. I sincerely thank Siju, Dr. Ditty, Dr. Lethesh for their help and co-operation.

The last few years have been quite an experience and certainly friends have made it a memorable time of my life. It gives me great pleasure to thank my seniors Dr. Joyce Jacob, Dr. Reshmi.R, Dr. Bolie Therattil, for their support. I am very happy to extend my sincere gratitude to my adorable labmates Dr. Ambili, Dr. Rajesh, Dr. Rose Philo, Dr. Dhanya, Dr. Reni, Nissam, Mothi, Soumini, Sandhya, Soumya and Honey. It is beyond the words to express my thankfulness to each one of them. I would like to thank Rose Miss for the research discussions and her help. Reni is like my family member and is always with me with her love and advice. Her unceasing support during my thesis writing is sincerely appreciated. I am also grateful to Nissam for his friendship, knowledge and availability in clarifying my research queries. Thank you Mothi for your warm friendship, support and encouraging suggestions. Special thanks to Sandhya for her constant help and encouragement. I remember Soumini, Honey and Soumya with gratitude for the nice time I had with them. Thank you Jiby for being a great friend throughout my stay at CUSAT. I cherished friendship from Sandhya, Reshma, Cisy, Bhavya, Pravitha, Jomon and Eason. I thank Asha, for having shared the same room with me and the valuable suggestions she has given to my thesis. I remember Dr. Jasmine with gratitude who became an inspiration in my life. Loving thanks to Amenla, Neethu and Pearl who has been with me in my early days of research work.

My heartfelt thanks to Dr. Vidya. She was with me in all the circumstances in my life. My deepest thanks go to Dr. Tintu, my helpful and trustful friend. I convey my thanks to Dr. Nimmy for her support and love. Loving thanks to Divya and Vineetha for their lovely friendship and love. I am grateful to Hamza (Sud-

Chemie) for his provocative ideas, nice friendship and also his help in doing various analyses.

I gladly remember my life in Athulya hostel. My sincere thanks to all my friends there. My hostel ambience never let me feel that I am away from my home. I will cherish those sweet and adorable memories throughout my life. I extend my gratitude to the present and ex-Matron and all mess workers of my hostel.

It is time to convey my hearty admiration to all my teachers from my school days to post graduation level. I feel proud to acknowledge all my teachers in school and Mar Thoma College, Thiruvalla for introducing me to the fascinating world of science. My days in School of Chemical sciences, CUSAT and NCL introduced me the ethics in science and has encouraged me a lot to pursue a career in research. I express my earnest respect to Mr. Murali, Dr. Koshy John, late Dr. C. V. Asokan, Dr. M. Padmanabhan and Dr. C. S. Gopinath for their motivations that helped me a lot on several occasions.

Words are not enough to express my love and gratitude to my family, the greatest gift God has given me. It gives me great pleasure to thank my Pappa and Mummy for their love, tremendous patience, encouragement and sincere prayers. All the knowledge that I have acquired today is the result of their upbringing. No words would be sufficient in describing the affection and support of my sisters, Mrs. Cinu and Mrs. Ciji throughout my life in all aspects. I wouldn't have overcome all the hurdles to achieve anything without their blessings, care and love. I am also very grateful to my brother-in-laws, Mr. Binoj and Mr. Gigy for their care and love they have shown to me. It gives me great pleasure to thank my nephews-Appu, Achu, Monu, Ponnu and Chachu for their beautiful smiles and for bringing lots of happiness to my life. I am indebted to my Ammachy for her affection and her desire to see my achievements. I am deeply obliged to all my uncles and aunts especially Vallyapappa

and late Vallya Mummy. She was one who extremely supported my research career. You all have been my constant source of strength and gladness.

I would like to pay high regards to the immense support of my husband, Anil Thomas, for his unparallel love and understanding that has driven me to excel even under difficult situations. I would like to thank my in-laws, Pappa and Mummy for their love, encouragement and support.

Finally, my thanks are due to IRELTDC, CUSAT and UGC-BSR for the financial support during my research work.

Cimi A. Daniel

PREFACE

The use of catalysts in chemical and refining processes has increased rapidly since 1945, when oil began to replace coal as the most important industrial raw material. Catalysis has a major impact on the quality of human life as well as economic development. The demand for catalysts is still increasing since catalysis is looked up as a solution to eliminate or replace polluting processes. Metal oxides represent one of the most important and widely employed classes of solid catalysts. Much effort has been spent in the preparation, characterization and application of metal oxides. Recently, great interest has been devoted to the cerium dioxide (CeO_2) containing materials due to their broad range of applications in various fields, ranging from catalysis to ceramics, fuel cell technologies, gas sensors, solid state electrolytes, ceramic biomaterials, etc., in addition to the classical application of CeO_2 as an additive in the so-called three way catalysts (TWC) for automotive exhaust treatment. Moreover, it can promote water gas shift and steam reforming reactions, favours catalytic activity at the interfacial metal-support sites. The solid solutions of ceria with Group IV transitional-metals deserve particular attention for their applicability in various technologically important catalytic processes. Mesoporous CeO_2–ZrO_2 solid solutions have been reported to be employed in various reactions which include CO oxidation, soot oxidation, water-gas shift reaction, and so on. Inspired by the unique and promising characteristics of ceria based mixed oxides and solid solutions for various applications, we have selected ceria-zirconia oxides for our studies. The focus of the work is the synthesis and investigation of the structural and catalytic properties of modified and pure ceria-zirconia mixed oxide.

The thesis is organized into eight chapters. Chapter 1 gives concise introduction and literature survey to the topic of study. Second chapter focuses the materials and methods adopted for the present work. Third chapter deals with the results of physico-chemical characterization of the prepared systems. Chapter 4-7 elucidates the activities of the prepared catalysts towards various reactions. Last chapter includes the summary of the investigation and the conclusions drawn from the work.

Contents

BET	Braunauer-Emmett-Teller
BJH	Barrett-Joyner-Halenda
Ce	Cerium
Cr	Chromium
CTAB	Cetyltrimethyl ammonium bromide
CZ	Ceria-Zirconia
DRS	Diffuse Reflectance Spectroscopy
DTG	Differential thermogravimetry
E_a	Activation energy
EB	Ethylbenzene
FTIR	Fourier Transform Infra-Red
GC	Gas chromatography
ICP-AES	Inductively Coupled Plasma-Atomic Emission Spectroscopy
IUPAC	International Union for Pure and applied chemistry
JCPDS	Joint Committee on Powder Diffraction Standards.
Mn	Manganese
Pr	Praseodymium
RS	Raman Spectroscopy
SEM	Scanning Electron Microscopy
TBHP	*tert*-Butyl hydroperoxide
TEM	Transmission electron microscopy
TGA	Thermogravimetry Analysis
TPD	Temperature Programmed Desorption
TPR	Temperature Programmed Reduction
V	Vanadium
XPS	X-ray Photoelectron Spectroscopy
XRD	X-ray diffraction
Zr	Zirconium

Chapter 1

INTRODUCTION AND LITERATURE REVIEW

Contents

Catalysis is a science relying on many disciplines. The advent of industrial catalytic technologies in the last century has, most often, resulted from a sequential interaction between chemists and chemical engineers, both communities developing their own fundamental and applied sciences, i.e., a multidisciplinary process. In recent years, environmental and economic considerations have promoted process innovation towards cleaner technologies. Therefore, it is desirable to use heterogeneous catalysts that can perform under milder reaction conditions. This chapter is comprised of a thorough literature survey on ceria based oxides with special emphasis on ceria-zirconia solid solutions including structural and redox properties; importance of its mesoporous nature, brief comment on the modification with metals and its potential applications with relevant references.

1.1. Prologue

In 1836, Swedish chemist J.J. Berzelius proposed the existence of a new force which he called the "catalytic force" and he defined catalysis as "*a power of substances that enables to awaken the affinities, which are asleep at reaction temperature, by their mere presence and not by their own affinity*".[1]

Throughout the rest of 19th century, the term catalysis remained heavily debated until around 1900 when Wilhelm Ostwald proposed its valid definition in terms of the concepts of chemical kinetics. The use of catalysts in chemical and refining processes has increased rapidly since 1945, when oil began to replace coal as the most important industrial raw material.[2] At the start of the 21st century, more than 80% of the products we use in our daily life have "seen" a catalyst at some point during their manufacture.[3]

Catalysts are materials that change the rate of a chemical reaction but do not change the thermodynamics of the reaction, without undergoing any change in itself. Catalyst offers remarkable increase in the activity of the reactants and selectivity towards a certain desirable reaction products is of greater importance since it reduces the generation of waste by-products. Heterogeneous catalysts cover almost 90% of the industrial catalytic processes. Due to its definite technical advantages, like production process, competitiveness and economy, heterogeneous catalysts are gaining more and more importance to the world's economy, to convert inexpensive raw materials into value added fine chemicals and fuel in an economic and environmentally efficient manner.

1.2. Metal Oxides as Heterogeneous Catalysts

Metal and their oxides control the vast panorama of heterogeneous catalysis. Metal oxides represent one of the most important and widely employed classes of solid catalysts, either as active phases or supports. Metal oxides are usually formed from their corresponding hydroxides, through calcination. The three key features of metal oxides, which are essential for their application in catalysis, are (a) coordination environment of the surface atoms; (b) redox properties of the oxide; (c) oxidation state of the surface.

Metal oxide can be widely applied in redox as well as acid-base catalytic reactions because they can exhibit both electron transfer and surface polarizing properties. The redox properties of oxides are relevant for the oxidation of toxic material. The surface acid-base properties of oxides have a crucial role in the selective organic transformations. Surface exposed cations and anions form acidic and basic sites as well as acid-base pair sites. Dehydrated surfaces possess both Lewis acid cationic sites as well as Lewis base anionic sites. Protons attach to bridging oxygen sites behave as Brönsted acids, whereas the -OH fragments adsorb to the cation sites and behave as Brönsted bases.

Alkali and alkaline earth metal oxides have been evaluated as catalyst for many reactions such as isomerization, dehydrogenation, aldol condensation etc. The *p*-block metal oxides like alumina, silica are extensively used as heterogeneous catalysts for alkylation, acylation and cyclization reactions. Transition metal oxides are active for a number of organic transformations such as oxidation, oxidative/non-oxidative dehydrogenation, reduction, ammoxidation, metathesis, esterification and water gas shift reaction.[4]

1.3. Rare Earth Oxides

Rare earth materials have key roles in our lives from personal items such as a portable compact disc player to a super computer or a huge atom-smashing accelerator. Most of these rare earth materials have been produced from rare earth oxides.[5] Interestingly, they display characteristic behavior and solid-state properties that make them interesting subjects for catalytic studies. For example, in catalysis they are known as the most active and selective catalysts for oxidative coupling of methane to form higher hydrocarbon products (mainly ethane and ethylene), a process of

considerable importance in utilizing the world's large reserves of natural gas.[6] Rare earth oxides are also used as supports for metals that catalyze the formation of methanol from CO_2 and H_2. La_2O_3 and CeO_2 have diverse environmental applications including important ingredients in automobile exhaust-gas conversion catalysts. The increased attention on these materials is due to its unique catalytic properties and increasing availabilities in high purities thereby permitting their fundamental investigations.[7]

1.4. Cerium Dioxide (CeO_2): Structure and Properties

Cerium dioxide is a significant rare earth oxide which has been explored for their structural and chemical properties, reduction behaviour and non-stoichiometry, oxygen storage capacity and metal-ceria interactions. CeO_2 is a promising candidate for its application in environmental catalysis, redox catalysis and wet catalytic oxidation of organic pollutants. Ceria is pale yellow in colour probably due to $O^{2-} \longrightarrow Ce^{4+}$ charge transfer. Ceria is known to crystallize in a fluorite (CaF_2) type of structure. It has a face-centred cubic unit cell (fcc) with space group Fm3m over the whole temperature range from room temperature to the melting point. Fig. 1.1 shows two unit cells of CeO_2 crystal. In this structure, each cerium cation is coordinated to eight equivalent oxygen anions at the corner of a cube and each anion is tetrahedrally coordinated by four cations.[8] The structure can be viewed as a ccp array of cerium ions with oxygen occupying all the tetrahedral holes where as the octahedral sites remain vacant.

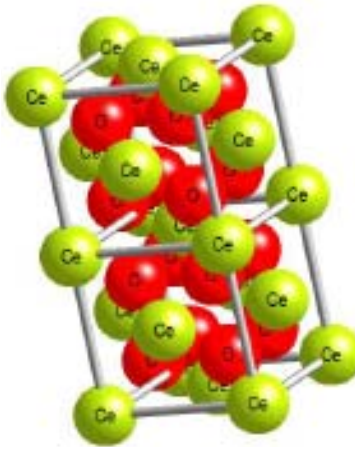

Fig. 1.1. Crystal structure of CeO_2; with two unit cells.

1.4.1. Defects in CeO_2

Defects in a crystal structure are the deviations from the perfect periodic lattice. Defects in ceria can be classified into intrinsic and extrinsic. Intrinsic defects may be present because of thermal disorder or can be created by reaction between the solid and the surrounding atmosphere. (redox processes) The two most common types of crystalline intrinsic defects in ionic materials are Frenkel and Schottky defects. CeO_2, readily exhibit Frenkel disorder in which an atom is displaced from its regular site to an interstitial site, thus forming a defect pair. Extrinsic defects are formed by impurities or by the introduction of aliovalent dopants.[8]

1.4.2. Oxygen Storage Capacity of CeO_2

Cerium oxide has been widely used as an oxygen storage component for three-way catalyst formulation.[9] Oxygen storage capacity (OSC) is defined as the capability to store and release oxygen. Equation (1.1) presents a very simplified picture of the redox behavior of CeO_2.

$$CeO_2 \leftrightarrow CeO_{2-x} + \tfrac{1}{2} O_2 \qquad (1.1)$$

$$Ce^{4+} \leftrightarrow Ce^{3+}$$

According to equation (1.1), oxygen storage is formally considered as the amount of oxygen released (left to right) or stored (right to left) under the net reducing/net oxidizing conditions.

Oxygen storage measurements determines the amount of a reducing gas (H_2, CO) which is oxidized after passing through oxygen presaturated catalyst.[8] Two different measurements of the oxygen storage capacity may be distinguished: a) The OSC (Oxygen Storage Capacity) is related to the most reactive oxygen species and the most readily available oxygen atoms. b) The OSCC (Oxygen Storage Capacity Complete) is the total or maximum oxygen storage capacity. OSCC contains information about the overall reducibility of the solid.

The most important application of ceria lays in this unique property namely its ability to shift easily between reduced and oxidized states. Anyway, the fluorite structure of ceria can withstand high levels of oxygen nonstoichiometry without changing its structural type.[10] CeO_2 containing materials have been receiving a great deal of attention in recent years due to their extensive use for Oxygen Storage Capacity (OSC) in three-way automotive catalysts and have more recently found application for hydrocarbon oxidation in diesel emissions. The technological applicability of CeO_2-containing materials is expanding very rapidly.[11]

1.5. Modification of CeO_2

Despite its widespread applications, pure cerium dioxide suffers from several drawbacks. Poor thermal stability, sintering, loss of surface area, low catalytic efficiency of bare ceria makes it difficult to meet the requirements of high-temperature applications.[12] Sintering at high temperatures can cause losing its crucial oxygen storage and release

characteristics. Therefore, much effort has been directed to find catalyst formulations that can enhance the thermal (textural) stability of CeO_2 without diminishing its special features, such as its unique redox properties and high oxygen mobility. To improve the property, ceria can be spread over a thermally stable, high-surface area support or mixing thoroughly with other oxides. Ceria stabilized on alumina or silica has been found to be an efficient catalyst, especially for environmental applications such as combustion or removal of pollutants from auto-exhaust streams. Transition and non-transition metal oxide, such as TiO_2, ZrO_2, SiO_2, M_2O_3(M- B, Al, Ga, In), SnO_2, MnO_x, HfO_2, Co_2O_3, CaO can be introduced into the ceria cubic structure to form a solid solution.[13] A solid solution is a homogeneous mixture of two or more kinds of atoms (metals) in the solid state. Mixed oxides of ceria maintain fluorite type structures. Modification improves its stability towards sintering. The second metal favours the transport of oxygen. Modification of ceria improves the catalytic activity of the resulting catalysts. Combination of the two metal oxides would result in the changes of structural, reductive and oxygen migration properties thereby affecting its catalytic efficiency. The second metal oxide can also enhance the defects by generating strain into the host lattice. It is reported that mixed oxides of ceria and hafnia, prepared by the citric-acid (Pechini) method, form solid solutions with enhanced phase stability and redox properties.[14] Devaiah *et al.* carried out the synthesis of ceria-hafnia (CH), ceria-zirconia (CZ), ceria-praseodymia (CP) and ceria-lanthana (CL) by modified co-precipitation method from ultrahigh dilute solutions.[15] Among these mixed oxides, CH sample shows highest CO oxidation activity and oxygen storage capacity. Recently, Yu *et al.* have studied the structural and catalytic properties of CeO_2–MO_x (M = Mg^{2+}, Al^{3+}, Si^{4+}).[13] They suggested that alumina act as a very effective surface stabilizer

because of its enhanced textural properties. CeO_2–Al_2O_3 mixed oxides exhibited highest catalytic activity for CO oxidation which is attributed to its excellent textural/structural properties, good homogeneity and redox abilities. Mixed La_2O_3–CeO_2 is the focus of much interest due to their increasing application in catalysis, absorption and related fields. Doped lanthana nanoparticles were reported as chemically stable photo-luminescent materials and doped ceria shows strongly improved performance as catalyst support and oxygen storage component in applications such as automotive exhaust control.[16] Among different mixed oxides of ceria, the most significant is ceria-zirconia. Ceria–zirconia solid solution shows enhanced thermal stability, oxygen storage capacity and catalytic properties.

1.6. Ceria-Zirconia Mixed Oxides

Ceria-zirconia (CZ) mixed oxides have been found to be of great interest because they combine the thermo mechanical stability of ZrO_2 with the oxygen-storage properties of CeO_2 due to its ability to create surface and bulk oxygen vacancies on the generation of Ce^{3+}/Ce^{4+} redox couples. Computational studies have shown that doping ceria with Zr cation lowers the reduction energy and increases the oxygen mobility.[17] Incorporation of zirconium into ceria leads to structural modification of the cubic fluorite structure of ceria that results in the decrease of the cell volume and activation energy for oxide ion diffusion. In 1980s, the first generation ceria-zirconia solid solution was invented as a remarkable oxygen storage material for automotive catalysts. This material mainly consisted of about 20 mol% zirconia as the doping compound to ceria.[18] In the 1990s, the second generation CZ were developed which could dissolve more than 20 mol% zirconia in ceria. Afterwards, the third generation CZ (known as

ACZ) was developed which further improved thermal stability. Based on the concept of diffusion barrier, alumina (A) added to CZ act as diffusion barrier layer which inhibited the coagulation of CZ and A at high temperature. By using these oxygen storage materials, the automotive catalysts could efficiently reduce NO_x emission from automobiles. Recently systematic investigation of a number of $Ce_xZr_{1-x}O_2$ solid solution have been initiated by the network of different laboratories which is supported by the European Union.[19] The first successful fabrication of cubic mesostructured CZ thin films have also been reported.[20] It is reported that the $Ce_{0.5}Zr_{0.5}O_2$ mixed oxide has the best oxygen storage capacity.[21] ZrO_2 addition created oxygen vacancies and increase channel diameter for oxygen migration in the lattice, which causes bulk oxygen release at low temperatures. This was associated with the ability of $ZrO_2$to modify sub lattice oxygen, generating defective structures and highly mobile oxygen atoms in the lattice that could be released, even at moderate temperatures. CeO_2-ZrO_2 oxides with an ordered mesoporous structure with crystalline walls are expected to provide enhanced catalytic performance due to their large surface area and a certain degree of size and shape selectivity.[20] Although the redox property of ceria has been widely studied, little has been published about the acid-base features of CZ solid solutions. This parameter has a key role in several catalytic applications. Cutrufello *et al.* have reported the acid-base properties of nanophase ceria-zirconia catalysts which are investigated by means of adsorption microcalorimetry, using NH_3 and CO_2 as probe molecules.[22] They also evaluated the catalytic activity of these catalysts for 4-methyl pentan-2-ol dehydration. The incorporation of increasingly high contents of zirconium into the ceria lattice has a complex influence on both the acidity and basicity of the pure parent oxide, in terms of both number and strength of the sites.

It was reported that there are five phases that exist in the CeO_2–ZrO_2 binary system from room temperature to 1000°C. The phase is monoclinic if the ceria content is lower than 5% while for ceria concentration is higher than 80%, the cubic phase was reported. In the intermediate region, true nature of the CZ phase diagram is still unclear. However, three tetragonal phases designated as *t*, *t'*, *t''* can be distinguished on the basis of XRD and Raman characterization. *t*- phase is stable one whereas *t'* and *t''* forms are metastable phases. *t''* phase is often referred to as a cubic phase since both give identical X-ray diffraction (XRD) patterns. The cations in the *t''* phase have the same positions as those in the cubic phase, but some oxygen ions are displaced from their positions in cubic fluorite. XRD is not sensitive to light elements (i.e., oxygen) in the presence of heavy elements (i.e., cerium), it is nearly impossible to separate the *t''* phase from the cubic phase by XRD alone.[23, 8]

1.7. Synthetic Approaches to Ceria Based Materials

Several preparation methods have been used for the synthesis of ceria-based materials. This includes sol–gel, precipitation and co-precipitation, hydrothermal method, spray pyrolysis, chemical vapour deposition etc.[24] The properties of the final material are found to be dependent on the preparation method adopted.

The sol-gel method is a homogeneous process which results in a continuous transformation of a solution into a hydrated solid precursor (hydrogel). A sol is a stable colloidal dispersion of small particles suspended in a liquid. These particles interact to form a continuous network of connected particles called a gel. In the sol preparation, the precursors undergo two chemical reactions: hydrolysis and condensation or polymerization, typically with acid or base as catalysts, to form small solid

particles or clusters in a liquid (either organic or aqueous solvent). The advantages of the sol-gel process in general are high purity, homogeneity, and low temperature. Precipitation is one of the most widely used methods for synthesizing solid materials from solution and may be used to prepare either single component catalyst and supports or mixed catalysts. This method utilizes a liquid-phase reaction to prepare insoluble compounds that are crystalline or amorphous precipitates. Co-precipitation method is the most commonly used wet-chemical process. Salts of the several metals are dissolved in the same solvent. Hydrothermal synthesis involves crystallization of substances from high-temperature aqueous solutions at high pressures. The preparation is usually carried out in an apparatus called autoclave. This method is used for the preparation of fine powders with nanosized to submicron particles. Spray pyrolysis is one of the effective methods to prepare homogenous and non-agglomerated sphere particles. The particles are formed by spraying a liquid precursor and by the reaction of the aerosol droplets in a furnace. In Chemical Vapour Deposition (CVD), reactive vapour precursors react to produce solid materials in the gas phase or at the solid-gas interface. CVD method is usually used to produce thin film material.[8]

Porous materials have been recently paid much attention due to their potential application in various fields such as catalysis, adsorption, sensing and fuel cells. According to IUPAC convention, depending upon the pore size they can be classified into three classes; (i) microporous, having pore size less than 2nm, (ii) mesoporous, having pore size within 2nm to 50nm and (iii) macroporous, having pore size greater than 50nm. Great interest has been focused on the mesoporous CZ metal oxides due to their potential application in various areas. Well-ordered mesoporous nonsiliceous metal

oxides have textural characteristics such as high surface area, large pore volume, uniform pore size distribution, high thermal and hydrothermal stability. Pore sizes of mesoporous materials allows easy accessibility for molecules with sizes up to a certain range.[25]

1.8. Mesoporous Solids

The use of templating techniques for the synthesis of mesoporous solids has recently opened up new opportunities in the design of novel high-surface area materials for catalytic applications. The cost effective methods for preparing mesoporous materials are through techniques that employ templates or structure directing agents. These templates can be divided into two groups: endo-templates (i.e., soft templates, such as surfactants, dendrimers, and block copolymers) and exo-templates (i.e., hard templates, such as porous carbons and resins).

Surfactants are surface-active agents; they cover the surfaces of the small particles in colloidal suspensions thereby stabilizing them. Surfactant can reduce the interfacial energy and thereby decrease the surface tension inside the pores by decreasing the capillary stress. This will reduce the shrinkage and collapse of the network during drying and calcinations, which help to maintain high surface area. At high temperature, the ordered supramolecular self-assembly is gradually dissociated to many single surfactant molecules, which lose the role as supramolecular templates. Better thermal stability of the final material is related to the structural arrangement and the morphology of the inorganic-organic composites.[8, 26] Fig. 1.2 shows the schematic diagram for the formation of mesoporous materials.

The surfactants can be of different types, with different properties. (1) Ionic surfactant (Anionic, zwitter ionic, cationic) - The surfactants are

covalently bonded to the inorganic precursor as a ligand. The mesoporous material that is formed using ionic surfactant has long ordering lengths, thick walls and large pores.

(2) Amphiphilic block copolymers - Materials formed using these types of surfactant are hydrothermally stable. Larger pores, up to 140Å, can be synthesized using this type of surfactants.

(3) Neutral templating - This involves non-charged species (often primary amines with carbon tail lengths between C-8 and C-18) in which interaction is based upon hydrogen bonding. The resultant framework structures are shown to have thicker walls.[27]

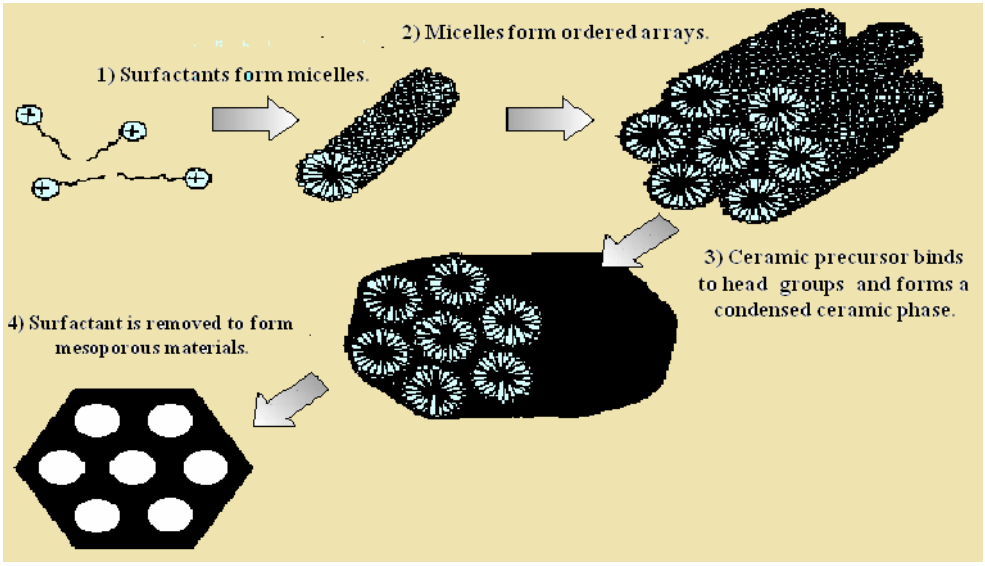

Fig. 1.2. Schematic diagram showing the formation of mesoporous materials.

1.8.1. Mesoporous Ceria-based Materials

Mesoporous $Ce_{0.5}Zr_{0.5}O_2$ with a distorted cubic structure was obtained with KLE polymer as the template.[20] Beck *et al.* systematically explored the role of alkyltrimethylammonium surfactants of the type $C_nH_{2n+1}(CH_3)_3NBr$ (n= 6-16) over the entire range of synthesis

temperatures, 100-200°C, for the formation of various porous molecular sieves.[28] Cetyltrimethylammonium bromide (CTAB), a frequently used cationic surfactant, can reduce the surface free energy and prohibit particle condensation and it has been widely applied in the controlled synthesis of nano-size materials and molecular sieves. Recently, the first successful synthesis of mesoporous ceria-zirconia-yttria mixed oxide (CZY) using CTAB as template was reported by Feng *et al.*[29]

In the surfactant assisted hydrothermal method, the hydrous ceria-zirconia oxide is prepared by the reaction of the precursor salt with ammonia. These hydrous oxides interact with cationic surfactants (CTAB) and can incorporate the organic molecule by exchange with surface OH groups. They can exchange either cations or anions, depending on the pH of the medium. It has been reported that hydrous oxide effectively incorporates cationic surfactants at a pH well above its isoelectric point, allowing a partial degree of ordering to develop over time.[30] The isoelectric point of hydrous zirconium oxide in aqueous solution is close to that of cerium and is dependent on the environment. Under highly basic conditions, incorporation of cationic surfactant take place ie., the following equilibrium shifts to the right with a negative charge on the surface.(Fig. 1.3)

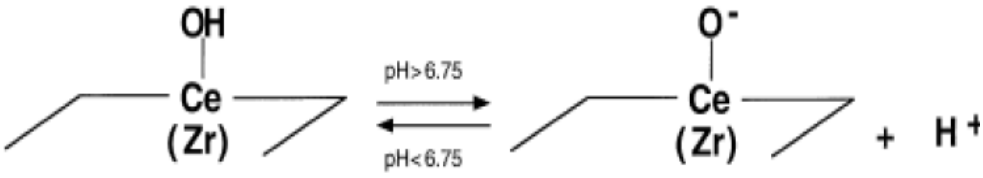

Fig.1.3. Equilibrium involved in the incorporation of surfactant.

The precipitation of hydrous mixed oxide at a pH > 9 in the presence of cationic surfactant should permit the cation exchange process

between H^+ and the surfactant together with the formation of an inorganic/organic composite which upon drying and calcinations will give a mesoporous mixed-oxide phase.[31] The strong similarity of the isoelectric points of Zr and Ce would enable exchangeable sites to be equally distributed over the surface and the extent of substitution of the hydroxyl groups to be comparable.[26]

1.9. Ceria-Zirconia as Support

In addition to their use as catalyst, ceria-zirconia mixed oxides can be used as a support for a variety of chemical processes.[32] Even though pure CZ solid solutions are active by themselves in the redox reactions, promotion by transition metals or noble metals can sharply enhance their activities. The support can disperse the metal particles and can influence the electronic and catalytic properties of the supported metal. The acid function of the support and the metal function can be tuned to promote the desired reaction selectivity. A model has been proposed on the basis of structural considerations to account for the metal support interaction M/CeO_2.[33] They propose the anchoring of the metal crystallite on the surface oxygen vacancies of ceria created by high temperature reduction. Ceria influences the catalytic property of the supported metal by metal-support interaction. The oxygen storage capacity, Ce^{4+}/Ce^{3+} redox couple and the defect sites such as anionic vacancies at the metal-ceria interface can directly contribute to the catalytic activity of the ceria-supported materials. Ceria-zirconia oxide solid solutions supported by precious metals (Pt, Pd and Rh) are promising components for automotive three-way catalysts.

Rakesh *et al.* tested various noble metals such as platinum, palladium, rhodium, ruthenium, iridium, gold supported ceria-zirconia

oxides for water gas shift activities in the temperature range between 200-320°C.[34] The observed reaction rates were found to be highly dependent on the synthesis technique, surface composition, and kinetic regime of operation, which potentially resulted in different reaction mechanisms for the different catalysts. Platinum was identified as the noble metal with the highest activity with optimum loading in the range of 1-2 wt.%. Ceria-zirconia mixed oxides seem to be very promising supports for gold (Au) nanoparticles for low temperature water gas-shift reaction and low-temperature CO oxidation.[35] High activity of $Au/Ce_{1-x}Zr_xO_2$ in low-temperature WGS reaction and CO oxidation is displayed by gold particles with an optimum size of 3–5 nm. The oxide support can modify the electronic properties of nanosized gold particles and this interaction defines the precise nature of the structure and properties at the gold/support interface. Trawczynski *et al.* have studied the effect of mixed CZ oxides as a carrier of Pd catalysts for combustion of oxygenated compounds.[36] They have evaluated Pd/CZ for ethanol combustion reaction and also for Pd-based TWC. The highest selectivity towards acetaldehyde, the major product of ethanol oxidation, was exhibited by Pd supported on pure zirconia. Pd catalyst supported on washcoat composed of alumina and 30wt. % of ceria-zirconia shows high activity in CO and NO conversion in the exhaust gases. One of the promising ways of methane utilization is the selective partial oxidation of methane into syngas (CO and H_2). However, the process is not cost-effective since the equipment required to produce pure oxygen is quite expensive. In this background, Sadykov *et al.* have carried out the selective methane oxidation over Pt supported CZ catalysts modified by Ca and F.[37] They suggested that lattice oxygen is a promising solution to overcome this problem. They have shown that Pt supporting

sharply enhances the catalyst performances and makes the samples selective in the syngas generation.

1.10. Preparation Method for Supported Catalysts

Preparation for supported catalyst involves two steps; (i) rendering a metal-salt component into a finely divided form on a support (dispersion) (ii) conversion of the supported metal salt to a metallic or oxide state. Dispersion can be done by impregnation, adsorption from solution, co-precipitation or deposition. In impregnation, supports are uniformly saturated with a solution of the metal salt and the solvent is subsequently evaporated. The dispersion can also be carried out by spraying the support with a solution of the metal compound or by adding the support material to a solution of a suitable metal salt, such that the required weight of the active component is incorporated into the support without the use of excess of solution. The second stage is called calcination or reduction. It is brought about by a thermal treatment in either an inert atmosphere or an active atmosphere of either oxygen or hydrogen. When the active atmosphere is hydrogen the process is known as reduction. [38, 39]

1.11. Significance of Metals Selected

Addition of modified metals strongly affects the redox behaviours of the catalysts, facilitating a low-temperature reduction of Ce^{4+}. On the basis of theoretical analysis, electron transfer between the metal and the oxide decreases the activation barrier for oxygen vacancy formation in the vicinity of the supported metal clusters. It is reported that transition metal modified ceria-zirconia are attractive catalysts for methane combustion asserting that they have a comparable activity with alumina supported noble metals.[40]

Supported vanadium oxide catalysts have been widely used for catalyzing several oxidation reactions.[41] Vanadium films supported on metal oxides such as TiO_2, CeO_2 and ZrO_2 have been studied for a wide variety of chemical processes including selective oxidation of alcohols, ammoxidation of aromatic hydrocarbons and the selective catalytic reduction of NO_x with ammonia.[42] Support has major influence on the reactivity. For instance, vanadia monolayers supported on TiO_2, CeO_2 and ZrO_2 usually exhibit high activity, while those supported on Al_2O_3 and SiO_2 exhibit much lower activity.

Supported chromium oxide catalysts have been of significant industrial importance for many decades. The industrial importance of supported chromium oxide catalysts have motivated a large number of studies relating to its specific surface properties and catalytic behaviour. Recently, it is reported that chromium substituted aluminophosphates are both active and fairly selective catalysts for the oxidation of secondary alcohols and hydrocarbons using either molecular oxygen or TBHP as the oxidant. Surface functionalized silica gel supported chromium showed excellent selectivity for the epoxidation of cyclohexene to cyclohexene oxide and for the oxidation of ethylbenzene to acetophenone, using air as the oxidant at 130ºC. Also, it was shown that chromium containing mesoporous molecular sieve efficiently catalyzes the oxidation of aliphatic and aromatic primary amines into the corresponding nitro derivatives using TBHP or H_2O_2 as oxidants. Parentis *et al.* have reported that silica supported chromium catalyst is very active and selective for the gas phase oxydehydrogenation and dehydrogenation of primary and secondary alcohols.[43] Cr/SiO_2 catalysts, known as the Phillips catalyst, is used for the production of high-density polyethylene (HDPE) and linear low density

polyethylene (LLDPE) and Cr/Al_2O_3 catalysts are used for the dehydrogenation of butane to butene. Research has been progressed towards the elucidation of the molecular structure of supported chromium oxides and it is found that different oxidation states of Cr can be present, which depend on the pretreatment, the Cr loading, the support type and the composition.

Recently, several authors have demonstrated that manganese oxide materials are efficient catalysts for the elimination of pollutants.[44] Manganese oxides have comparable catalytic activities with noble or supported noble metals; hence, they can be a cheaper alternative. MnO_x-CeO_2 mixed oxides have been developed as environmental friendly catalysts for the abatement of contaminants in both liquid phase and gas phase, such as oxidation of ammonia, phenol and pyridine. It is reported that MnO_x-CeO_2 is a superior catalyst for NO reduction by NH_3. The high activity is attributed to the highly dispersed Mn species and the more active oxygen species that is formed. Mn/Ce composite catalysts are found to be effective for the wet oxidation of phenol, ammonia etc. MnO_x catalysts supported on Al_2O_3, TiO_2 and ZrO_2 (Y_2O_3) have been tested in ethanol and ethyl acetate oxidation. MnO_x– CeO_2 catalysts have been evaluated for the oxidation of ethanol and hexane.[45, 46]

It was found that the oxygen exchange in Ce-Pr mixed oxides occurred at lower temperature in comparison with CeO_2.[47] The addition of Pr caused the distortion of the cations around the oxygen vacancies and the decrease of the activation energy for oxygen migration. In the mixed oxide, it can form mixed valence states of Pr^{3+} and Pr^{4+} under ambient conditions and facilitate oxygen vacancies. Further, in ceria-praseodymia solid solutions, both elements have 3+ and 4+ oxidation states that are

readily formed and the anion vacancy would be very much mobile in this system.[48] Wu et al. have reported that Pr doped CeO_2–ZrO_2 solid solution was found to be active for CH_4–CO_2 reforming to produce synthesis gas which is suitable for Fischer–Tropsch synthesis. It is suggested that the reaction controlling step is closely related to the reaction between CH_4 and surface oxygen species.[49]

1.12. Applications of Ceria Based Materials

Ceria-based materials have been receiving a great deal of attention in recent years due to their extensive use in very broad fields, ranging from catalysis, ceramics, fuel cell technologies, gas sensors, solid state electrolytes, glass-polishing materials, cosmetics etc.[17] It promotes noble metal dispersion, increases thermal stability of Al_2O_3 support, promotes Water Gas Shift (WGS) and steam reforming reactions, favors catalytic activity at the interfacial metal-support sites, promotes CO removal through oxidation by employing its lattice oxygen.[12] Some of the major applications are outlined below.

1.12.1. Automotive Three-way Catalysis

One of the major technological applications of cerium based oxides is in three way catalysis where significant amount of cerium is consumed annually. Houdry, a mechanical engineer founded a company to develop catalytic converter in 1953 when the results of early studies of smog were published. Catalytic converter is a vehicle emission control device for converting toxic byproducts of combustion to less toxic substance by means of catalyzed chemical reaction. Catalytic converter can be of 2 types; two way or three way. In two way catalytic converter, it can oxidize carbon monoxide and hydrocarbon whereas in three way, it can simultaneously catalyze three reaction; oxidation of carbon monoxide and

hydrocarbon and reduction of nitrogen oxides. This task can be accomplished by using a simple oxidation catalyst and noble metal catalysts promote the oxidation of incomplete oxidation products from the internal combustion engine.[8] The most widely used exhaust control device consists of several components- catalyst core, washcoat and catalytic material. The catalyst core is usually a ceramic monolith with a honeycomb structure. Washcoat is a carrier for the catalytic material. It is impregnated on the walls of the monolith. It is made of alumina, cerium and zirconium. Cerium is present as CeO_2 as high as 20%. It is used to disperse catalytic material which is a precious metal; platinum palladium and rhodium. Pt and Pd are efficient for the oxidation reaction whereas rhodium for the reduction. So commercially used three way catalysts is a bimetallic combination of Pt, Rh or Pd, Rh catalysts. Ceria has multiple roles in three way catalyst. It can promote the low temperature water-gas shift reaction. Because of its redox property, it can store and release oxygen under lean (oxygen rich) and rich fuel conditions respectively. It can stabilize precious metal dispersion against thermal damage and also minimize the sintering of alumina washcoat. The automotive three-way catalyst system operates under a certain range of air-to fuel (A/F) ratios, controlled by an electric fuel-injection system linked to an oxygen sensor device. However, even the exhaust gases controlled by the system alternate between slightly rich to slightly lean conditions.[50] If the air-fuel ratio is close to a stoichiometric value of 14.6, the catalyst converts all the pollutants to CO_2, H_2O and N_2 gases effectively. (Fig. 1.4) Deviation from this value affects the conversion thereby resulting in the incomplete combustion of pollutants. The role of ceria and ceria related material is to widen the A/F window. This is due to its ability to switch between Ce^{3+} and Ce^{4+}. Zirconia also

plays an integral role in providing oxygen storage which broadens the conversion efficiency for all three pollutants during rich/lean perturbations.

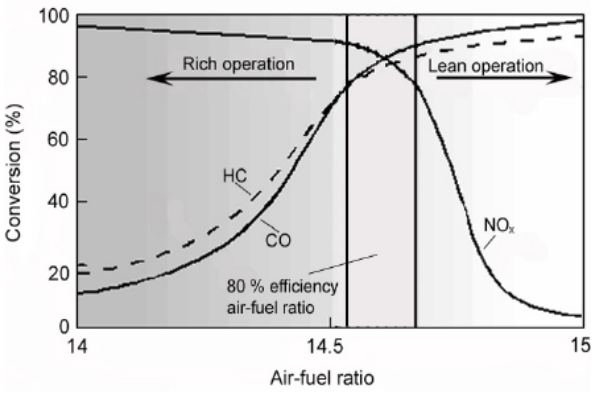

Fig. 1.4. Conversion efficiency of NO_x, CO and HC as a function of the air-fuel ratio in a three-way catalytic converter.

1.12.2. Solid Oxide Fuel Cells

Fuel cells are electrochemical devices which directly convert chemical energy stored in fuel to electric power. Recently fuel cells have attracted considerable attention because of its enhanced efficiency than well established fossil fuel combustion technologies and lower emissions.[51] Among the variety of fuel cells, solid oxide fuel cell (SOFC) is considered to be the most promising power source of incoming decades because of high efficiencies, low cost and fuel flexibility. Fig. 1.5 depicts the design of a solid oxide fuel cell. A single SOFC unit consists of an anode, a cathode and a solid ceramic electrolyte that is sandwiched between the two. Fuel (usually hydrogen or methane) is fed to the anode and oxidant (O_2 or air) flows through the cathode. Negatively charged oxygen ions migrate through the electrolyte membrane. This electrochemical reaction generates electrons, which flow from the anode to an external load and back to the cathode. It operates at high temperatures (~1000°C) to give the ion conductivity of electrolyte material enough to be used. Popular electrolytes

used are yttria stabilized zirconia (YSZ) and scandia stabilized zirconia. They can deliver promising power output only at high temperatures. At intermediate temperatures, YSZ electrolytes exhibit insufficient electro catalytic activity for oxygen reduction and poor ionic conductivity. This demands an electrolyte with high ionic conductivity at intermediate temperatures (600–850°C). SOFC comprised of rare-earth doped ceria electrolyte has been attracting more attention in the past two decades since it exhibits sufficiently high oxide ionic conductivity at intermediate temperature. The main features of ceria containing SOFC are low operating temperature, higher ionic conductivity, chemical inertness, high crystalline-phase and chemical purity.[52] Gadolinium-doped ceria (GDC, $Gd_{0.1}Ce_{0.9}O_{1.95}$) can be used as highly conductive solid electrolytes.[53] Lin *et al.* fabricated a cell using samaria-doped ceria (SDC) which performs well at intermediate temperatures. Simplicity in the cell fabrication and maintenance, attractive cell power output suggest that this technology may be useful in many fields.[51]

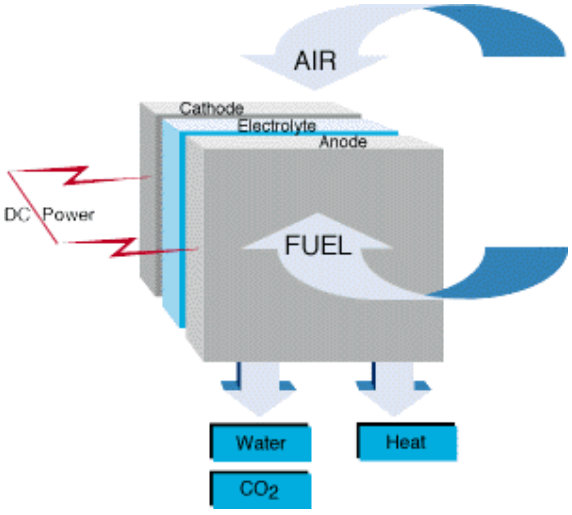

Fig.1.5. Design of a solid oxide fuel cell.

1.12.3. Catalytic Wet Oxidation (CWO)

The aim of CWO is catalytic abatement of organic pollutants present in wastewater to less toxic compounds that are then amenable to biological treatment for final purification.[54] Wet oxidation is carried out under high pressure of oxygen at high temperature to decompose organic pollutants in waste waters. Currently, Copper (II) salts are used as the homogeneous wet-oxidation catalyst. Since the water is contaminated by toxic copper ion after treatment, the recovery of copper salt is crucial which is rather difficult. In this context, heterogeneous catalysts have attracted much attention. Interestingly, ceria and related compounds are active both in the oxidation of lower carboxylic acids (especially acetic acid) and of ammonia. The former are very refractory to oxidation and they are key compounds in the degradation of organic pollutants. Ammonia is one of the potent pollutants which cause eutrophication of the receiving water system. The nitrogen compounds contained in various organic compounds are converted into ammonia by wet oxidation and its further oxidation is rather difficult. MnO_x-CeO_2 was reported as a best choice for the wet oxidation of ammonia. Mn/Ce catalysts were found to be effective for oxidation of carboxylic acids also. The redox properties of the catalyst are an important factor in controlling the activity. In the low-temperature region the valence state of Mn in Mn-Ce composite oxide exceeds 3+ whereas in pure Mn oxide it is below 3+. Cerium provides oxygen to Mn at low temperatures and withdraws oxygen at high temperatures. This is due to the oxygen storage capacity of CeO_2. Ceria-zirconia doped with MnO_x and CuO was also found to be active for the acetic acid oxidation. The presence of small amounts of copper and manganese enhances its low temperature oxidation ability with low level of catalyst leaching during reaction.[8]

1.12.4. Removal of Sulfur Oxides

The control of sulfur oxides emissions is becoming a major issue since it is the major source of acid rain. Ceria can be used as sorbent or catalyst additive for the development of new solutions to de-SO_x technologies. Ceria can react easily with sulphur compounds resulting in the formation of sulphates, sulphites, oxysulfides and sulphides. The presence of metals like Ni and Cu increases the rate of reaction. It is the redox property of ceria that makes possible the storage and release of sulphur compounds. In the refinery Fluid Catalytic Cracking process (FCC), sulfur containing components in crude oils can give rise to sulfur oxide in the gases emitted from catalyst regenerator unit. Cerium can be used as an additive to the FCC-catalyst to capture SO_X as sulphate and released as more easily trapped form of sulfur, H_2S.[8, 50]

1.12.5. Catalytic Applications

Ceria-based catalysis has demonstrated high efficiency in a variety of chemical transformations widely used for the synthesis of fine chemicals and specialties. The redox and acid–base properties of ceria, either alone or in the presence of transition metals, are important parameters that allow to activate complex organic molecules and to selectively orient their transformation. Mishra *et al.* have studied hydrogen transfer reaction of cyclohexanone with isopropanol over CeO_2–ZnO composite catalyst.[55] The catalyst showed 51.3 mol% conversion of cyclohexanone. Recently, Rose *et al.* have reported acetalization of cyclohexanone with methanol producing dimethyl acetal using different transition metals (iron, chromium, nickel & copper) modified mesoporous ceria catalysts.[56] The protection of carbonyl groups is important specifically during the manipulation of multifunctional organic molecules since dimethyl acetal

display higher stability towards strong bases, Grignard reagents, lithium aluminium hydride, strong oxidants and esterification reagents than their parent carbonyl compounds. Among different catalysts, ceria modified with iron was shown to be active for protection of cyclohexanone. Ceria has been used as a catalyst for ketonization of small organic acids which is a valuable reaction for biorenewable applications. Between temperature regimes of 150−300°C, cerium oxide can undergo bulk transformations.[57] Very recently, it was reported that magnetite nanoparticle supported ceria catalyst can catalyze multicomponent synthesis of functionalized 1,4 dihydropyridines under benign reaction conditions.[58] Notably, 5.22 mol% of the catalyst is sufficient to catalyze the multicomponent reaction in ethanolic medium at room temperature. Catalyst can be recycled and reused without loss of activity. Dehydration of 4-methyl-2-pentanol to 4-methyl-1-pentene, monomer for the manufacture of thermoplastic polymers is catalyzed by CeO_2-ZrO_2, CeO_2-La_2O_3 and CeO_2-ZrO_2 supported on SiO_2 between 250°C and 400°C. Allylic alcohols can be selectively produced by the vapor-phase dehydration of 1,3-diols over CeO_2. Mesityl oxide (4-methyl-2-penten-2-one) was selectively hydrogenated in the gas phase at 175°C over 2CuO-CeO_2 and 2Cu-CeO_2 reduced catalysts to produce methyl isobutyl ketone (4-methylpentan-2-one). Coumarins can be prepared using sulphated $Ce_xZr_{1-x}O_2$ solid catalyst under solvent-free conditions at 120°C. Ce–MCM-41 and ceria–yttria catalysts were found to be active for the acylation of alcohols, amines, and thiols with acetic anhydride without solvent or in the presence of acetonitrile.[59] Ceria nanorods with well-defined surface planes can be synthesized and utilized for the hydrogenation of nitroaromatics with N_2H_4 as a reducing agent.[60] In the

near future, the very rich chemistry of cerium oxides can boost research on new catalysts with better properties for organic synthesis.

1.12.6. Other Applications

Cerium oxide is the most efficient polishing agent for most glass compositions. The chemical reaction between the glass silica substrate and the cerium oxide particles causes formation of a silicate layer which makes the glass surface more fragile and less resistant to mechanical erosion and physical modifications. Cerium oxide polishing powders are used in spectacles, precision optics lenses for camera, CRT displays and they remove damaged layers of glass providing a smooth and glossy surface.[5]

Considerable interest is given to CeO_2 for its application as UV-blocking agents.[5] Sunscreen materials have been developed to protect the damaging effect of UV-rays on human skin. Even though popular inorganic sunscreen agent is titanium oxide, it can oxidize sebum and degrade other ingredients in the sunscreen cosmetics since is an excellent photocatalyst. CeO_2 has characteristics ideal for its use as inorganic sunscreen because it is transparent to visible light and has excellent ultraviolet radiation absorption properties, due to the appropriate refractive index (2.1) and the band gap energy (3.1eV) respectively.

1.13. Reactions Selected for Present Study

1.13.1. Transesterification Reaction

Transesterification is industrially as well as academically important reaction. Transesterification is a pivotal organic transformation that provides easy synthesis route for a number of applications in many organic processes. Numerous reports were available in the literature on the transesterification reactions over solid catalysts.[61] Transesterification is a

vital step in several industrial processes such as (i) production of higher acrylates from methylmethacrylate, (ii) polyethylene terephthalate (PET) from dimethyl terephthalate (DMT) and ethylene glycol, (iii) intramolecular transesterifications leading to lactones and macrocycles, (iv) alkoxy esters (biodiesel) from vegetable oils, and (v) co-synthesis of dimethyl carbonate (an alkylating agent, octane booster and precursor for polycarbonates) and ethylene glycol from ethylene carbonate and methanol.[62] Transesterification is more beneficial than the ester synthesis from carboxylic acid and alcohol, due to poor solubility of some of acids in organic solvents, whereas the esters are commonly soluble in most of the solvents. Some esters, especially methyl and ethyl esters are readily or commercially available and thus serve conveniently as starting materials in transesterification reaction.[63] Malonic esters are among the most important intermediates in organic synthesis, since they can be transformed into useful building blocks and serve as a valuable tool for the synthesis of various complex compounds and for pharmaceutics. The transesterification of these compounds has been known as a useful process because it allows the preparation of more complex products from more easily accessible synthons.[64]

1.13.2. Ethylbenzene Oxidation

The study and the development of innovative metal-catalyzed systems for the oxygenation of organic molecules with sustainable oxidant is a very attractive perspective for the chemical industry. A sustainable catalytic oxidation should present the following fundamental features : i) capability to activate oxygen species, with solvent-free protocols, or in environmentally friendly solvents. ii) high selectivity iii) oxidative, hydrolytic and thermal stability in the reaction conditions.[65] Catalytic oxidation, both in vapour and

liquid phases, is one of the most important areas because of the production of commercially important compounds. In recent years, the development of liquid phase processes have been accelerated because of certain process economic advantages such as higher yield, improved selectivity and milder reaction conditions.[43] Processes involving the oxidation of hydrocarbons are of great importance to industrialized economies because of their role in converting petroleum hydrocarbon feed stocks such as alkanes, olefins, and aromatics into industrial organic chemicals important in the polymer and petrochemical industries.[66]

Among them, one of the notable reaction is the direct oxidation of alkylbenzene to the corresponding aralkyl ketones. The selective oxidation of ethylbenzene to acetophenone is an industrially important reaction since acetophenone formed is the raw material for the production of pharmaceuticals, perfumes, resins and alcohol, esters, aldehydes and tear gas. It is used as a flavouring agent in many sweets and drinks, and as a solvent for cellulose ether. Therefore it is desirable to increase selectivity to acetophenone in the ethylbenzene oxidation reaction.[67] Initially, oxidation of ethyl benzene has not drawn much attention due to the complexity of the products that could be formed. But the effective utilization of ethyl benzene to more value added products is an interesting proposition. Synthesis of acetophenone by Friedel Craft's acylation of aromatic compound by acid halide or acid anhydride using stoichiometric amount of anhydrous aluminium chloride or a homogeneous acid catalyst leads to a the formation of a large volume of highly toxic and corrosive wastes.[68] The oxidation of ethyl benzene to acetophenone using stoichiometric quantities of $KMnO_4$ is not recommended because of the difficulty in the separation of products from the reaction mixture and the large amount of wastes. Therefore, heterogeneous transition metal (viz. Co, Mn, Cu

or Fe) catalysts have been developed for the liquid phase oxidation of ethyl benzene by oxygen/air. However, this also suffers from disadvantages such as formation of tarry waste products, poor product selectivity and harsh reaction conditions. It is therefore of great practical interest to develop a more efficient, easily separable, reusable and environmental friendly catalyst for the production of acetophenone. [69]

1.13.3. Benzene Hydroxylation

Hydroxylated aromatic compounds are the most important raw materials in chemical industry. The oxidation of benzene to phenol is most probably a champion catalytic reaction. A variety of approaches, number of tested catalysts, and amount of efforts have been dedicated to its realization. It probably appears to be very simple but is very difficult to achieve. This elegant chemical transformation will continue to challenge catalytic researchers in the next century. Phenol has an important role as intermediate in the manufacture of petrochemicals, agrochemicals and plastics processes. Moreover, benzene is a monocyclic Volatile Organic Compound (VOC) mostly found in petroleum derivatives such as gasoline and diesel fuels. [70] VOCs are toxic to humans (carcinogenic and mutagenic) and can cause atmospheric pollution (photochemical smog and destruction of ozone layer). Catalytic oxidation is a promising technology for the oxidation of petrochemical materials to make products of economical value. Catalytic oxidation has been applied for odor control and treatment of emissions containing evaporated solvents. The direct hydroxylation of benzene to phenol using a variety of catalysts, electrochemical oxidation systems, and photochemical systems have been extensively investigated.[71] One-step hydroxylation of benzene to phenol is of great interest because of its environmentally benign nature.[72]

1.13.4. Soot Oxidation

The ability of cerium oxide to act as an oxidizing agent prompted the potential use of various cerium derivatives as additives to aid combustion. During the combustion process these derivatives can catalyze the low temperature oxidation of carbon. Diesel engines are the workhorses for the modern society since they are the controlling source behind commercial transport being employed in on-road (buses, trains etc.) as well as off-road industrial vehicles.[73] Nevertheless the diesel engine is one of the largest contributors to environmental pollution problems due to the emissions of diesel particulate materials (DPM) and nitrogen oxides (NO_x). This particulate matter (soot) which is released into the atmosphere can cause a great threat to the environment and the health of human beings. They can cause and enhance respiratory, cardiovascular and allergic diseases.[74] Among the several techniques that have been developed for reducing particulate emissions from diesel engines, filtering followed by catalytic oxidation is one of the most promising. The particulate capture is done using Diesel Particulate Filter (DPF) or other similar devices but the main drawback is that particulate traps suffer from blocking and need periodic regeneration. Catalytic regeneration has been suggested as the best approach and intensive efforts are being made to develop suitable catalysts. The regeneration catalysts should possess excellent catalytic activity at low temperature with high thermal and chemical stability. Among this kind of catalysts, some advances were followed in CeO_2-based formulations during the last years. It has the potential to increase the soot oxidation rate by the participation of its active oxygen and thereby lower the onset temperature of the soot oxidation.[75]

Kinetic analysis of thermal decomposition processes has been the subject interest for many investigators all along the modern history of thermal decomposition. The analysis allows one to design any kind of device, in which the thermal decomposition takes place. Thermogravimetric analysis (TGA) is a common method to study the kinetics of solid-state reactions. Most evaluations are performed by fitting kinetic data to various reaction models.[76] A substantial number of methods have been suggested in which kinetic parameters can be evaluated from the data of non-isothermal experiments. In 1964, Coats and Redfern presented an integral method, which become one of the most widely used methods in non-isothermal kinetic analysis. Coats-Redfern method assumes various orders of reaction and compares the linearity in each case to select the correct order. The equations are given below.[77]

$$\log\left[\frac{1-(1-\alpha)^{1-n}}{T^2(1-n)}\right] = \log\frac{AR}{\beta Ea}\left[1-\frac{2RT}{Ea}\right]-\frac{Ea}{2.303RT} \quad for\ n \neq 1$$

$$\log\left[\frac{-\log(1-\alpha)}{T^2}\right] = \log\frac{AR}{\beta Ea}\left[1-\frac{2RT}{Ea}\right]-\frac{Ea}{2.303RT} \quad for\ n = 1$$

By plotting the appropriate left-hand side of the above equations versus l/T, the slope equals ($-E_a/2.303R$). Activation energy (E_a) can be calculated from these equations.

1.14. Aim and Scope of the Thesis

Catalysis has wide range applications in chemical industry and has a major impact on the quality of human life as well as economic development. In recent years catalysis is also looked upon as a solution to eliminate or replace polluting processes due to inherent characteristics of catalytic processes as clean technologies. Ceria and ceria based mixed oxides deserve particular attention for their applicability in various

technologically important catalytic processes. Ceria-zirconia oxides are effective catalysts or carriers for industrial or environmentally friendly reactions, such as automotive exhaust gas conversion, methane reforming processes, water–gas shift reaction etc. In this context, due to its unique characteristics, we have selected ceria-zirconia for our studies. Ceria-zirconia mixed oxide modified with various metals can improve surface properties thereby enhance the catalytic activity. The scarcity of systematic studies in the literature does not allow a basis for the role of the dopant in modifying the textural, phase stability and activity of CeO_2 based catalysts for various reactions. The thesis will provide a systematic and comprehensive study to understand the surface properties and catalytic activities of several metal modified ceria-zirconia mixed oxides. The study and development of modified ceria-zirconia catalysts for chemical processes have very attractive perspectives since the use of CeO_2 based catalysts has shown a rapid increase in the last years. Different reactions have been carried out to implement benchmark catalytic activity of these materials. The thesis is aimed at the design of modified ceria-zirconia catalysts for different chemical process which are appealing in an industrial perspective such as hydroxylation of aromatic hydrocarbons,[78] transesterification reaction[79] and also carbon (soot) oxidation.[80]

1.15. Objectives of the Present Work

The main objectives of this work are as follows:

- To prepare ceria-zirconia mixed oxide by surfactant assisted hydrothermal method using cetyltrimethyl ammonium bromide as cationic surfactant.

- To modify ceria-zirconia mixed oxide with metals such as Vanadium (V), Chromium (Cr), Manganese (Mn) and Praseodymium (Pr).
- To investigate the surface properties of the systems by employing various spectroscopic and non-spectroscopic techniques namely X-ray diffraction (XRD), Nitrogen adsorption isotherm, Thermal Analysis (TGA), Fourier Transform Infrared Spectroscopy (FT-IR), UV-vis diffuse reflectance spectroscopy (UV-Vis DRS), Raman spectroscopy (RS), X-ray photoelectron spectroscopy (XPS), Scanning electron microscopy (SEM), Transmission electron microscopy (TEM), Temperature programmed reduction (TPR) and Temperature programmed desorption(TPD-NH_3) .
- To evaluate the catalytic activity of the prepared catalysts towards trans-esterification reaction of diethyl malonate with butanol. The influence of different reaction parameters on catalyst activity is to be studied in detail.
- To investigate the activity of the prepared catalysts for the liquid phase oxidation of ethyl benzene with *tert*-butyl hydroperoxide oxidant.
- To assess efficiency of the systems for the oxidation of benzene using hydrogen peroxide as oxidant under liquid phase condition.
- To study the activity of the catalysts towards soot oxidation reaction using a model soot by thermo gravimetric analysis method and to estimate the kinetic parameters of soot oxidation reaction using kinetic model.

References

[1] J.J. Berzelius, Jber. Chem. 15 (1835) 237.

[2] L. Lawrie, Handbook of Industrial Catalysts, Springer (2011) ISSN 1574-0447.

[3] C. Marcilly, Journal of Catalysis 216 (2003) 47.

[4] M. Maitri, Ph. D thesis, Synthesis, characterization and catalytic studies of heteroatoms incorporated ZnO, University of Pune (2009).

[5] G. Adachi, N. Imanaka, Z.C. Kang, Binary Rare Earth Oxides, Kluwer Academic Publishers (2004).

[6] A. M. Gamal, Hussein, Journal of Analytical and Applied Pyrolysis, 37 (1996) l49.

[7] P.M. Rosynek, Catalysis Reviews: Science and Engineering, 16 (1977) 111.

[8] A. Trovarelli: Catalysis by Ceria and Related Materials, Catalytic Science Series, World Scientific Publishing Company, UK, Vol. 2. (2002)

[9] M. Boaro, F. Giordano, S. Recchia, V.D. Santo, M. Giona, A. Trovarelli, Applied Catalysis B: Environmental 52 (2004) 225.

[10] T.G. Kuznetsova, V.A. Sadykov, ISSN 0023-1584, Kinetics and Catalysis, 49 (2008) 840.

[11] D. Harshini, D.H. Lee, J. Jeong, Y. Kim, S.W. Nam, H.C. Ham, J.H. Han, T. Lim, C.W. Yoon, 148–149 (2014) 415.

[12] M.B. Reddy, A. Khan, Catalysis Surveys from Asia, 9 (2005).

[13] Q. Yu, X. Wu, C. Tang, L. Qi, B. Liu, F. Gao, K. Sun, L. Dong, Y. Chen, Journal of Colloid and Interface Science 354 (2011) 341.

[14] G. Zhou, J.R. Gorte, J. Phys. Chem. B 112 (2008) 9869.

[15] D. Devaiah, H.L. Reddy, K. Kuntaiah, M.B. Reddy, Indian Journal of chemistry 51A (2012) 186.

[16] S. Liang, E. Broitman, Y. Wang, A. Cao, G. Veser, J Mater Sci 46 (2011) 2928.

[17] Q. Yuan, H. Duan, L. Li, L. Sun, Y. Zhang, C. Yan, Journal of Colloid and Interface Science 335 (2009) 151.

[18] H. Sobukawa, R& D Review of Toyota CRDL, Vol.37, No.4

[19] M. Daturi, C. Binet, J. Lavalley, A. Galtayries, R. Sporken, Phys. Chem. Chem. Phys. 1 (1999) 5717.

[20] Q. Yuan, Q. Liu, W. Song, W. Feng, W. Pu, L. Sun, Y. Zhang, C. Yan, J. Am. Chem. Soc. 129 (2007) 6698.

[21] L. Meng, L. Liu, X. Zi, H. Dai, Z. Zhao, X. Wang, H. He, Front. Environ. Sci. Engin. China 4 (2010) 164.

[22] M.G. Cutrufello, I. Ferino, V. Solinas, A. Primavera, A. Trovarelli, A. Auroux, C. Picciau, Phys. Chem. Chem. Phys. 1 (1999) 3369.

[23] F. Zhang, C. Chen, J. Am. Ceram. Soc., 89 (2006) 1028.

[24] C. Liang, J. Qiu, Z. Li, C. Li, Nanotechnology 15 (2004) 843.

[25] A.W. Bosman, H.M. Hanssen, E.W. Meijer, Chem. Rev. 99 (1999) 1665.

[26] P. Aniruddha, M.Sc Dissertation, Preparation and characterization of mesoporous CeO_2-ZrO_2 nanopowders using dodecylamine and sodium dodecyl sulfate as surfactant, National Institute of Technology, Rourkela.

[27] K.J.P. Rose, Ph. D thesis, Studies on catalysis by mesoporous ceria modified with transition metals, Cochin University of Science And Technology (2012).

[28] J.S. Beck, J.C. Vartuli, G.J. Kennedy, C.T. Kresge, W.J. Roth, S.E. Schramm, Chem. Mater. 6 (1994) 1816.

[29] R.M. Feng, X.J. Yang, W.J. Ji, C.T. Au, Materials Chemistry and Physics 107 (2008) 132.

[30] M.J. Hudson, J.A. Knowles, J. Mater. Chem. 6 (1996) 89.

[31] P.J. Fincy, Ph. D thesis, Catalysis by nanocrystalline ceria modified with transition metals, Cochin University of Science And Technology (2004)

[32] M.P. Yeste, C.J. Hernandez-Garrido, D.C. Arias, G. Blanco, M.J. Rodrıguez-Izquierdo, M.J. Pintado, S. Bernal, A.J. Perez-Omil, J.J. Calvino, J. Mater. Chem. A 1 (2013) 4836.

[33] Troveralli, Catal. Rev. Sci. Eng. 38 (1996) 439.

[34] R. Rakesh, R.R. Willigan, Z. Dardas, T.H. Vanderspurt, American Institute of Chemical Engineers Journal 52 (2006) 5.

[35] J. M. Rynkowski, I. Dobrosz-Gomez, DOI: 10.2478/v10063-008-0015-6

[36] J. Trawczynski, W. Walkowiak, Journal of KONES Internal Combustion Engines 11 (2004) 3.

[37] V.A. Sadykov, T.G. Kuznetsova, S.A. Veniaminov, D.I. Kochubey, B.N. Novgorodov, E.B. Burgina, E.M. Moroz, E.A. Paukshtis, V.P. Ivanov, S.N. Trukhan, S.A. Beloshapkin, Yu. V. Potapova, V.V. Lunin, E. Kemnitz and A. Aboukais, React. Kinet. Catal. Lett. 76 (2002) 83.

[38] Lowrie Lloyd, Handbook of Industrial Catalysts, Springer Science and Business Media, LLC (2011) ISSN 1574-0447.

[39] G.J.K. Acres, A.J. Bird, J.W. Jenkins, F. King, The Design and Preparation of Supported Catalysts, 10.1039/9781847553164-00001

[40] T. Kuznetsova, V. Sadykov, L. Batuev, E. Moroz, E. Burgina, V. Rogov, V. Kriventsov, D. Kochubey, Journal of Natural Gas Chemistry 15 (2006) 149.

[41] T. Radhika, S. Sugunan, Catalysis Communications 8 (2007) 50.

[42] S. G. Wong, R. M. Concepcion, M. J. Vohs, J. Phys. Chem. B 106 (2002) 6451.

[43] L.M. Parentis, N.A. Bonini and E.E. Gonzo, React. Kinet. Catal. Lett. 76 (2002) 243.

[44] C. H. Genuino, S. Dharmarathna, C.E. Njagi, C.M. Mei, L.S. Suib, J. Phys. Chem. C 116 (2012) 12066.

[45] G. Maya, Ph. D thesis, Catalysis by transition metal modified ceria and ceria-zirconia mixed oxides prepared via sol-gel route, Cochin University of Science And Technology. (2006).

[46] D. Delimaris, T. Ioannides, Applied Catalysis B: Environmental 84 (2008) 303.

[47] R. Rui, W. Duan, W. Xiaodong, F. Jun, W. Lei, W. Xiaodi, Journal of Rare Earths 29 (2011) 1053.

[48] B.M. Reddy, G. Thrimurthulu, L. Katta, J. Phys. Chem. C 113 (2009) 15882.

[49] Q. Wu, J. Chen, J. Zhang, Fuel Processing Technology 89 (2008) 993.

[50] P. Bharali, Ph. D thesis, Design of novel nanosized ceria-based multicomponent composite oxides for catalytic applications, Osmania University. (2009)

[51] Y. Lin, C. Su, C. Huang, J.S. Kim, C. Kwak, Z. Shao, Journal of Power Sources 197 (2012) 57.

[52] W. Sun, W. Liu, Journal of Power Sources 217 (2012) 114.

[53] S. Park, C.W. Na, J.H. Ahn, U. Yun, T. Lim, R. Song, D. Shin, J. Lee, Journal of Power Sources, Volume 218 (2012) 119.

[54] A. Trovarelli, C.D. Leitenburg, M. Boaro, G. Dolcetti, Catalysis Today 50 (1999) 353.

[55] B.G. Mishra, G.R. Rao and B Poongodi, Proc. Indian Acad. Sci. (Chem. Sci.) 115 (2003) 561.

[56] K.J.P. Rose, S. Sugunan, IOSR Journal of Applied Chemistry (IOSRJAC) 1 (2012) 24.

[57] W. Ryan, Snell, H. Brent Shanks, ACS Catal. 3 (2013) 783.

[58] B.M. Gawande, D.B.V. Bonifacio, S.R. Varma, D.I Nogueira, N. Bundaleski, C. Amjad, A. Ghumman, M.N.D.O. Teodoro, S.P. Branco, Green Chem. 15 (2013) 1226.

[59] L. Vivier, D. Duprez, ChemSusChem. 3 (2010) 654.

[60] H. Zhu, Y. Lu, F. Fan, S. Yu, Nanoscale 5 (2013) 7219.

[61] S. Saravanamurugan, Sujandi, D. Han, J. Koo, S. Park, Catalysis Communications 9 (2008) 158.

[62] D. Srinivas, R. Srivastava, P. Ratnasamy, Catalysis Today 96 (2004) 127.

[63] E.D. Ponde, H.V. Deshpande, J.V. Bulbule, A. Sudalai, S.A. Gajare, J. Org. Chem. 63 (1998) 1058.

[64] S. Tural, Turk J Chem, 32 (2008) 169.

[65] C. L. Hill, Nature 401(1999) 436.

[66] A.K. Suresh, M.M. Sharma, T.Sridhar, Ind. Eng. Chem. Res. 39 (2000).

[67] V. Raji, M. Chakraborty, A.P. Parikh, Ind. Eng. Chem. Res. 51 (2012) 5691.

[68] P.H. Groggins, R.H. Wagel, Ind. Eng, Chem. 26 (1934) 1313.

[69] K. Morikawo, T. Shirasaki, M. Okada, Adv. Catal. 20 (1969) 97.

[70] C.H. Genuino, S. Dharmarathna, C.E. Njagi, C.M. Mei, L.S. Suib, J. Phys. Chem. C 116 (2012) 12066.

[71] O. Shoji, T. Kunimatsu, N. Kawakami, Y. Watanabe, Angew. Chem. Int. Ed. 52 (2013) 1.

[72] H. Xiao-ke, Z. Liang-fang, G. Bin, L. Qiu-yuan, L. Gui-ying, H. Chang-wei, Chem. Res. Chinese Universities 27 (2011) 503.

[73] R. Prasad, V.R. Bella, Bulletin of Chemical Reaction Engineering & Catalysis 5 (2010) 69.

[74] N.K. Rao, P. Venkataswamy, M.B. Reddy, Ind. Eng. Chem. Res. 50 (2011) 11960.

[75] M. Dhakad, S.S. Rayalu, R. Kumar, P. Doggali, S. Bakardjieva, J. Subrt, T. Mitsuhashi, H. Haneda, N. Labhsetwar, Catal Lett 121 (2008) 137.

[76] R. Ebrahimi-Kahrizsangi, M.H. Abbasi, Trans. Nonferrous Met. Soc. china 18 (2008) 217.

[77] T. Bolie, Ph. D thesis, Studies on the surface properties and catalytic activity of metal chromites on thermal decomposition of ammonium perchlorate, Cochin University of Science And Technology (2010).

[78] Y. Tang, J. Zhang, Transition Metal Chemistry 31 (2006) 299.

[79] S. Pallavi, V.A. Ramaswamy, K. Lazar, R. Veda, Applied Catalysis A: General 273 (2004) 239.

[80] B. Azambre, S. Collura, P. Darcy, J.M. Trichard, P.D. Costa, A. García-García, A. Bueno-López, Fuel Processing Technology 92 (2011) 363.

Chapter 2

MATERIALS AND METHODS

Contents

The importance of heterogeneous catalysts has surpassed the interest in the fundamental chemistry because of their wide industrial applications. Recent catalyst research has been focused towards the better understanding of the structure-activity/selectivity relationships. In the present chapter, a detailed description of the experimental procedure and chemicals used for the catalyst preparation, characterization and activity studies are given in detail.

2.1. Prologue

For many years, the development and preparation of heterogeneous catalysts were considered more as alchemy than science, with the prevalence of trial and error experiments. However, this approach is expensive, time-consuming and does not offer guarantee on the final results. But, now-a-days the approach is scientific and involves a wide number of specific competencies of solid state chemistry, analytical chemistry, physical chemistry and spectroscopy. Development of catalysts with unique properties is entirely based on the synthetic strategies followed for the preparation of such materials. The fundamental aspects in the preparation and characterization of solid acid catalysts are discussed elaborately in this chapter.

2.2. Catalyst Preparation

2.2.1. Experimental Methodology

The catalysts were prepared by employing surfactant assisted hydrothermal method where cationic surfactant cetyl trimethyl ammonium bromide was used as a synthetic template, by which nanophases of ceria-zirconia solid solutions were obtained.

2.2.2. Preparation of Ceria-Zirconia Mixed Oxide

Ceria−zirconia mixed oxide was prepared by adopting a surfactant assisted method using cerium nitrate, $Ce(NO_3)_3.6H_2O$ (Spectrochem Pvt. Ltd) and zirconium oxychloride, $ZrOCl_2.8H_2O$ (Loba Chemie). The required amount of precursors were dissolved separately in deionized water and mixed together. It was slowly added to a solution containing cetyl trimethyl ammonium bromide (Sigma Aldrich) (surfactant/cerium nitrate=3.5 molar ratio) under stirring conditions followed by the addition of ammonium hydroxide, NH_4OH, (28%, Qualigens) into the mixture. Upon complete mixing, excess ammonium hydroxide was added dropwise until the precipitation was complete (pH = ~11). The precipitate was then loaded into a stoppered Teflon bottle and heated hydrothermally at 100ºC for 48 hrs. The resulting slurry was filtered off and thoroughly washed with distilled water until free from surfactant and anionic impurities. The mixed hydroxide paste was then allowed to dry at 80°C for 12 hrs. Finally, it was calcined at 500°C for 4 hrs. After cooling, the solid residues were ground using a ceramic mortar and pestle until fine powders were obtained. For comparison purpose, CeO_2−ZrO_2 mixed oxide with different mole ratio, ceria: zirconia 2:1, 1:1, 1:2 (mole ratio based on metal salt) were prepared. The modification with transition metal is done with CZ ratio of 1:1.

2.2.3. Preparation of Metal modified Ceria-Zirconia

The modified ceria-zirconia catalyst was prepared by wet-impregnation of the ceria-zirconia support, calcined at 500°C with required amount of aqueous solution of corresponding metal salt. It was mechanically stirred for 6hrs and then dried at 110°C for 4 hrs. It was powdered and calcined at 400°C to obtain metal modified ceria-zirconia oxide. The metal and its sources used are given in the table 2.1.

Table 2.1 Metals used for modification

Sl. No	Metal	Source
1	Vanadium	Ammonium metavanadate NH_4VO_3, (CDH laboratory reagent)
2	Chromium	Chromium(III) nitrate $[Cr(H_2O)_6](NO_3)_3.3H_2O$, (Loba Chemie)
3	Manganese	Manganese (II) acetate $Mn(CH_3COO)_2$, (Qualigens)
4	Praseodymium	Praseodymium (III) nitrate hexahydrate $(PrNO_3)_3.6H_2O$, (S.D. Fine Chemicals Ltd)

2.2.4. Prepared Catalysts

The catalysts prepared for the present work with its notation are listed in Table 2.2.

Table 2.2 Catalysts Prepared

Catalysts Prepared	Notation
Ceria-Zirconia	C2Z1
	CZ
	C1Z2
Vanadium modified ceria-zirconia (with 4,8,12 weight% of vanadium)	4VCZ
	8VCZ
	12VCZ
Chromium modified ceria-zirconia (with 4,8,12 weight% of chromium)	4CrCZ
	8CrCZ
	12CrCZ
Manganese modified ceria-zirconia (with 4,8,12 weight% of manganese)	4MnCZ
	8MnCZ
	12MnCZ
Praseodymium modified ceria-zirconia(with 4,8,12 weight% of praseodymium)	4PrCZ
	8PrCZ
	12PrCZ

2.3. Characterization Techniques

A complete characterization of the prepared materials requires information from a number of physical, chemical and spectroscopic techniques. Understanding the structural and electronic properties of the catalyst by spectroscopic techniques is one of the major goals in catalysis research because they can provide fundamental information about catalytic structures and also give insight into the relation between physical and chemical properties of the catalyst and its activity. This in turn helps in designing new catalyst or to improve the catalytic performances. The various characterization techniques employed in the present study are Inductively Coupled Plasma-Atomic Emission Spectroscopy (ICP-AES), Powder X-ray diffraction, BET-BJH-surface area & pore size analysis, thermogravimetry/differential thermogravimetry (TG/DTG), Fourier Transform-Infra Red spectroscopy (FTIR), UV-visible diffuse reflectance spectroscopy (UV-vis DRS), Raman spectroscopy (RS), X-ray photoelectron spectroscopy (XPS), scanning electron microscopy (SEM), transmission electron microscopy (TEM), Temperature Programmed Reduction (TPR) and surface acidity measurements like temperature programmed desorption (TPD) and cumene cracking reaction. The brief introduction to the theory and principle of various characterization techniques are briefly described in this section.

2.3.1. Elemental Analysis- Inductively Coupled Plasma-Atomic Emission Spectroscopy (ICP-AES)

Inductively coupled plasma-atomic emission spectrometry (ICP-AES) has been extensively applied for the elemental analysis. ICP-AES is an emission spectrophotometric technique, exploiting the fact that excited

electrons emit energy at a given wavelength as they return to ground state. The fundamental characteristic of this process is that each element emits energy at specific wavelengths peculiar to its chemical character. Although each element emits energy at multiple wavelengths, in the ICP-AES technique it is most common to select a single wavelength for a given element.[1] The intensity of the radiation emitted at the chosen wavelength is proportional to the amount (concentration) of that element in the analyzed sample. Thus, by determining spectra wavelength emitted by a sample and by determining their intensities, the analyst can quantify the elemental composition of the given sample relative to a reference standard. The advantages of ICP-AES are low detection limits, good precision and/or accuracy, wide dynamic ranges of calibration curves, and capability of simultaneous multi element analysis.[2]

ICP systems can analyze about 60 different elements at the same time with a single source (the plasma). Plasma is a cloud of highly ionized gas, composed of ions, electrons and neutral particles. The gas is usually Argon which is ionized by the influence of a strong electrical field either by a direct current or by radio frequency. In plasma-based systems the temperature is considerably hotter (~6000 to 10000 K) which results in more effective excitation of atoms.[3] Atoms are excited (ionized) by the intense heat of the plasma and the emission of a photon occurs via resonance fluorescence.

An ICP-AES system can be divided into two basic parts; the inductively coupled plasma source and the atomic emission spectrometry detector. The predominate form of sample matrix in ICP-AES today is a liquid sample: acidified water or solids digested into aqueous forms.

ICP-AES were done on Thermo electron IRIS INTERPID II XSP DUO model. Solution of ceria-zirconia catalysts were prepared by digesting the solid in a solution of HF. The solution is then made up to 100ml in a standard flask using 5% HNO_3. Then the sample is introduced by solution nebulization. Nebulization converts the sample into rapid atomization form.[4]

2.3.2. X-Ray Diffraction (XRD)

XRD is one of the oldest and most frequently exploited techniques in catalyst characterization. It helps determining the crystallinity, phase purity, crystal structure and crystallite sizes of catalyst materials.[5] Although it has become a standard mandatory technique for solids in the identification of crystalline phases, yet it is extensively used for the determination of unit cell parameters, analysis of structural imperfections, crystallite size determination and recently in the refinement of the structures.

The theory behind XRD involves the interaction between the incident monochromatized X-rays (like Cu Kα or Mo Kα source) with the atoms of a periodic lattice. X-rays scattered by atoms in an ordered lattice interfere constructively in directions given by Bragg's equation.

$$n\lambda = 2d \sin\theta,$$

where λ is the wavelength of the X-rays, d is the distance between two lattice planes, θ is the angle between the incoming X-rays and the normal to the reflecting lattice plane and n is an integer known as the order of reflection. X-ray diffraction system consists of an X-ray source, a goniometer, sample holder, detector and computer for instrument control and data analysis.[6] X-ray tubes generate X-rays by bombarding a metal target with high energy (10-100 keV) electrons that knock out core

electrons. An electron in an outer shell fills the hole in the inner shell and emits X-ray photons. Two common targets are Mo and Cu, which have Kα X-ray emissions at 0.71073 Å and 1.5418 Å, respectively.

The most important use of diffraction data is for phase identification. Each crystalline powder gives a unique diffraction pattern, which is the basis for a qualitative analysis by X-ray diffraction. The diffraction pattern of a particular phase is characteristic and it helps to determine phase purity and degree of crystallinity. Interpretation of the XRD data is accompanied by the systematic comparison of the obtained spectrum with a standard one, taken from any X-ray powder data file catalogues, published by the American society for testing materials (JCPDS). The smallest diffracting domain in any specimen is called a crystallite. Crystallites up to several hundred nanometers have broadened peak profiles resulting from incomplete destructive interference at angles near the Bragg angle. From this broadening, crystallite size can be determined by a single line analysis known as Scherrer method.

Debye-Scherrer equation is

$$D = k\lambda/\beta \, Cos\theta$$

where D is the crystallite size, k is the Scherrer constant (= 0.9 assuming that the particles are spherical), λ is the wavelength, β is the line width (obtained after correction for the instrumental broadening) and θ is the diffraction peak angle. Unit cell parameter (a_o) of cubic lattice can be calculated from,

$$a_0 = d\,(h^2 + k^2 + l^2)^{1/2}.$$

For mesoporous materials reflections are observed in X-ray powder patterns at low 2θ angles ($0.5<2\theta< 10^0$). These reflexes are due to the long-range order induced by the very regular arrangement of the pores. Generally the d-spacing of the mesopores are rather big so the X-ray diffraction at low angles is observed.

Powder XRD of the prepared samples were taken on a Bruker AXS D8 advance model with Ni filtered Cu Kα radiation (λ-1.5406 Å) within the 2θ range 5-80 ^{0} at a speed of 2^0/min. Low angle XRD measurements of the samples were taken on a Panalytical Xpert PRO MPD model with Ni filtered Cu Kα radiation (λ=1.5406 Å) within the 2θ range 0.1-5° at a speed of 0.25°/min at room temperature.

2.3.3. Adsorption Measurements

Gas adsorption is a prominent method to obtain a comprehensive characterization of porous material with respect to the specific surface area, pore size distribution and porosity. Nitrogen adsorption is the most commonly used one.[7] The amount of adsorbed nitrogen is measured as a function of the applied pressure, giving rise to the adsorption isotherm.

2.3.3.1. Specific Surface Area: BET Method

The Brunauer-Emmett-Teller (BET) method is the most acceptable procedure for measuring surface areas of various materials by physical adsorption of gases at their boiling temperatures.[8] In principle the amount of adsorbate (nitrogen) required to form a monolayer of molecules over the surface of catalyst is given by the following BET equation,

$$P/Va(P_0-P) = 1/VmC + C-1/VmC\ P/P_0$$

where

P is the pressure

P_0 is the saturation vapour pressure,

Va is the amount of gas adsorbed at the relative pressure P/P_0

Vm is the monolayer capacity

C is the BET constant

A plot of P/Va (P_0-P) versus relative pressure of P/P_0 is a straight line with a slope of (C–1)/(VmC) and intercept of 1/(VmC), respectively. Vm is calculated from slope and intercept. Subsequently the specific surface area of the sample can be determined by the following equation.

$$Specific\ surface\ area\ (m^2 g^{-1}) = \frac{v_m \times N_A \times A_M}{W \times V_0}$$

where,

N_A is the Avagadro constant (6.023 X 10^{23} molecules mol^{-1})

A_M is cross sectional area of adsorbate molecule, (For N_2, A_M=0.162 nm^2 at 77 K)

W is the weight of the sample

V_0 is 22414 mL mol^{-1}

An adsorption isotherm is obtained by measuring the amount of gas adsorbed across a wide range of relative pressures at a constant temperature (typically liquid N_2, 77K). Conversely desorption isotherms are achieved by measuring gas removed as pressure is reduced. The shape of the isotherm depends on the porous texture of the measured solid.[9] The isotherms may be grouped into six types.

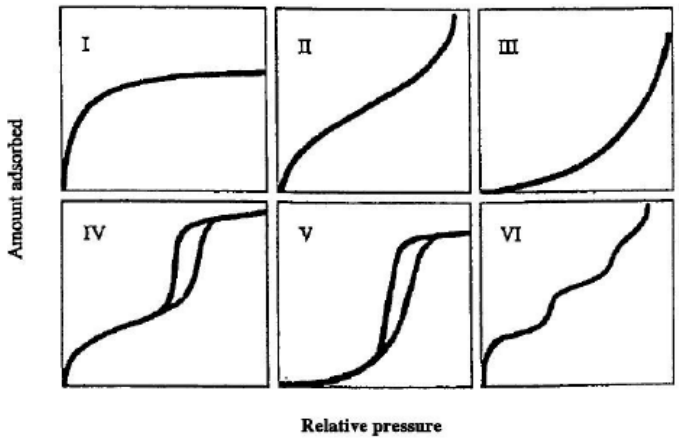

Fig. 2.1: Type of adsorption isotherms

Type I adsorption isotherm corresponds to microporous solids. Type II and III give adsorption isotherms of macroporous absorbents with strong and weak affinities respectively. Types IV and V characterize mesoporous adsorbents with strong and weak affinities, respectively. For lower temperatures they show adsorption hysteresis. Type VI corresponds to stepwise adsorption at very weak adsorbate-solid interactions. Hysteresis loop, which is associated with capillary condensation taking place in mesopores. IUPAC classified the various hysteresis loops that are observed experimentally as types H1, H2, H3 and H4 as shown in Fig. 2.2 and their interpretation is given as H1- typical for type IV isotherms, H2- characteristic for "ink-bottle" pores, H3 and H4- slit pores.

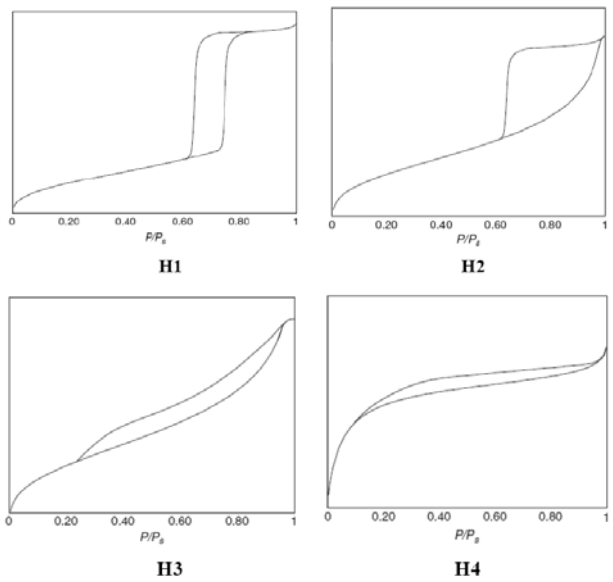

Fig. 2.2: IUPAC classification of hysteresis loops

2.3.3.2. Pore volumes and Pore size distribution

Several computational procedures are available for the derivation of pore size distribution of mesoporous samples from physisorption isotherms. Most popular among them is the Barrett-Joyner-Halenda (BJH) model.[10] First, the volumes desorbed from the sample at different partial pressures are converted to liquid volumes (multiplying by 0.00156). The next step is to use the Kelvin equation to calculate the value of the volume of the liquid in the capillary. The Kelvin equation shows that the smaller the pore radius, the lower the vapour pressure, P, in the pore

$$P/P_0 = \exp(-2\upsilon\gamma/ r_k RT) \qquad (2.3)$$

Pore volume is a property that has been utilized extensively in characterizing a molecular sieve material due to its ability to adsorb selected molecules. It is always determined using several probe molecules such as n-hexane, water, nitrogen, etc. These probe molecules of various

sizes also have been used to gain information on the size of the pore openings, using gravimetric adsorption methods.

In the present investigation, simultaneous determination of surface area, pore size distribution and total pore volume of the samples were achieved in a *Micromeritics Tristar 3000* surface area and porosity analyzer. Prior to the analysis the samples were degassed at 90°C for half an hour and then at 200°C for overnight.

2.3.4. Thermal Analysis

Thermal methods are based upon the measurement of the dynamic relationship between temperature and some property of a system such as mass, heat of reaction or volume. In a thermo gravimetric analysis, the mass of sample is recorded continuously as its temperature is increased linearly at a predetermined rate from ambient to a high temperature.[6] TG records the loss in weight as a function of temperature or transitions that involve dehydration or decomposition. The changes in weight results from physical and chemical bonds forming and breaking at elevated temperatures. These processes may evolve volatile products or form reaction products that result in a change in weight of the sample. The apparatus needed for thermogravimetric analysis includes: a sensitive analytical balance, a furnace, a furnace temperature controller and a recorder that provides a plot of sample mass as a function of temperature. Samples are placed in a crucible that is positioned in the furnace on a quartz beam attached to an automatic recording balance. DTG curve is the derivative of the thermogram. Many modern instruments are equipped with electronic circuitry to provide such a curve as well as the thermogram itself. The derivative curve may reveal information that is not detectable in the ordinary thermogram. In catalysis, these techniques are used to study the

genesis of catalytic materials *via* solid-state reactions where α-alumina is used as a reference material.

Thermal analyses of the synthesized samples were carried out on Perkin Elmer TGA (Delta series TGA 7) with a steady heating rate of 20°C /min. The samples were heated from ambient temperature to 800°C in nitrogen atmosphere.

2.3.5. Fourier Transform-Infrared (FT-IR) Spectroscopy

Fourier transform infrared (FT-IR) spectroscopy deals with the vibration of chemical bonds in a molecule at various frequencies depending on the elements and types of bonds. The absorption frequencies represent excitations of vibrations of the chemical bonds and thus are specific to the type of bond and the group of atoms involved in the vibration. The energy corresponding to these frequencies correspond to the infrared region (4000-400 cm^{-1}) of the electromagnetic spectrum. In a FTIR instrument, the polychromatic source is modulated into an interferogram that contains the entire frequency region of the source and hence all frequencies are measured simultaneously. In Fourier transform, IR signal is digitalized to obtain the numerical data. The infrared spectrum can be divided into two regions: one called the functional group region and the other finger print region. The functional group region is generally considered to range from 4000 to 1400 cm^{-1}. The "fingerprint region" of an IR spectrum falls in the 600 cm^{-1} to 1400 cm^{-1} range. This region is where most of the bending vibrations (and some stretching vibrations) occur. Though this region is not useful to obtain structural information, it is still characteristic for a given molecule.

IR spectroscopy has been used to study powdered heterogeneous catalysts since the 1960's.[1] Informations on some of the peculiarities of the surface such as the presence of surface hydroxyl groups can be obtained. The hydroxyl groups on the surface of oxide supports are extremely important in catalyst preparation because they provide sites where catalyst precursors may anchor to the support. One drawback of IR is that almost all compounds absorb IR radiation so that the spectra of reaction mixtures can be very complex, which cause difficulty in straightforward interpretation and assignments. However, data manipulation and processing techniques like deconvolution, spectral subtraction are helpful in extracting the desired informations.[14]

The Infrared induced vibrations of the samples were recorded using *Thermo NICOLET 380 FTIR* Spectrometer by means of KBr pellet procedure. Spectra were measured in the transmission mode and the samples were evacuated before making the pellet and the spectra were taken under atmospheric pressure and room temperature. The changes in the absorption bands were investigated in the 400-4000 cm^{-1}.

2.3.6. UV-VIS Diffuse Reflectance Spectroscopy (UV-Vis-DRS)

Diffuse reflectance spectroscopy (DRS) is a technique based on the reflection of light in the ultraviolet (UV), visible (Vis) and near-infrared (NIR) region by a powdered sample. In a DRS spectrum, the ratio of the light scattered from an '*infinitely thick*' closely packed catalyst layer and the scattered light from an infinitely thick layer of an ideal non-absorbing (white) reference sample is measured as a function of the wavelength, λ. It is a non-invasive technique that uses the interaction of light absorption and scattering to produce a characteristic reflectance spectrum, providing information about the structure and composition of the medium. It gives

information regarding electronic transition between orbitals or bands in the case of atoms, ions and molecules in gaseous, liquid or solid state.

One of the advantages of DRS is that the obtained information is directly chemical in nature since outer shell electrons of the transition metal ions are probed. This further provides information about the oxidation state and coordination environment of transition metal ions in the solid matrices. Thus DRS is a sensitive technique to examine the type of the metal sites, *viz.,* framework or extra-framework, in which that metal ion or cluster exists.[18] The disadvantage of DRS is that the signals are usually broad and overlap with each other, leading to a biased spectral analysis. In addition, the origin of the specific electronic transition is sometimes difficult to isolate due to its dependence on the local coordination environment, the polymerization degree and the specific oxidation state.

Diffuse reflectance UV-VIS spectra of the samples were recorded in the range 200-800nm using a conventional spectrophotometer (Labomed UV-VIS Double Beam UVD-500) with an integrating sphere assembly using $BaSO_4$ as reference standard with a CCD detector.

2.3.7. Raman Spectroscopy

Raman spectroscopy (RS) is based on the inelastic scattering of photons, which loose energy by exciting vibrations in the sample. For Raman scattering to occur, the polarizability of the molecule must vary with its orientation. Raman spectroscopy is useful for analysing molecules without a permanent dipole moment which would not show up in IR spectrum. Raman spectroscopy is widely used for the investigation of oxides, supported and bulk metals, supported oxides and has found steadily increasing application in the characterization of supported transition metal

oxide catalysts.[11] All characteristic vibrational features of oxides of the transition metals like V, Cr, Mo and W fall in the frequency range below 1100 cm^{-1} and these oxides have high Raman scattering cross-sections because of their relatively high covalent bond character. Various studies have demonstrated that the simultaneous use of reference compounds and the correlation between Raman frequency and bond length makes this spectroscopy very well suited to study the molecular structures of supported metal oxides. A disadvantage of this technique is the small cross sections for Raman scattering, that most of the scattered intensity goes into the Rayleigh band, which is typically about three orders of magnitude greater than the Stokes bands.

In contrast to XRD, which allows determining just cation sublattice symmetry, the Raman spectra provide information about oxygen anions position and reflect the oxygen lattice vibrations, being sensitive to crystalline symmetry.[12] Since the information provided by IR spectroscopy is less relevant due to its lower sensitivity (broadening of the peaks and LO–TO splitting) to unit cell distortions, Raman spectroscopy was applied to determine the coordination symmetry of cations in the mixed CeO_2–ZrO_2 oxides.[13]

Raman spectra were recorded on Horiba Jobin Ivan Lab Ram HR system at a spatial resolution of 2 mm in a backscattering configuration. The 514.5 nm line of Argon ion laser was used for excitation.

2.3.8. X-ray Photoelectron Spectroscopy (XPS)

X-ray photoelectron spectroscopy (XPS) is a well-known surface technique, also known as Electron Spectroscopy for Chemical Analysis (ESCA). XPS is a widely used technique for obtaining chemical information of various material surfaces. XPS is based on the photoelectric

effect. An atom absorbs a photon of energy hυ, a core or valence electron with binding energy E_b is ejected with kinetic energy, E_k.[14]

$$E_k = h\nu - E_b - \varphi s$$

where,

Ek is the kinetic energy of the photoelectron

hυ is the energy of photon

Eb is the binding energy of atomic orbital from which the electron originates

φs is the spectrometer work function

The low kinetic energy (0 ≤ 1500 eV) of emitted photoelectrons limit the depth from which it can emerge, so that XPS is a very surface-sensitive technique and the sample depth is in the range of few nanometers. Photoelectrons are collected and analyzed by the instrument to produce a spectrum of emission intensity versus electron binding (or kinetic) energy. The binding energies of the photoelectrons are characteristic of the element from which they are emitted, so that the spectra can be used for surface elemental analysis. Small shifts in the elemental binding energies provide information about the chemical state of the elements on the surface. The peak area can be used to find out the surface compositions of the material.

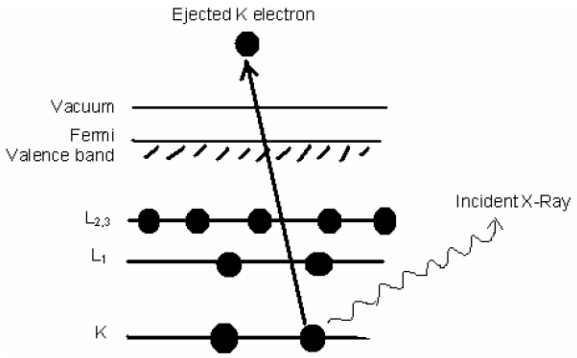

Fig. 2.3: Schematic diagram of the XPS process, showing photo ionization of an atom by the ejection of a 1s electron.

The process of photoemission is shown schematically in Fig. 2.3, where an electron from the K shell is ejected from the atom (1*s* photoelectron). Once a photoelectron has been emitted, the ionized atom must relax in some way. This can be achieved by the emission of an X-ray photon, known as X-ray fluorescence. The other possibility is the ejection of an Auger electron through a secondary process. XPS is one of the most frequently used techniques in catalysis. It yields information on the elemental composition, the oxidation state of the elements and in favorable cases, on the dispersion of one phase over another.

XPS spectra were recorded in an electron spectrometer equipped with Thermo VG Clamp -2 Analyzer and a Mg Kα X-ray source (1253.6 ev, 30 mA x 8 kV). A thin sample wafer of 12 mm in diameter was used for measurements.

2.3.9. Scanning Electron Microscopy (SEM)

Scanning Electron Microscopy (SEM) is one of the most widely used techniques for characterization of size and morphology of the catalysts which provides topographical information like optical microscopes do. SEM is carried out by passing a narrow electron beam over the surface and detecting the yield of either secondary or backscattered electrons as a function of the position of the primary beam. Contrast is caused by the orientation: parts of the surface facing the detector appear brighter than parts of the surface with their surface normal pointing away from the detector. The secondary electrons have mostly low energies and originate from the surface region of the sample. Backscattered electrons come from deeper and carry information on the composition of the sample. The interaction between the beam and the sample produces different types of

signals providing detailed information about the surface structure and morphology of the sample.[14]

In SEM analysis finely powdered sample was applied on to a double sided carbon tape placed on a metal stub. The stub was then inverted in such a manner that the free side of the carbon tapes generally picked up a small amount of the sample, thereby creating a thin coating. It was then sputtered with a thin layer of gold to obtain better contrast and provide improved cohesion.[15] Beam of electrons is focused on a spot volume of the specimen, resulting in the transfer of energy to the spot. The secondary electrons, produced, are attracted and collected by a positively biased grid or detector and then translated in to a signal. Scanning microscopy allows for producing high-resolution images of a sample surface, revealing details about 1 to 5 nm in size. Due to its position aside of the lens, SEM micrographs yield a characteristic three-dimensional appearance useful for understanding the surface structure of a sample. SEM permits a direct examination of the surfaces of complex catalyst systems. Using this technique, the effect of processing conditions on surface morphology can conveniently be studied and predictions on the performance of a catalyst can be made.[16]

The scanning electron micrographs of the samples were taken using JEOL Model JSM-6390LV scanning electron microscope with a resolution of 1.38eV. The powdered samples were dusted on a double sided carbon tape, placed on a metal stub and was coated with a layer of gold to minimize charge effects.

2.3.10. Transmission Electron Microscopy (TEM)

Transmission Electron Microscopy (TEM) is typically used for high resolution imaging of thin films of a solid sample for nanostructural and

compositional analysis. The technique involves: (i) irradiation of a very thin sample by a high energy electron beam, which is diffracted by the lattice of a crystalline or semicrystalline material and propagated along different directions, (ii) imaging and angular distribution analysis of the forward-scattered electron (unlike SEM where backscattered electrons are detected) and (iii) energy analysis of the emitted X-rays.

TEM uses transmitted and diffracted electrons. A primary electron beam of high energy and high intensity passes through a condenser to produce parallel rays which impinge on the sample. Transmitted electrons form a two-dimensional projection of the sample mass which is magnified by the electron optics to produce bright field image. The dark field image is obtained from the diffracted electron beam which is slightly off angle from the transmitted beam. TEM uses high energy electrons (100-200keV). The images can be resolved over a fluorescent screen or a photographic film. Image is a two dimensional projection of the sample.

TEM provides real space image on the atomic distribution in the bulk and surface of a nanocrystal.[17] TEM is commonly applied for studying supported catalysts. Detection of supported particles is possible provided that there is sufficient contrast between particles and support. This may impede applications of TEM on well dispersed supported oxides.

TEM analyses were performed on a CM200 (Philips) with operating voltage 20-200kV providing a resolution of 2.4 Å.

2.3.11. Temperature Programmed Reduction (TPR)

Temperature Programmed Reduction methods typically involve monitoring surface or (bulk) processes between the solid catalyst and its gaseous environment *via.,* continuous analysis of the gas phase composition as the

temperature is raised linearly with time. The procedure for temperature-programmed analysis is as follows: A simple container (U-tube), filled with a solid or catalyst, is positioned in a furnace with temperature control equipment. A thermocouple is placed in the solid for temperature measurement. Container is filled with an inert gas. A thermal conductivity detector is used to measure the concerned active gas before and after the reaction. TPR determines the number of reducible species present in the catalyst and reveals the temperature at which the reduction occurs. An important aspect of TPR analyses is that the sample need not have any special characteristics other than containing reducible metals. It is used for determining the effect of catalyst precursors and also the type of interaction between the active precursor and the support.[19]

TPR profiles of the calcined samples were obtained on micromeritics TPR apparatus which was interfaced with a computer. Sample placed in a U-shaped quartz tube was first purged in a He flow for 1h and then cooled to ambient temperature. The TPR profiles were recorded on the degassed sample by passing a 10% H_2/Ar gas mixture in which the sample was heated at a constant rate of 10°C/min from room temperature to 800°C.

2.3.12. Acidity Determination

The acidic or basic properties of solid surfaces are interesting aspects of surface structure. Understanding the acidic nature of solid surface is of great importance in the field of catalysis. The nature of active sites as well as its number and strength have decisive role in determining the conversion and selectivity of acid catalyzed reactions. So the determination of the number, nature and strength of the acid sites are necessary to understand the catalytic activity and selectivity. Two distinct types of surface acidity have been identified in the literature,[20] (a) Lewis acidity and (b) Brönsted acidity. If the active metal sites are capable of accepting a lone pair of electrons from the

substrate molecules and activate them for further reaction, such acidic sites are said to be Lewis acidic sites. Brönsted acidity is attributed to the acidic protons on surface hydroxyl groups.

2.3.12.1. Temperature Programmed Desorption (TPD-NH_3)

Acidity of solid catalysts can be investigated by different methods like Temperature Programmed Desorption (TPD), infrared (IR) spectroscopy techniques and calorimetric measurements of the heat of adsorption of base molecules. Temperature programmed desorption can provide a measure of the number density of each type of site by the intensity of the desorption features and the strength of the sites based on the desorption temperatures of the probe molecule. The TPD method is simple, rapid, reproducible and can provide a quantitative determination of the activation energies of desorption. [21]

In TPD technique, basic, volatile, probe molecules such as NH_3, pyridine, quinoline or n-butylamine are initially allowed to adsorb on an activated solid catalyst at a defined temperature. The adsorbed molecules are then allowed to desorb in a flow of N_2 or Ar by heating the catalyst material in a programmed manner. The amount of gas desorbed from the catalyst is estimated by a TCD close to the reactor outlet. Based on the amount of base molecules desorbed, the total acidity and the relative strength of the acid sites can be determined. Ammonia is commonly used because of its size, stability and strong basic strength. At first, ammonia is adsorbed on the sample. Then the temperature is raised at a constant rate and the amount desorbed at different temperatures is recorded. In a TPD spectrum, one or more peaks may be observed; the peaks at low temperatures corresponding to NH_3 desorbing from the weaker acidic sites and the ones at higher temperatures corresponding to the stronger acidic sites. The areas under these peaks give information about the amount of

acidic sites of different acidity, whereas the peak temperatures give information about the relative acid strengths.

TPD analysis was carried out as follows: Catalyst was charged into the quartz reactor of the conventional TPD apparatus. It was first degassed in a He flow for 1h and then cooled to room temperature. Ammonia was then purged into the reactor at room temperature for half an hour until the acid sites were saturated with NH_3. Physisorbed NH_3 was removed by evacuating the catalyst sample at 50°C for 1 h under the flow of helium. Furnace temperature was increased from room temperature to 800°C at a heating rate of 10°C/min. Desorbed ammonia was detected using TCD detector.

2.3.12.2. Cumene Cracking Reaction

The catalytic activity of solid acid catalysts is not only correlated with the surface concentration of acid sites, but also with their nature (Lewis or Brönsted sites). Cracking of cumene (isopropylbenzene) is a model reaction used for a long time to test acid catalysts. This molecule has a very simple cracking scheme due to the fact that the benzene ring is not attacked easily. Therefore, this reaction can be used to differentiate between Lewis and Brönsted acid sites. The major reactions taking place during the cracking of cumene are dehydrogenation to give α-methyl styrene over Lewis acid sites and dealkylation to give benzene, ethylbenzene and propene over Brönsted acid sites.[22] Therefore, the ratio of Lewis to Brönsted acid sites can be calculated by the comparison of the amount of α-methyl styrene to benzene.

The vapour phase cumene conversion reaction was carried out at atmospheric pressure in a fixed bed down-flow glass reactor at a temperature of 400°C. The previously activated catalyst was packed between silica beads in the reactor with glass wool. The liquid reactant was fed into the reactor with the help of a syringe pump at a flow rate of 4ml/h. The products were analyzed by Chemito GC 1000 gas chromatograph with FID detector using BP-1 capillary column. Analysis conditions are specified in Table 2.6.

2.4. Catalytic Activity Studies

The liquid phase reactions studied are given below

2.4.1. Transesterification of Diethyl Malonate

Transesterification reactions were performed in a round bottom flask fitted with a water-cooled condenser. The flask was immersed in an oil bath in order to make the working temperature constant, which was connected with a condenser. In a typical run, a mixture of diethyl malonate (Spectrochem Pvt. Ltd) and *n*-butanol (Merck), in a definite molar ratio, was added to the flask containing the catalyst. The reaction was monitored periodically by withdrawing samples at regular intervals and analyzed on a gas chromatograph Chemito GC 1000. Analysis condition is given in Table 2.3. The products were further confirmed by GC–MS (GCMS, Shimadzu, QP 2010). The products of the reaction mixture were quantified using the authentic samples by considering the relative area of the peak.

2.4.2. Side-chain Oxidation of Ethylbenzene

The reaction was performed in the liquid-phase in a 50 ml two-necked round bottom flask equipped with a magnetic stirrer, thermometer and a reflux condenser. The temperature was maintained using an oil bath.

Initially, desired amount of catalyst was charged into the dried RB flask. Acetonitrile (Ranbaxy Fine Chemical) was added to the flask followed by ethylbenzene (Spectrochem Pvt. Ltd) and stirred for 10 min. Finally, oxidant TBHP (Sigma Aldrich, 70 wt %) was added dropwise to the above reaction mixture. The progress of the reaction was monitored by withdrawing aliquots of the reaction mixture and analyzing the same in a gas chromatograph Chemito GC 1000 equipped with a capillary column BP-1 attached to a FID detector, operated with a heating program described in Table 2.3. Conversion rate and selectivity were calculated based on the relative area of authentic samples with standard ones.

2.4.3. Direct Hydroxylation of Benzene to Phenol

The oxidation reaction was carried out in a 50mL double neck round bottom flask connected with a reflux condenser and kept in an oil bath which is mounted on a magnetic stirrer. In a typical reaction, the catalyst powder was suspended in a mixture of acetonitrile (Ranbaxy Fine Chemical) and benzene (Qualigens) and stirred for 10 min. Then H_2O_2 (30%, S.D. Fine Chem. Ltd.) was added dropwise to the system with stirring. The top of the refluxing condenser was closed by a standard size cork. After separation of catalyst, the liquid portion was analysed at regular intervals through Chemito 8610 GC with an FID detector and an OV-17 packed column.

2.4.4. Soot Oxidation

Soot oxidation tests were performed in a Thermogravimetric analyzer (TGA7 Perkin Elmer). Carbon black (ISAF grade) was used as model soot whose physico-chemical characterisation is reported in chapter 7. The activity studies have been performed using air as the source of

oxygen. Since the physical contact between soot and the catalyst was found to have a great impact on soot oxidation rates, we carefully paid attention to the mixture of these two compounds. This will be discussed in chapter 7 in detail. For *tight contact* experiments, each catalyst was accurately mixed with soot in an agate mortar in order to achieve a tight contact. For *loose contact* experiment, soot and catalyst were mixed with a spatula. During the TG measurements, around 7 mg of mixture was heated at a constant rate (20°C /min) from room temperature to 850°C, while the gas flow was kept fixed at 400 ml/min. For evaluating activity we used the light-off temperature, $T_{50,}$ temperature at which 50% of soot is converted.[23]

Analysis conditions of various reactions using gas chromatography are presented in Table 2.3.

Table 2.3. Analysis conditions of various reactions

Reaction	GC	Analysis Condition		
		Temperature(°C)		Temperature Programme
		Injector	Detector	
Cumene cracking	GC1000, BP-1 Capillary column, FID detector	230	230	70°C-2min-10°C/min-250°C-2min
Transesterification of diethyl malonate	GC1000, BP-1 Capillary column, FID detector	250	250	55°C-0.2min-20°C/min-120°C-0.1min-25°C/min-250°C-1min
Ethylbenzene oxidation	GC1000, BP-1 Capillary column, FID detector	250	250	60°C-2min-10°C/min-125°C-2min-2°C/min-140°C-1min-15°C/min-200°C -1min
Benzene hydroxylation	GC 8610, OV-17 Packed column, FID detector	250	250	60°C-2min-4°C/min-80°C-0.5min-10°C/min-150°C-1min-15°C/min -250°C -1min

References

[1] http://www-odp.tamu.edu/publications/tnotes/tn29/technot2.htm

[2] K. Yoshida, H. Haraguchi, Anal. Chem. 56 (1984) 2580.

[3] Dunnivant, Ginsbach, Flame Atomic Absorbance and Emission Spectroscopy and Inductively Coupled Spectrometry-Mass Spectrometry Whitman College 9 (2009)

[4] A. Montaser, Inductively Coupled Plasma Mass Spectroscopy,

[5] W. H. Bragg, W. L. Bragg, The Crystalline State, McMillan, New York 1 (1949).

[6] S. Mahinder, A textbook of Analytical Chemistry Instrumental Techniques, Dominant Publishers and distributors, New Delhi (2005).

[7] S.J. Gregg, K.S.W. Sing, Adsorption, Surface Area and Porosity, Academic Press, London (1982).

[8] S. Brunauer, P.H. Emmett, E. Teller, J. Am. Chem. Soc, 60 (1938) 309.

[9] K.S.W. Sing, D.H. Everett, R.A.W. Haul, L. Moscou, R.A. Pierotti, J. Rouquerol, T. Siemieniewska, Pure Appl. Chem. 57 (1985) 603.

[10] E.P. Barret, L.G. Joyner, P.H. Halenda, J. Amer. Chem. Soc. 73 (1951) 373

[11] P.L. Villa, F. Trifiro, I. Pasquon, React. Kinet. Catal. Lett. 1 (1974) 341.

[12] A. Atribak, Bueno-Lopez, A. Garcia-Garcia, Journal of Molecular Catalysis A: Chemical 300 (2009) 103.

[13] S. Damyanova, B. Pawelec, K. Arishtirova, M.V.M. Huerta, J.L.G. Fierro, Applied Catalysis A: General 337 (2008) 86.

[14] J.W. Niemantsverdriet, Spectroscopy in catalysis-An introduction, Wiley-VCH Verlag GmbH,D-69469, Weinheim(Federal Republic of Germany), 2000

[15] E. Wachs, Characterization of Catalytic Materials, Butterworth Heinemann: Manning (1992).

[16] A.M. Reimschussel, R.J. Fredericks, Journal of material science 4 (1969) 885.

[17] Z.L. Wang, Characterization of Nanophase Materials, Ed.in: Wiley-VCH, Weinheim (2000) 37.

[18] B.M. Weckhuysen, I.P. Vannijvel, R.A. Schoonheydt, Zeolites 15 (1995) 482.

[19] D.K. Chakrabarty, B. Viswanathan, Heterogeneous catalysis, New age International (P) limited, Publishers, New Delhi.

[20] K. Tanabe, Solid Acids and Bases, Academic Press, New York (1970).

[21] P. Berteau, B. Delmon, Catal. Today, 5 (1989) 121.

[22] P. Fincy, S. Sugunan, Reac Kinet Mech Cat. 103 (2011) 125.

[23] E. Aneggi, C.D. Leitenburg, G. Dolcetti, A. Trovarelli, Catalysis Today 114 (2006) 40.

Chapter 3

PHYSICO-CHEMICAL CHARACTERIZATION

Contents

The characterization tools used to study heterogeneous catalysts including atomic-level techniques not only reveals the surface structure and properties but also offer numerous advantages as alternative investigative procedures providing useful insights into the physics and chemistry of surfaces. This chapter demonstrates the results and discussion pertaining to the structural characteristics of modified and un-modified ceria-zirconia mixed oxide systems by various spectroscopic and non-spectroscopic techniques.

3.1. Prologue

Although catalysis by solids is a surface phenomenon, bulk properties of oxides require considerable attention, if one has to understand the chemistry of heterogeneous catalysis. Bulk properties govern several important aspects of surface reactions, including the nature and distribution of defects, and the stabilization of surface structures. Applying the tools of surface science to the study of well-defined model catalysts has emerged and matured over the past two decades. The characterization techniques, especially atomic-level techniques of surface science, can be used to study heterogeneous catalysts, providing useful insights into the physics and chemistry of catalyst surfaces. This chapter illustrates the results of various characterization techniques and their detailed discussions. An extensive characterization of the prepared catalysts was carried out and presented here.

3.2. Physico-Chemical Characterization

The structural characterization has been investigated using Inductively Coupled Plasma-Atomic Emission Spectroscopy (ICP-AES) Analysis, Powder X-ray diffraction (XRD), BET-BJH-surface area & pore

size analysis, Thermogravimetry/differential thermo gravimetry (TG/DTG), Fourier Transform-Infra Red spectroscopy (FTIR), UV-visible diffuse reflectance spectroscopy (UV-vis DRS), Raman spectroscopy (RS), X-ray photoelectron spectroscopy (XPS), scanning electron microscopy (SEM), transmission electron microscopy (TEM), Temperature Programmed Reduction (TPR) and surface acidity measurements like temperature programmed desorption (TPD) and cumene cracking reaction.

3.2.1. Elemental Analysis–ICP-AES Analysis

In order to investigate the presence of various elements in as-prepared samples, ICP-AES analysis was carried out for all the prepared catalysts. The data shown in the Table 3.1 give the amount of Ce, Zr and the different metals present in each sample. It is observed that the experimental atom percentage is quite closer to the theoretical values. The results show that the method of preparation adopted is effective for the preparation of metal modified ceria zirconia catalysts with required composition.

Table 3.1. Elemental composition of prepared catalysts

Catalysts	Composition (atom %)					
	Theoretical			Experimental		
	Ce	Zr	Metal	Ce	Zr	Metal
C2Z1	56.6	43.4	--	64.1	35.9	--
CZ	39.5	60.5	--	43.4	56.6	--
C1Z2	24.6	75.4	--	34.7	65.3	--
4VCZ	36.3	55.5	8.2	38.8	55.3	5.9
8VCZ	33.1	51.3	15.8	30.0	54.4	15.6
12VCZ	30.4	46.8	22.8	33.6	44.2	22.2
4CrCZ	36.2	55.7	8.1	38.7	55.3	6.0
8CrCZ	33.2	51.3	15.5	35.0	57.7	7.3
12CrCZ	30.5	46.9	22.6	33.1	43.2	23.7
4MnCZ	36.5	55.8	7.7	30.0	58.2	11.8
8MnCZ	33.7	51.5	14.8	32.8	60.5	6.7
12MnCZ	30.9	47.6	21.5	33.0	47.5	19.5
4PrCZ	38.1	58.7	3.2	36.3	59.5	4.2
8PrCZ	36.9	56.8	6.3	33.2	59.4	7.4
12PrCZ	35.7	54.7	9.6	30.5	60.0	9.5

3.2.2. X-Ray Diffraction Analysis

3.2.2.1. Wide Angle XRD Analysis

Powder X-ray diffraction analysis is used to explore the structural properties of the material. The prepared materials show XRD pattern (Fig.3.1) corresponding to the cubic fluorite structure.[1] No XRD patterns pertaining to ZrO_2 is observed. This indicates that cerium and zirconium ions are uniformly distributed in the structure to form a homogeneous solid solution thereby stabilizing fluorite structure by zirconia substitution.[2]

It was reported that when ZrO_2 concentration exceeds 95%, the equilibrium is 100% monoclinic phase and at high ceria concentration ($Ce_{1-x}Zr_xO_{2-y}$ with x<20%), the stable phase is the cubic fluorite structure.[2] For the other composition (20%<x<95%), there are two tetragonal phases, *t*' and *t*". The important point is that the *t*"phase and the cubic phase '*c*' give identical X-ray diffraction (XRD) patterns. Therefore it is practically impossible to separate the *t*" phase from the cubic phase by XRD alone since the cations in the *t*" phase have the same positions as those in the cubic phase. This might definitely be the case for the present $Ce_xZr_{1-x}O_2$ mixed oxides, given that the widths of the diffraction peaks made it impossible to distinguish between cubic and tetragonal phases.[3] Therefore, other techniques, particularly Raman spectral analysis, can be used as a complementary study.

Moreover, a careful examination of the patterns shows that the shift in position of peaks occurs with variation in the zirconium content. The characteristic peak of pure ceria is seen at 2θ value of 28.5°, 33.0°, 47.5°, 56.5° corresponding to the planes (111), (200), (220) and (311) respectively with space group Fm3m (JCPDS database (75-0162)). We have correlated

2θ values corresponding to various planes with various compositions of ceria-zirconia mixed oxides (Fig.3.1. (b)). 2θ values of pure ceria are shifted to higher values as the Zr content increases in agreement with the literature reports.[2] Shift of peaks towards higher 2θ values is due to the small ionic radius of Zr^{4+} (0.84 Å) in comparison with that of Ce^{4+} (0.97 Å).

Unit cell parameter is calculated from the d-spacing value using the formula, [4]

$$a_0 = d_{111} (h^2+k^2+l^2)^{1/2}$$

The calculated lattice parameter of as-prepared samples is shown in Table 3.2. The lattice parameter decreases in the order C2Z1>CZ>C1Z2. The shrinkage of lattice cells indicated the substitution of smaller ionic size Zr^{4+} with Ce^{4+}.[5] Furthermore, relative to pure ceria (5.4 Å) the lattice shrinkage of CZ samples indicates the penetration of Zr^{4+} cations into the cubic lattice of CeO_2.[6] XRD data show that the calculated average crystallite size of the prepared oxides is around 5nm and it is not effectively affected by the incorporation of zirconium content (Table 3.2).

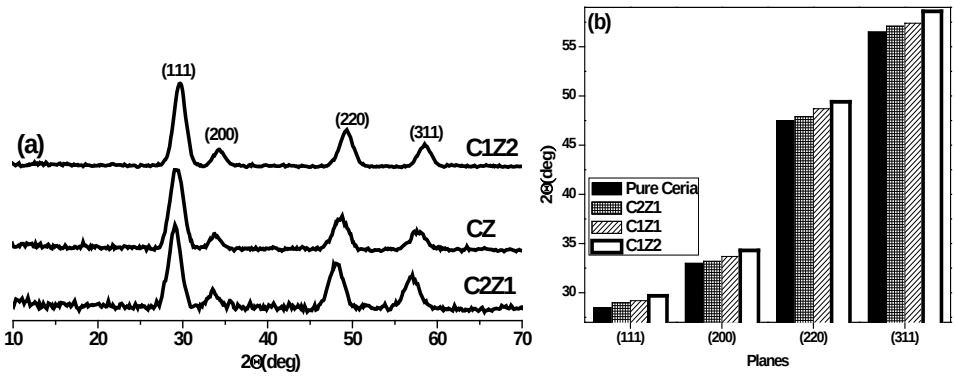

Fig. 3.1: (a) Powder X-ray diffraction patterns of ceria-zirconia support (b) Variation of 2Θ values with different ceria-zirconia compositions.

3.2.2.1.1. Modified Ceria-Zirconia Catalysts

i. Vanadium impregnated ceria-zirconia

The X-ray powder diffraction patterns of vanadium modified samples are presented in Fig.3.2 (a). Mainly, diffraction lines due to cubic fluorite type phase are observed. The absence of prominent lines due to vanadia crystalline phases in 4VCZ sample indicates the existence of highly dispersed or amorphous vanadium oxides on the CZ surface.[7] 8VCZ and 12VCZ, with higher concentration of vanadium, shows additional peaks at 2Θ value of around 26.4° and 34.1°. Earlier studies suggested that the formation of $CeVO_4$ in such a way that vanadium oxide selectively interacts with the ceria part of the ceria-zirconia to form $CeVO_4$ at high temperature.[8] Above a particular concentration, V_2O_5 can interact with the support material and form compounds or multilayer species. Radhika *et al.* investigated different loadings of vanadia supported on ceria and observed the presence of mixed phase $CeVO_4$ for loading above 6 wt%.[8] Other spectroscopic analysis of the samples, described in the subsequent sections, indeed provides unequivocal evidence to this conclusion. The crystallite size of ceria-zirconia is little influenced by metal loading.

ii. Chromium impregnated ceria-zirconia

XRD patterns of the Cr incorporated CZ are shown in Fig.3.2 (b). Detailed analysis revealed that for 4CrCZ, the XRD profiles look similar to that of the cubic fluorite structure of ceria. There are no extra peaks of other phases present in the XRD profile. It suggests that the chromium species are well dispersed and the crystallite size may be smaller than the detection limit.[9] Nevertheless, examination of the XRD pattern for 12CrCZ

shows additional diffraction peaks at 2Θ values of around 24.8°, 36.3°, 41.7°, 63.8°, 65.5° which are due to the formation of Cr_2O_3 phase (JCPDS 01-070-3765). 8CrCZ shows small peaks due to Cr_2O_3 phase. An estimate of average crystallite size by the line broadening method gives a value of around 4.6 nm.

iii. Manganese impregnated ceria-zirconia

Within the detection limits of the XRD technique, there is no evidence for the presence of crystallographic phases of manganese oxide in 4 and 8 wt% manganese impregnated catalysts. (Fig.3.2(c)) On the other hand, for 12MnCZ, diffraction peak is observed at 2Θ value of 18.6° in addition to those of ceria. Observed d-lines matched the speculated values for the tetragonal Mn_3O_4 phase (JCPDS; 1–1127).[10]

iv. Praseodymium impregnated ceria-zirconia

The XRD patterns of Pr modified catalysts are presented in Fig.3.2 (d). XRD pattern can be indexed satisfactorily to the fluorite structure with a space group *Fm*3*m*. Interestingly, no XRD pattern corresponding to crystalline praseodymia is noted. The fact that we could not trace any crystalline phase of praseodymia even on increasing the Pr content to 12 wt% substantiates the postulate that X-ray amorphous microcrystals of praseodymia phase are dispersed on the given support. Lattice parameter and crystallite size are given in Table 3.2.

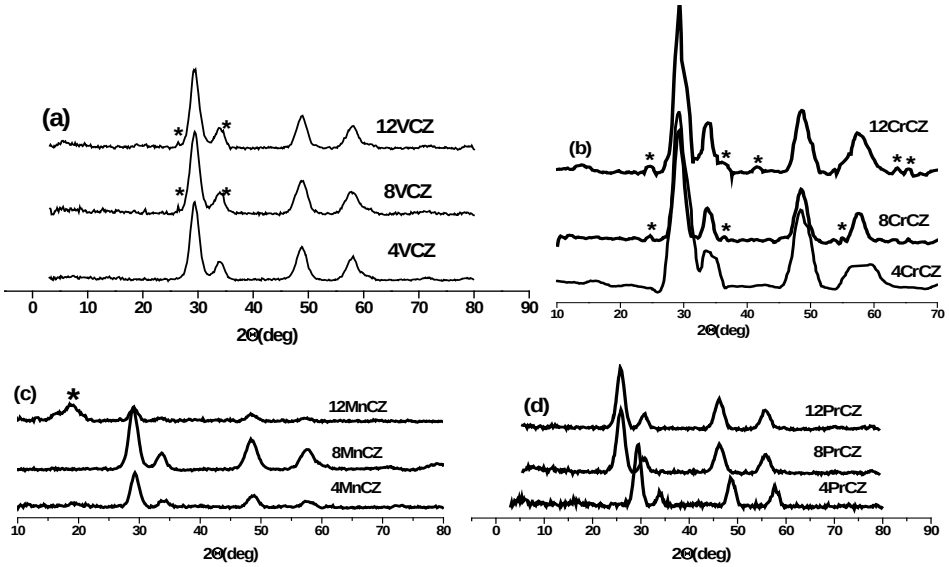

Fig. 3.2: Powder XRD patterns of modified ceria-zirconia catalysts

Table 3.2. XRD data of prepared catalysts

Sample	d-spacing (Å)	Average crystallite size (nm)	Lattice parameter (Å)
C2Z1	3.06	5.07	5.31
C1Z1	3.05	4.35	5.28
C1Z2	2.99	5.21	5.19
4VCZ	3.04	4.65	5.26
8VCZ	3.03	4.57	5.26
12VCZ	3.05	4.62	5.28
4CrCZ	3.04	4.66	5.27
8CrCZ	3.05	4.90	5.28
12CrCZ	3.03	4.64	5.26
4MnCZ	3.05	5.17	5.28
8MnCZ	3.06	5.16	5.30
12MnCZ	3.05	5.24	5.29
4PrCZ	3.03	4.94	5.25
8PrCZ	3.03	4.95	5.25
12PrCZ	3.06	4.86	5.30

3.2.2.2. Low Angle XRD Analysis

The low angle XRD patterns of representative CZ and 8VCZ materials are shown in Fig.3.3. For mesoporous materials reflections are observed in X-ray powder patterns at low 2θ angles ($0.5 < 2\theta < 10^{\circ}$). Because d-spacings are rather larger for the mesopores, the reflections appear at low angles. These are due to the long-range order induced by the very regular arrangement of the pores. The well-defined XRD pattern can be indexed to the (100) Bragg reflections, appeared at 2θ values around 0.3°-0.7° which is characteristic of 2D hexagonal structure. The appearance of low-angle diffraction peaks indicates that mesoscopic order is preserved in the calcined metal oxide materials. The observed peak indicates a good structural regularity of the samples.

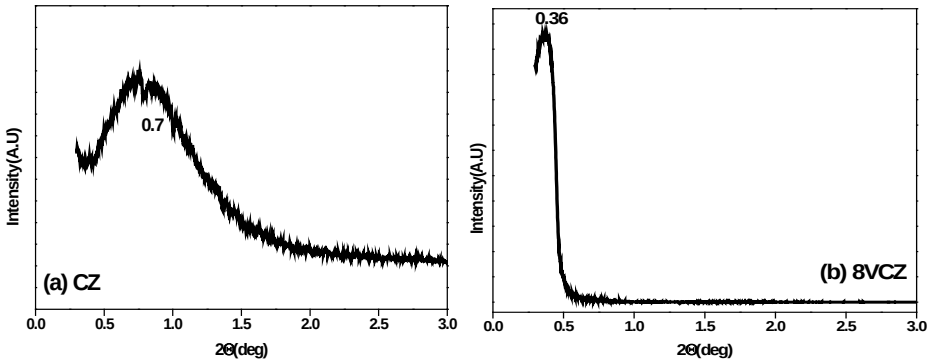

Fig. 3.3: Low angle XRD patterns of CZ and 8VCZ

3.2.3. Surface area and Porosity Measurements

Information on the textural properties of porous solids is typically obtained from low-temperature (77 K) nitrogen adsorption isotherms, which have been used to get information about the mesoporosity, the total (BET) surface area, the total pore volume and also the pore size distribution. Table 3.3 lists the textural parameters calculated from the nitrogen adsorption–desorption isotherms: the BET surface area, total pore

volume and pore size. The representative isotherms and the calculated pore size distributions are shown in Fig.3.4. and Fig.3.5.

The BET results show that reasonably high surface area is obtained for all the samples. As can be seen from the Table 3.3, in the case of pure ceria-zirconia, CZ possess a high surface area of 132 m^2/g. Increasing ceria or zirconia decreases the surface area. It is generally known that the mixed oxides with highest possible specific surface area are of great interest in view of their practical utility.

3.2.3.1. Modified Ceria-Zirconia Catalysts

i. Vanadium impregnated ceria-zirconia

Modification of ceria-zirconia support with metal causes reduction in surface area. A steady decrease in surface area is observed with the addition of vanadium. This surface area decrease is primarily due to blockage of the pores by the supported species. The decrease in surface area was partly due to the solid state reaction between the support and supported species resulting in the formation of new phases at higher loadings.[11]

ii. Chromium impregnated ceria-zirconia

The deposition of chromium on ceria-zirconia causes a decrease in BET surface area and pore volume of the support. 4CrCZ shows a high surface area of 125 m^2/g. It declines to 103 for 8CrCZ and 73 m^2/g for 12CrCZ. The reduction in the textural property mentioned above is explained by the plugging of pores on the support by chromia phase. [9,12]

iii. Manganese impregnated ceria-zirconia

With manganese loaded sample, 4%, 8% and 12% catalysts bear a BET surface area of 67, 64 and 57 m^2/g respectively. This decreased

surface area may be attributed to the blockage of the surface by the metals during impregnation.

iv. Praseodymium impregnated ceria-zirconia

As can be noted from the Table 3.3, Pr modified catalysts also exhibit a decreasing trend in surface area with increasing metal content. This shows the homogeneous distribution of praseodymium metal into the surface vacant site attained by wet impregnation method.

Table 3.3. Textural properties of the prepared catalysts.

Catalyst	Surface area (m^2/g)	Total Pore Volume (cm^3/ g)	Pore diameter (nm)
C2Z1	125	0.13	3.40
CZ	132	0.16	3.84
C1Z2	76	0.11	3.01
4VCZ	106	0.14	4.30
8VCZ	92	0.09	4.03
12VCZ	89	0.13	4.86
4CrCZ	125	0.21	3.58
8CrCZ	103	0.13	3.85
12CrCZ	73	0.10	3.34
4MnCZ	67	0.09	2.01
8MnCZ	64	0.09	3.72
12MnCZ	57	0.08	2.56.
4PrCZ	91	0.11	3.72
8PrCZ	59	0.10	5.70
12PrCZ	49	0.06	3.91

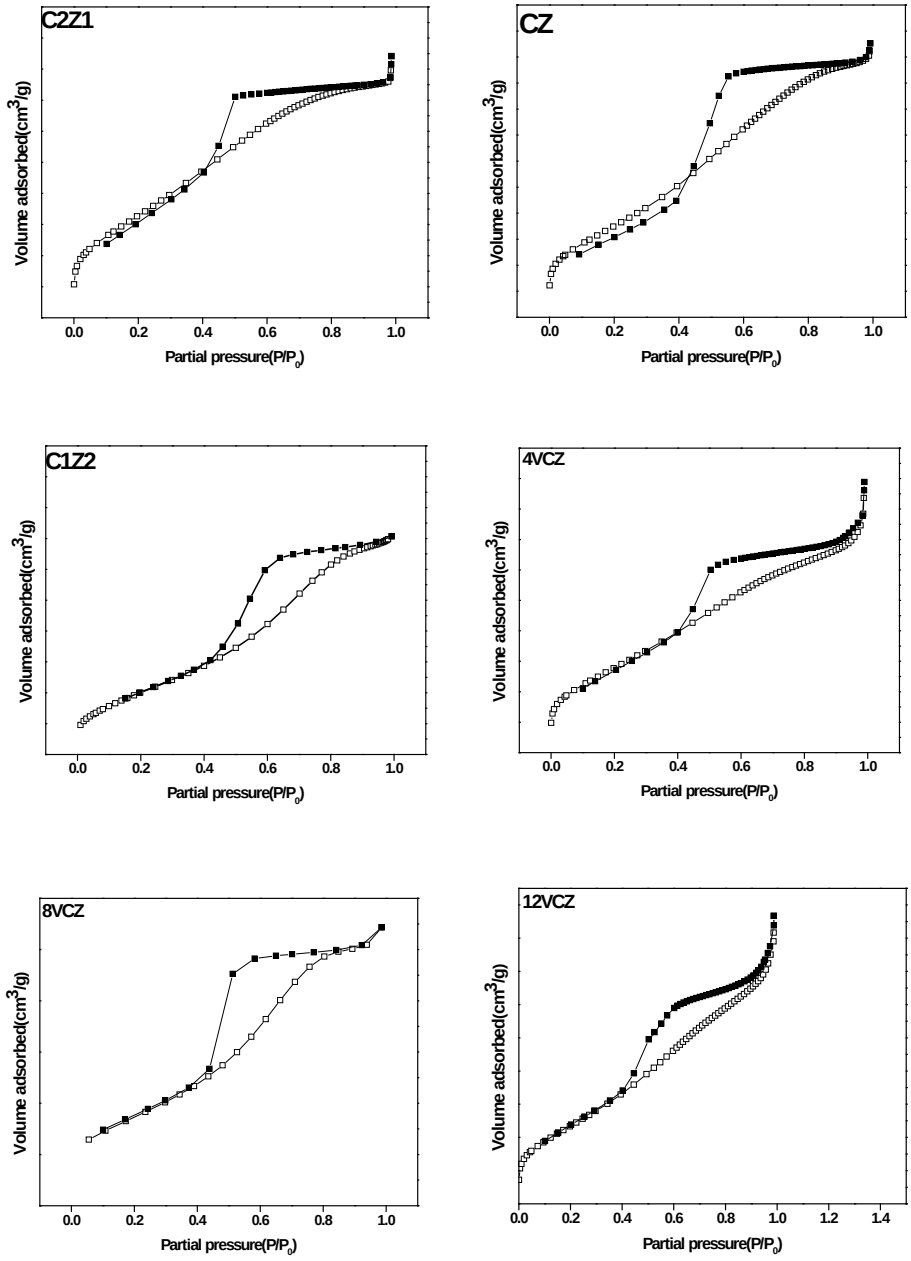
C2Z1
CZ
C1Z2
4VCZ
8VCZ
12VCZ
Volume adsorbed(cm3/g)
Partial pressure(P/P0)
0.0
0.2
0.4
0.6
0.8
1.0
1.2
1.4

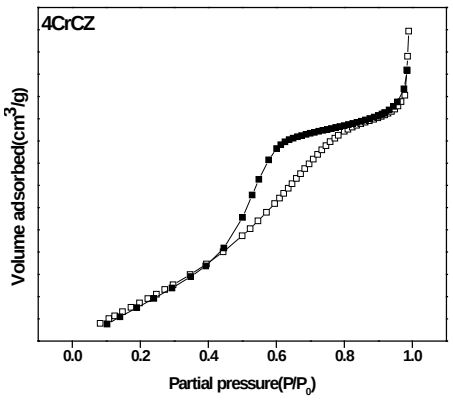
4CrCZ
Volume adsorbed(cm3/g)
0.0
0.2
0.4
0.6
0.8
1.0
Partial pressure(P/P0)

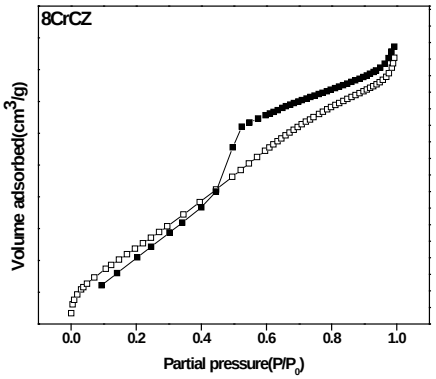
8CrCZ
Volume adsorbed(cm3/g)
0.0
0.2
0.4
0.6
0.8
1.0
Partial pressure(P/P0)

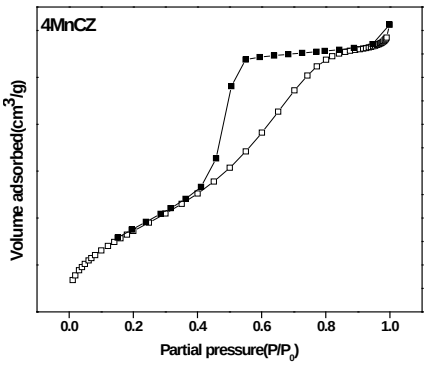
4MnCZ
Volume adsorbed(cm3/g)
0.0
0.2
0.4
0.6
0.8
1.0
Partial pressure(P/P0)

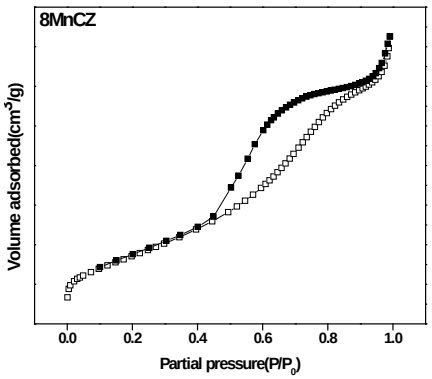
8MnCZ
Volume adsorbed(cm3/g)
0.0
0.2
0.4
0.6
0.8
1.0
Partial pressure(P/P0)

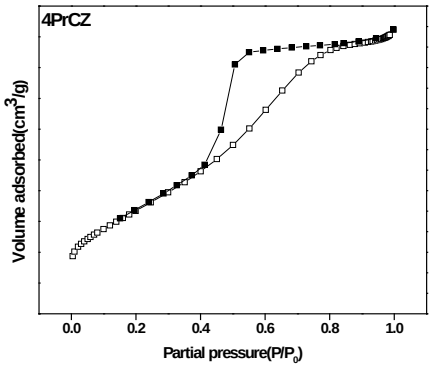
4PrCZ
Volume adsorbed(cm3/g)
0.0
0.2
0.4
0.6
0.8
1.0
Partial pressure(P/P0)

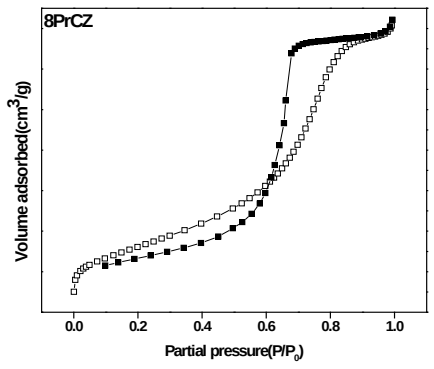
8PrCZ
Volume adsorbed(cm3/g)
0.0
0.2
0.4
0.6
0.8
1.0
Partial pressure(P/P0)

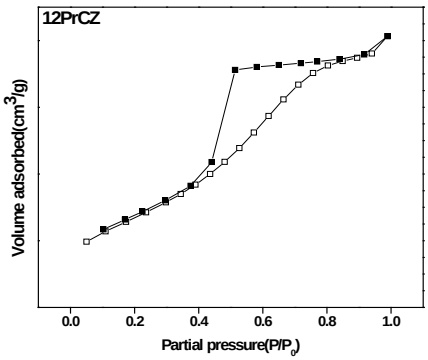

Fig. 3.4: N_2 adsorption/desorption isotherms of modified and pure ceria-zirconia catalysts.

As can be noted from Fig.3.4, that all the adsorption-desorption isotherms can be classified as type IV typical of mesoporous material. The shape of the curve indicates the absence of a narrow pore size distribution as suggested by the lack of the typical step in the adsorption isotherm which is observed with ordered mesoporous structure. According to IUPAC classification, the hysteresis loop is of type H2 with a relatively steep desorption branch in the range of relative pressure P/P_0= 0.4-0.5. This hysteresis loops is typical for wormhole-like structure[13] indicating complex mesoporous structure.

The pore size distributions have been determined by referring to Barrett-Joyner-Halenda (BJH) model applied to the desorption isotherm branch. The values of average pore diameters are summarized in Table 3.3. The plot of the pore-size distribution reveals that the prepared material possesses porous structures with a size distribution of 20-60 Å.

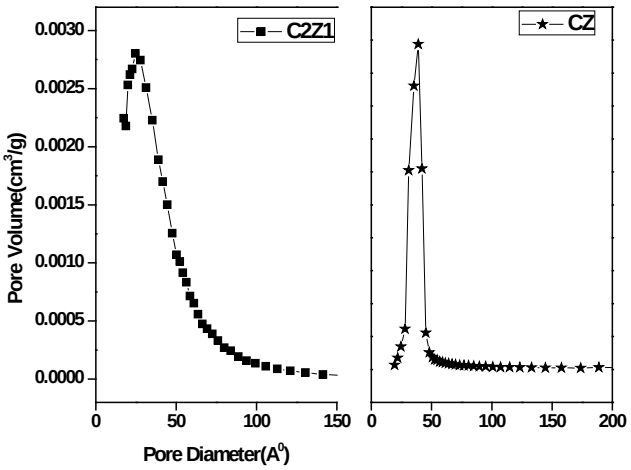
C2Z1
CZ
Pore Volume(cm³/g)
Pore Diameter(A⁰)

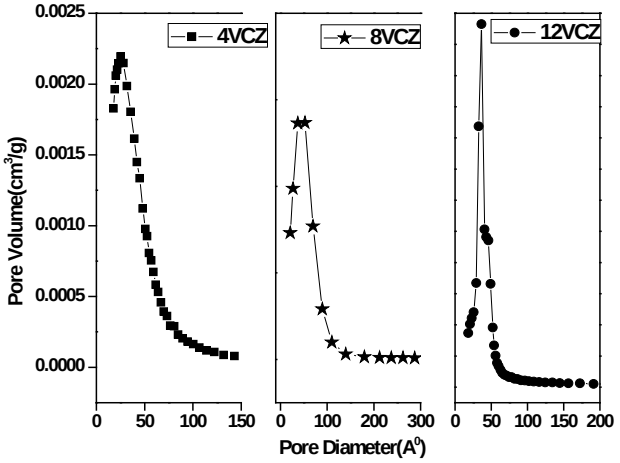
4VCZ
8VCZ
12VCZ
Pore Volume(cm³/g)
Pore Diameter(A⁰)

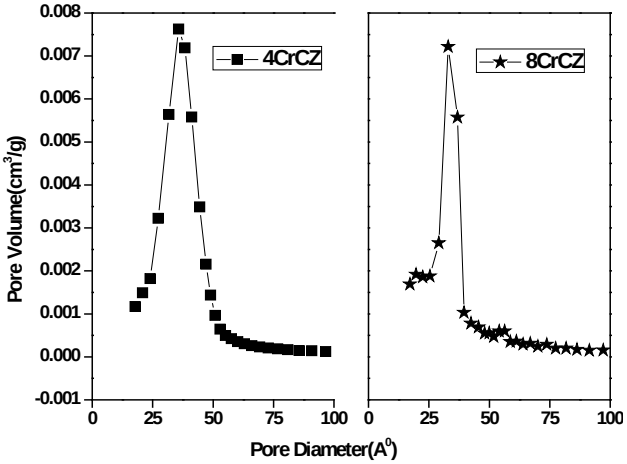
4CrCZ
8CrCZ
Pore Volume(cm³/g)
Pore Diameter(A⁰)

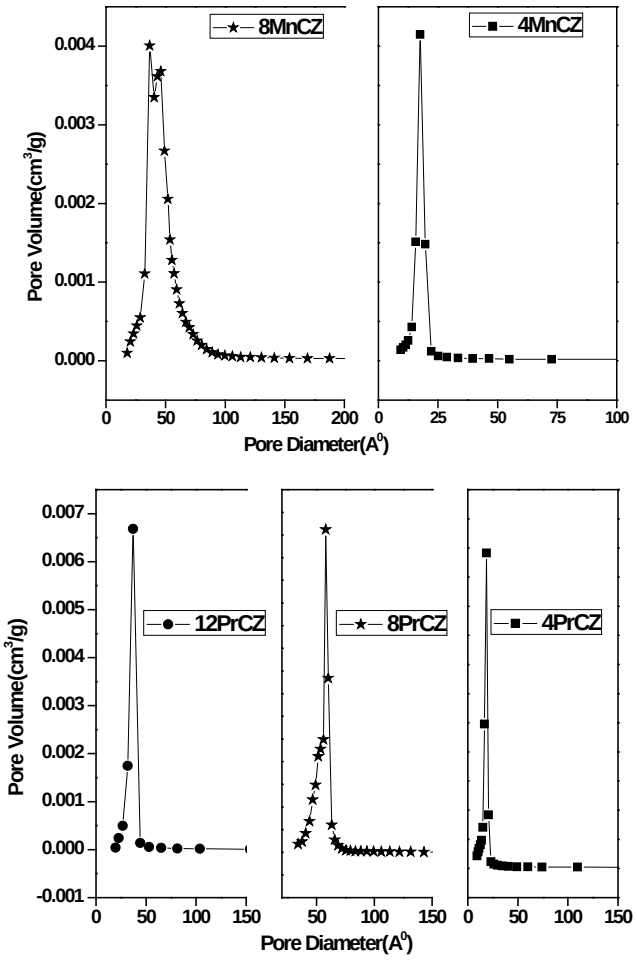

Fig. 3.5: Pore size distributions of modified and pure ceria-zirconia catalysts.

3.2.4. Thermogravimetric Analysis

In order to evaluate the thermal stability of pure ceria-zirconia samples, thermal analysis of as-synthesized samples was carried out. The TG and DTG curve obtained is shown in Fig.3.6. Two weight losses are observed in the thermogram. The first loss occurs at around 170°C which may correspond to the dehydration of physically adsorbed water and loss of water held on the surface by hydrogen bonding. The second weight loss at around 250°C is due to the decomposition of cetyltrimethylammonium

bromide surfactant. As seen from the figure, the offset temperature of surfactant removal is at around 370°C. It was reported that thermal degradation of pure CTAB was showing weight loss between 180–340°C.[14] No further weight loss is observed confirming the structural stability of the prepared catalyst. Hence the catalysts which are calcined at 500°C contain only metal oxides without any impurity.

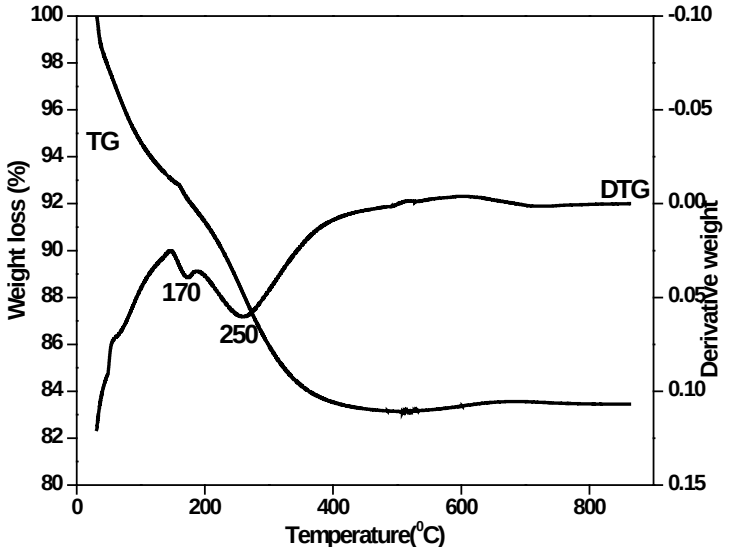

Fig. 3.6: Thermogram of pure ceria-zirconia catalyst.

3.2.5. Fourier Transform Infrared Spectroscopy

A broad band observed in the region 3000-3500 cm^{-1} corresponds to O-H stretching vibration. (Fig.3.7) Band at around 1600 cm^{-1} is due to the H_2O bending vibration.[15] This indicates the presence of coordinated water molecules. A small peak at around 1340 cm^{-1} is due to Ce-OH stretching vibration. The weak peak at around 1010 cm^{-1} is due to the presence of Ce-O-Zr bond. Moreover no characteristic absorption peak is found at 1384cm^{-1}, suggesting that nitrates are completely removed during filtration and washing.

3.2.5.1. Modified Ceria-Zirconia Catalysts

IR spectra of metal modified samples can give information about the possible existence of metal oxide phases on the surface. The most pronounced absorptions expected for these phases, however, are covered by the strong ceria-zirconia absorptions below 800 cm^{-1}.

In line with the earlier findings, vanadium modified catalysts show absorption bands in the range 795-810 cm^{-1} and 1000-1100 cm^{-1} in addition to those observed for ceria. [8] For 8VCZ and 12VCZ, the IR bands observed at around 1020 cm^{-1} region are generally attributed to the V=O stretching vibration. The band observed at 810 cm^{-1} is assigned to the coupled vibrations between V=O and V-O-V. The FT-IR spectra of 12CrCZ demonstrated an additional peak at around 1104 cm^{-1}. In conformity with literature reports, this is generally attributed to the chromium–oxygen groups.[9] Careful inspection of the spectra for 12MnCZ allows the identification of manganese oxide phase. Three small peaks are found from 400 to 650 cm^{-1} due to Mn–O vibrations. Peaks at around 435, 520, 615 cm^{-1} may probably due to those of Mn_3O_4.[10] No peak corresponds to Pr-O vibration, with characteristic vibrational frequency of 415 cm^{-1}, is found in the spectrum.[16]

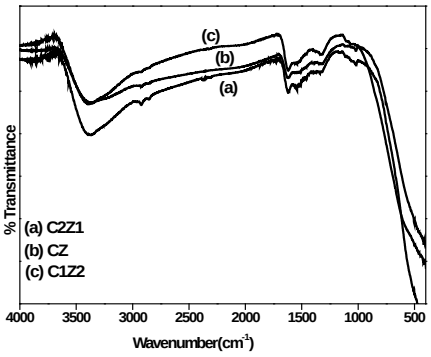

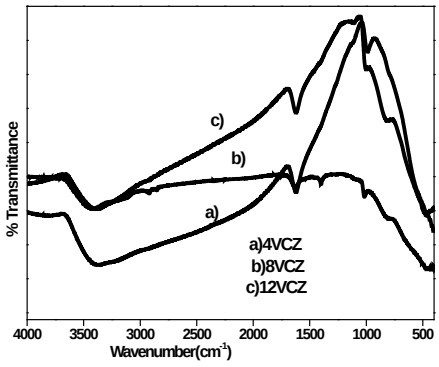

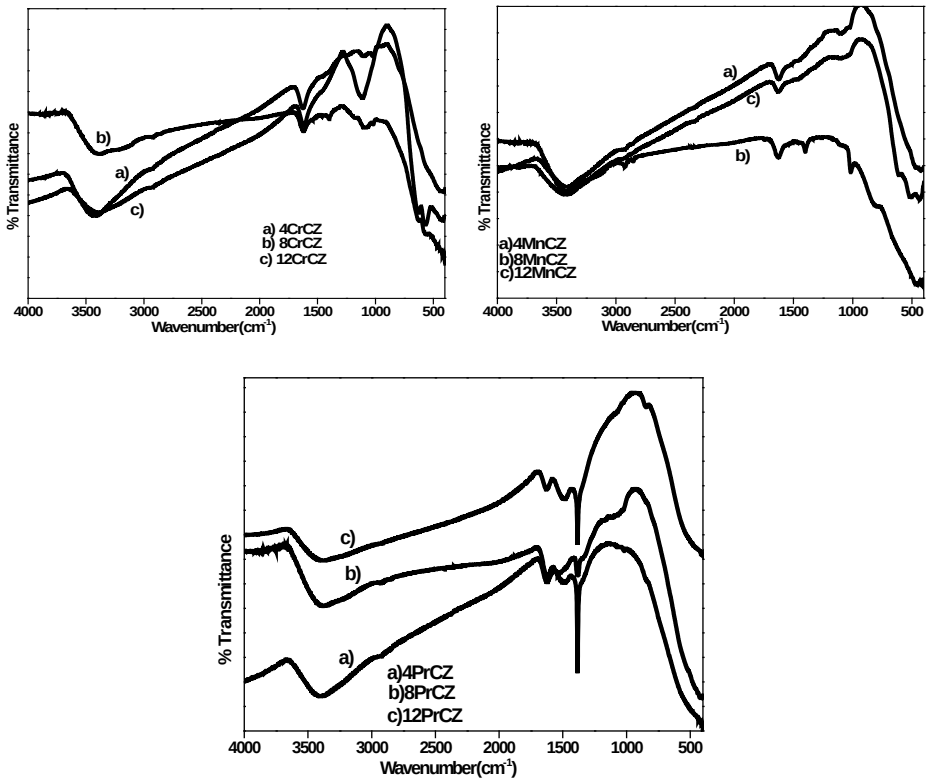

Fig. 3.7: IR spectra of modified and pure ceria-zirconia catalysts.

3.2.6. Ultraviolet-Visible Diffuse Reflectance Spectroscopy

UV-vis DRS is a useful technique for studying the local coordination environment and electronic state of isolated transition metal ions as well as aggregated transition metal oxides in spite of its difficulties in interpreting large bandwidths and specular reflectance often observed. In the case of ceria-zirconia mixed oxide, a broad band is observed between 250-340 nm in the spectra (Fig.3.8(a)). The bands in the range of 250–350 nm are in agreement with literature report 17. These can be assigned to $Ce^{3+} \leftarrow O^{2-}$ (~250 nm) and $Ce^{4+} \leftarrow O^{2-}$ (270-297 nm) charge transfer transitions. The broad shoulder-type band at 320–340 nm on the higher wavelength side in the DR spectra may consist of interband and $Zr^{4+} \leftarrow O^{2-}$ transitions of the substituted fluorite lattice.

3.2.6.1. Modified Ceria-Zirconia Catalysts

i. Vanadium impregnated ceria-zirconia

UV-vis diffuse reflectance spectroscopic studies have been carried out for the modified catalyst also. (Fig.3.8 [(b),(c),(d)(e)]). A broad band is extending up to 550 nm for V impregnated catalysts. Ligand-to-Metal Charge Transfer (LMCT) transitions of V^{5+} appear in the 200–500 nm region which are usually found to be very broad.[18]

ii. Chromium impregnated ceria-zirconia

For Cr modified sample, 4CrCZ exhibits peak similar to that of the support. No peaks due to Cr species are detected. On the other hand, 8% and 12% Cr loaded samples (particularly 12CrCZ) show two peaks at 450 and 590 nm which are characteristic of Cr^{3+} in Cr_2O_3.[2] Cr^{6+} cannot be distinguished from the spectrum since the peak may be overlapped with support peak.

iii. Manganese impregnated ceria-zirconia

For Mn modified catalysts, three broad bands are found at around 260-360, 450-520 and 570-640 nm. The former can be attributed to the transitions of the support itself. The latter two peaks can be assigned to $^5E_2$ - $^5T_2$ transition of Mn^{3+} species and to the $^6A_1$ - $^4T_2$ transition of Mn^{2+} species.[19]

iv. Praseodymium impregnated ceria-zirconia

Pr modified sample shows similar spectra as that of the support. In addition to that, a small band is observed in the visible region (~590 nm) which may be associated with Pr^{3+} ion transitions in 8PrCZ and 12PrCZ.[20]

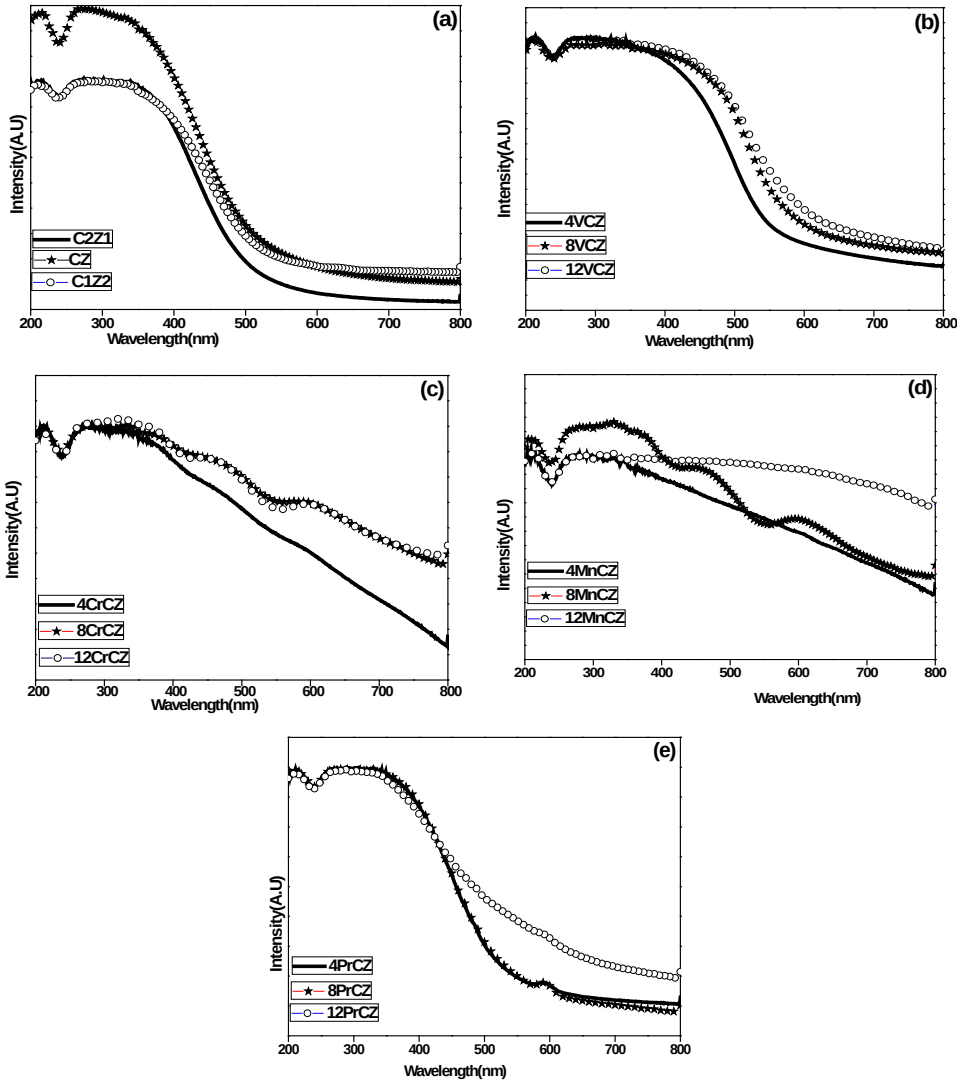

Fig. 3.8: UV-Vis-DRS spectra of modified and pure ceria-zirconia catalysts.

3.2.7. Raman Spectroscopy

Raman spectroscopy is widely used for the investigation of oxides, supported and bulk metals, supported oxides. Raman bands reflect both the surface and bulk information due to the weak absorption of samples in the visible range. Fig.3.9 shows the Raman spectra of mixed ceria-zirconia oxides. It has been reported that the Raman spectrum of bare CeO_2 has a

single band centered at around 465cm^{-1} that corresponds to the single allowed Raman mode (F_{2g}) of the fluorite-type structures.[21,22] In line with the reported studies, the spectrum pertaining to C2Z1 shows a profile similar to that observed for pure ceria with a single predominant band at 465 cm^{-1}. This band corresponds to the triply degenerate F_{2g} mode and can be viewed as a symmetric breathing mode of oxygen atoms around cerium ions.[18] These vibrational modes occur from three equivalent motions of oxygen atoms on the three axes. F_2 mode splits into one symmetric component F_{2g}, which only involves movements of the oxygen atoms (Raman active), and another asymmetric F_{1u} which involves movements of both the oxygen and cerium atoms (IR-active).[23]

It is clear from the figure that intensity of strong band at ~465 cm^{-1} decreases much in intensity for CZ when compared to C2Z1. Moreover, when the Zr content increases further as in C1Z2, the main peak in the Raman spectra broadens considerably whereas the six broad bands characteristic of the tetragonal symmetry occur at about 125, 206, 310, 465, 590 and 640 cm^{-1}. Escribano *et al.* suggested that this may be due to the presence of tetragonal and cubic solid solution phase though the cubic phase is still largely predominant.[23] However, it is difficult to predict the co-existence of both phases due to the broadness and overlapping of ZrO_2 and CeO_2 bands.[2] It is also supposed that the reduced intensity of predominant Raman peak may be due to the strong interaction between zirconium and cerium oxide species occurring under the high temperature calcination process which resulted in the formation of oxygen vacancies by the reduction of cerium. A small shoulder peak at approximately 600 cm^{-1} is attributed to oxygen vacancies in the ceria lattice.[22,24] This peak can be assigned as non-degenerate Longitudinal Optical (LO) mode of ceria arising due to relaxation of symmetry rules. The presence

of oxygen vacancies is likely to enhance the catalytic performance of these systems. The weak band observed at around 300 cm^{-1} for C1Z2 can be ascribed to the displacement of oxygen atoms from their ideal fluorite lattice positions.[23]

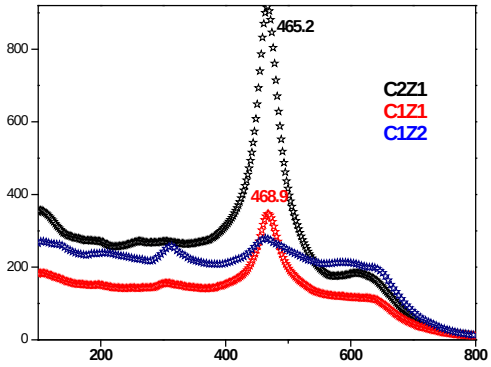

Fig. 3.9: Raman spectra of ceria-zirconia catalysts.

3.2.7.1. Modified Ceria-Zirconia Catalysts

Raman spectroscopy is also helpful for the elucidation of structures of complex transition metal oxides presenting either as bulk phases or as two-dimensional supported phases because Raman spectroscopy directly probes structures and bonds by their vibrational spectra. It is a very powerful characterization technique to obtain detailed surface information about the molecular structure of the metal oxide over-layer on oxide supports. The Raman spectra were recorded for all 8% metal modified ceria-zirconia catalysts. (Fig.3.10)

i. Vanadium impregnated ceria-zirconia

Raman spectra of vanadium modified ceria-zirconia is shown in Fig.3.10(a). A ceria phase has been evidenced in all the catalysts. From the fingerprint Raman spectrum, we can find the nature of V species in ceria-zirconia. Vanadium modified sample (8VCZ) exhibits Raman peak

around 462 cm^{-1}, which is characteristic of F_{2g} mode of cerium ions.[18] In addition to this, numerous Raman bands are found around 992, 698, 526, 405, 301 and 285 cm^{-1} which are typical of crystalline V_2O_5.[11, 25] Peaks are observed at 790 and 857 cm^{-1} due to the formation of $CeVO_4$. It is proposed that the VO_4^{3-} surface species interact with ceria to form stable $CeVO_4$ compound under the influence of high-temperature calcinations. The earlier report suggested that for solids with isolated VO_4^{3-} units, Raman band lies in the range of 830–855 cm^{-1}.[18] It is associated with the breathing mode of the vanadium tetrahedron. In $CeVO_4$, vanadium ions are located at the centre of oxygen tetrahedron with a vanadium-oxygen distance similar to that of an isolated VO_4^{3-}. Therefore, the band at 857 cm^{-1} can be assigned to such a mode of $CeVO_4$.

ii. Chromium impregnated ceria-zirconia

The Raman spectrum of chromium modified sample is characterized by the 462 cm^{-1} band which corresponds to F_{2g} symmetry in the cubic phase. Raman modes are found at 306, 345, 548, 608 and 627 cm^{-1}. This is ascribed to the presence of Cr_2O_3. The most intense band at 548 cm^{-1} is of A_{1g} symmetry, the others are of E_g symmetry.[26, 27] This indicates that Cr_2O_3 phase [Cr(III)] is the main surface component of the catalyst. Small peak at 840 cm^{-1} may be due to the presence of Cr^{6+}. This can be assigned to polychromate species.[28] It is reported that supported chromium shows more than a single oxidation state depending on Cr loading, preparation procedure and pre-treatment conditions applied.[29]

iii. Manganese impregnated ceria-zirconia

FT-Raman spectra of manganese modified ceria-zirconia oxide, shown in Fig.3.10(c), display a broad peak at 450 cm^{-1} characteristic of cubic fluorite-like structure. Comparison of the Raman spectra of the support and 8MnCZ

gives information about the manganese oxide phase. It displays peaks around 626, 368 and 310-315 cm^{-1}. Peak at 626 cm^{-1} is, rather, strong which can be related to the hausmannite phase (Mn_3O_4). The other two peaks are small, which is in good agreement with those previously reported.[30] Hausmannite contains both manganous and manganic ions (exists as $MnO.Mn_2O_3$) and belongs to mixed valence compounds.

iv. Praseodymium impregnated ceria-zirconia

The Raman spectra for 8PrCZ (Fig.3.10 (d)) revealed one main peak centered at about 468 cm^{-1} which is typical of the F_{2g} Raman active mode of the fluorite-structured materials. For Pr modified catalysts, no characteristic peaks are found due to Pr oxides showing that Pr is well dispersed in the support.

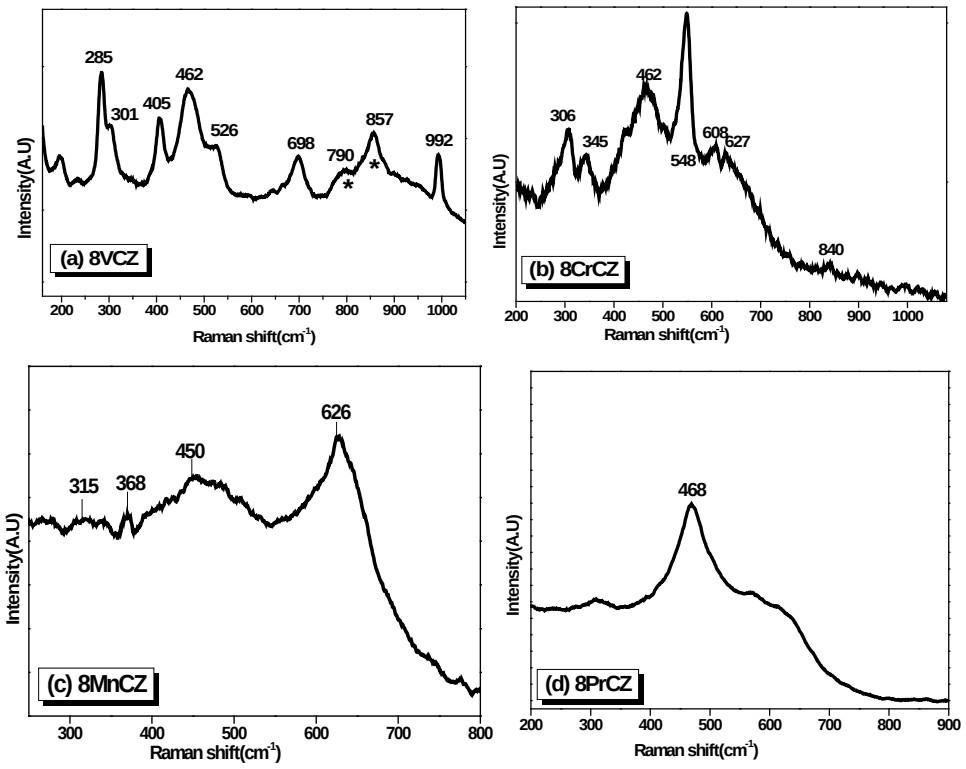

Fig. 3.10: Raman spectra of modified ceria-zirconia catalysts.

3.2.8. X-ray Photoelectron Spectroscopy

Representative catalysts have been investigated with XPS technique to investigate the oxidation state of the elements. The photoelectron peaks of Ce 3d, Zr 3d and O 1s of C1Z2 are depicted in Fig.3.11[(a), (b), (c)] respectively. The Ce 3d core level spectra of ceria is complicated which occur not only because of multiple oxidation states but also because of the mixing of Ce 4f levels and O 2p states during the primary photoemission process.[31] Peaks labeled as 'v' correspond to Ce $3d_{5/2}$ contributions and those denoted as 'u' represent the Ce $3d_{3/2}$ contributions which are reported elsewhere.[2] Peaks observed in the XPS spectrum is in agreement with the literature reports.[32,33] The four main $3d_{5/2}$ features at 880.6, 884.9, 891.0, and 898.6 eV correspond to V, $V^{/}$, $V^{//}$, $V^{///}$ components, respectively. Main $3d_{3/2}$ features about 900.6, 903.1, 909.8, and 914.5 eV correspond to U, $U^{/}$, $U^{//}$ and $U^{///}$ components, respectively. The main peaks of $V^{///}$ and $U^{///}$ represented the $3d^{10}4f^{0}$ initial electronic state correspond to the Ce^{4+} ion. Peaks of $V^{/}$ and $U^{/}$ represented the $3d^{10}4f^{1}$ initial electronic state belong to the unique photoelectron features of the Ce^{3+} state. Others are satellite peaks. Thus C1Z2 exhibited peaks that are due to the presence of both Ce^{4+} and Ce^{3+} ions, thus implying that cerium is present at the surface in both 4+ and 3+ oxidation states. The core level XP spectra of Zr 3d corresponding to the C1Z2 sample is presented in Fig.3.11 (b). The peaks at 182.6 and 184.9 eV correspond to Zr $3d_{5/2}$ and Zr $3d_{3/2}$, respectively (Zr^{4+}). The difference in the binding energies (BE) between the Zr $3d_{5/2}$ and Zr $3d_{3/2}$ photoemission feature is 2.3 eV, which is in agreement with the literature.[34] The position of the primary O 1s feature found at 530.1 eV is attributed to the lattice oxygen associated with the C1Z2 metal oxides.[2](fig.3.11(c))

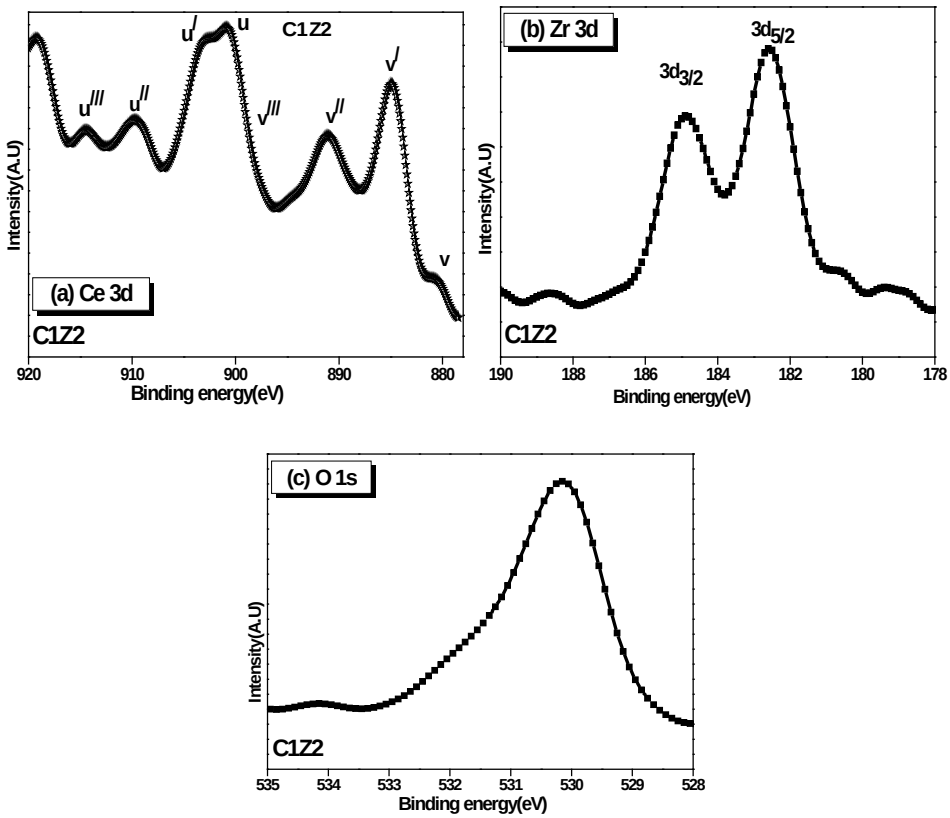

Fig. 3.11: XPS spectra of C1Z2.

The spectra of Ce 3d, Zr 3d and O 1s core-levels of CZ are shown in Fig. 3.12 [(a), (b), (c), (d)]. The peaks are identified in the spectrum which is similar to those reported for C1Z2. Hence as can be seen from Fig. 3.12 (b), Ce ions are present in both 4+ and 3+ oxidation states in CZ sample also. The binding energy of the Zr 3d photoelectron peak reveals the presence of Zr^{4+} species. The binding energy of 529–530 eV is characteristic of the lattice oxygen.

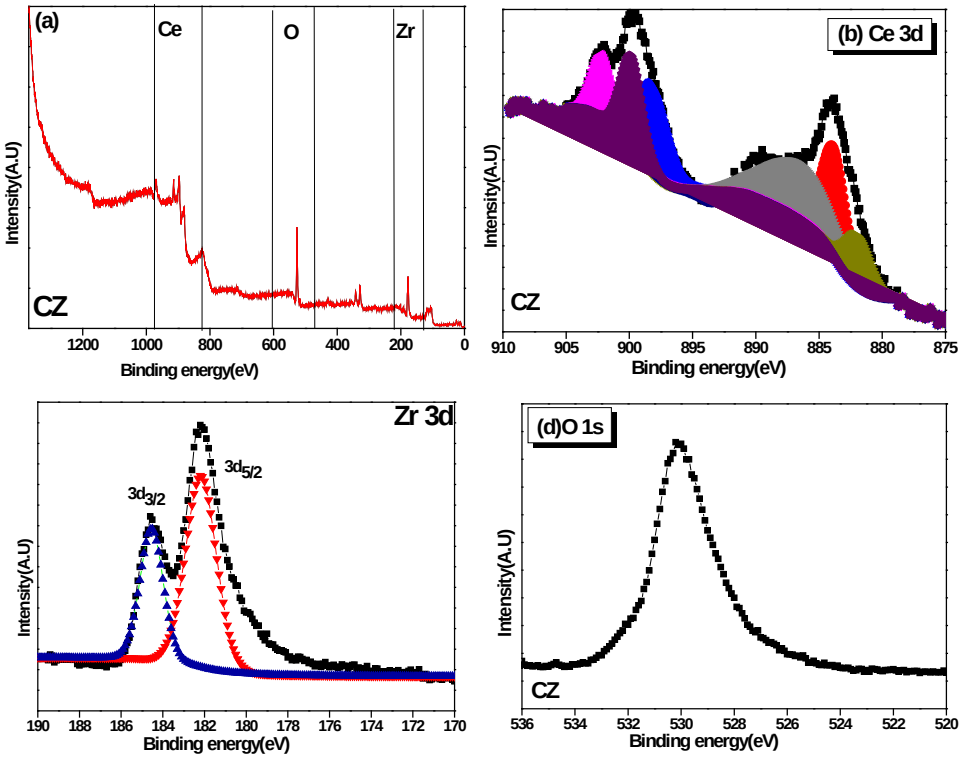

Fig. 3.12: XPS spectra of CZ.

3.2.8.1. Modified Ceria-Zirconia Catalysts

XPS was also employed to investigate the oxidation state of modified metal in the mixed oxides. The spectra were recorded for 12VCZ, 12MnCZ, 12CrCZ and 12PrCZ. Results are given in Fig.3.13.

i. Vanadium impregnated ceria-zirconia

Vanadium 2p core level photoelectron spectra of the representative 12VCZ are given in Fig. 3.13 (a). The spectrum is broad. On deconvoluting, it can be resolved into two individual peaks whose binding energies are at 521.0 and 517.4 eV corresponding to V $2p_{1/2}$ and V $2p_{3/2}$ respectively.[11] This peak can be attributed to the presence of V^{5+} species. The presence of $CeVO_4$ cannot be distinguished since vanadium cation is in 5+ valence state in the species also.

ii. Chromium impregnated ceria-zirconia

The core level electronic spectrum of Cr 2p is shown in Fig. 3.13 (b). It was reported in the literature that the BE of Cr $2p_{3/2}$ signals at 577 eV could be assigned to Cr^{3+} ions whereas those at 579 eV attributed to Cr^{6+} ions. In 12CrCZ spectra, two bands centered at 577 and 586.5 eV can be assigned to $2p_{3/2}$ and $2p_{1/2}$ components respectively. Peak in the $2p_{3/2}$ region is broad with a small shoulder at around 580 eV which may be attributed to Cr^{6+} ions. It has been reported that Cr ions exist in various oxidation states in supported chromium materials.[35] The spectra for Ce 3d, Zr 3d and O 1s core-levels of 12CrCZ are shown in Fig.3.13 (c).

iii. Manganese impregnated ceria-zirconia

Manganese 2p spectum of representative 12MnCZ is shown in Fig. 3.13 (d). Mn 2p doublet analysis shows that binding energies of various manganese ions are very close to each other, rendering the exact identification of oxidation states impossible due to overlap of the energy ranges for various oxidation states of Mn. Mn 2p peak is rather broad due to multiple splitting which may imply the co-existence of Mn^{2+} and Mn^{3+} ions at the surface of the catalysts. Spin-orbit multiples of Mn 2p have components Mn $2p_{3/2}$ and Mn $2p_{1/2}$. $2p_{3/2}$–$2p_{1/2}$ doublet is observed at 642.9 eV and 653.7 eV respectively. It was reported that Mn ($2p_{3/2}$) core level at 641.3 eV can be attributed to Mn in 2+ as well as to 3+ oxidation states.[36] The spin–orbit splitting is the difference between binding energy values of Mn $2p_{3/2}$ and Mn $2p_{1/2}$ levels. The observed spin–orbit splitting is 11.6 eV. The binding energy value and spin–orbit splitting matches with the previously reported values for hausmannite phase (Mn_3O_4).[37]

iv. Praseodymium impregnated ceria-zirconia

Fig.3.13 ((e) and (f)) illustrates spectrum of praseodymium (Pr) modified sample. The spectrum for Pr modified catalyst is rather broad. Deconvolution of the peaks allows an unambiguous identification of the oxidation states of metal. According to the literature report, in the spectrum of Pr 3d two sets of spin-orbit multiples are observed at binding energies of ~933 and ~953 eV corresponding to $3d_{5/2}$ and $3d_{3/2}$ electrons of Pr.[33,20] Because of the high redox property of PrO_2, there is a possibility of the coexistence of mixed valence +3 and +4 cations (Pr^{4+}/Pr^{3+}) at equilibrium for the stable Pr_6O_{11} ($4PrO_2 \cdot Pr_2O_3$). As expected, $3d_{5/2}$ sublevel consists of two peaks at 933.4 and 929.2 eV which can be assigned to Pr^{4+} and Pr^{3+} respectively. Two features of $3d_{3/2}$ observed at 953.6 and 950.1 eV correspond to Pr^{4+} and Pr^{3+} respectively. This indicates that the prepared sample contains both 3+ and 4+ oxidation states of praseodymium at the surface region.

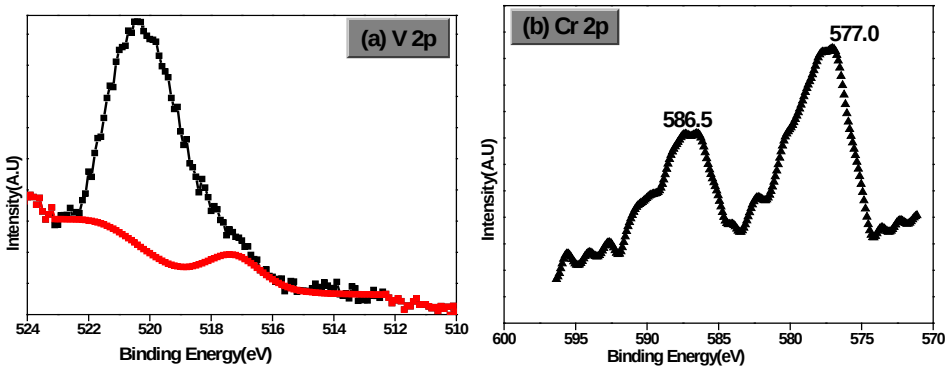

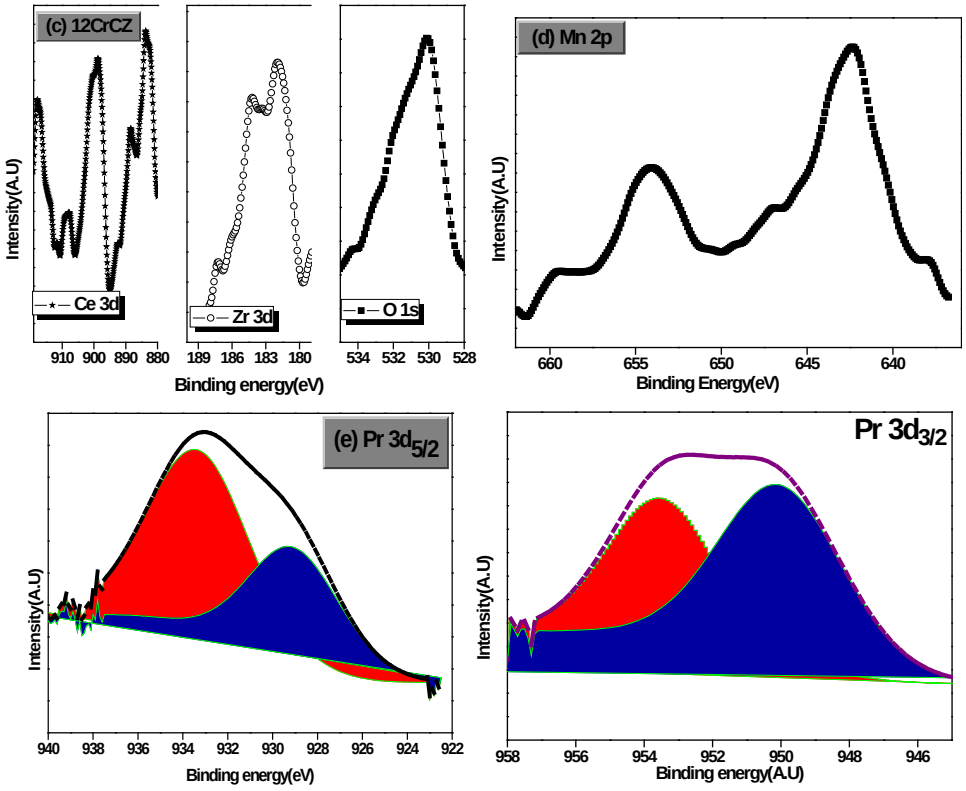

Fig. 3.13: XPS spectra of modified ceria-zirconia catalysts.

3.2.9. Scanning Electron Microscopy

SEM analysis of the prepared systems gives an idea about the surface topography of the catalysts. Fig.3.14 presents the scanning electron micrographs of the prepared systems.

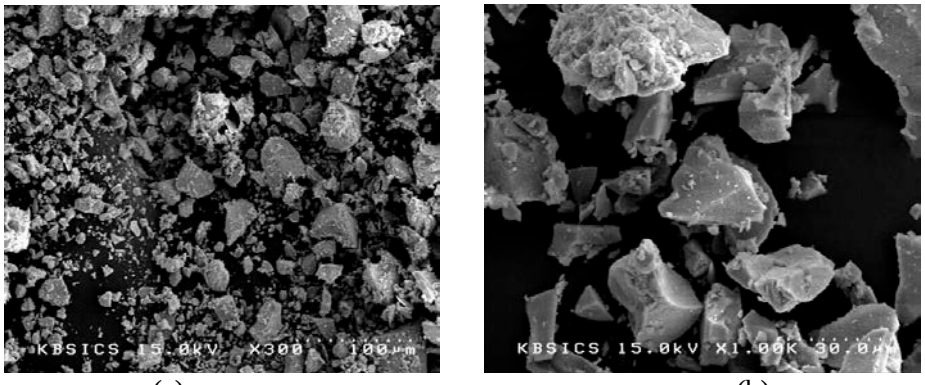

(a) (b)

Fig. 3.14: SEM images of representative catalysts (a) C1Z2 (b) 8CrCZ

From the SEM pictures it can be identified that particle aggregation has taken place i.e., the samples possess densely packed agglomerates of crystallites. The particles are irregular shaped and larger sized due to the collapse in structure during calcination.

3.2.10. Transmission Electron Microscopy

The surface morphology and structural properties of the prepared catalysts are illustrated by TEM and HR-TEM techniques, shown in Fig.3.15. Micrographs showed that the sample is in polycrystalline form and is constituted by small crystallites. The lattice fringes of nano crystalline material can also be well detected by the high resolution TEM image. (Fig.3.15 (a)) HRTEM image of CZ sample indicates that particles crystallize as cubic fluorite type structure of ceria, exposing preferentially the crystal plane (111) with a d spacing of 3.1 Å, in addition to (200) plane with 2.7 Å nm interplanar spacings.[13] The images reveal a porous structure of the oxide. As observed from figures, agglomeration of dense nanoparticles has taken place. Statistical analysis of these micrographs has been carried out. Particle size histogram can be plotted from TEM images and it reveals that the average particle size ranged from 5-13 nm for different catalysts as shown in Fig.3.15. However 8MnCZ consists of particles of about 18 nm in size. These results are in good agreement with those obtained from XRD peak broadening measurements.

The selected area electron diffraction (SAED) pattern of the sample exhibited concentric rings that are essentially continuous, implying that the samples consisted of many very small crystallites (Fig.3.15 (d)). Inter planar spacings were calculated from the pattern and can be indexed to cubic fluorite phase. Also, SAED pattern confirms the formation of thermodynamically most stable (111) surface plane. The shapes of the particles observed from TEM images are almost similar to those usually

seen in previous works for ceria–zirconia specimens.[3, 22] Transmission images confirm that the adopted preparation method is favorable for maintaining the highly ordered structure.

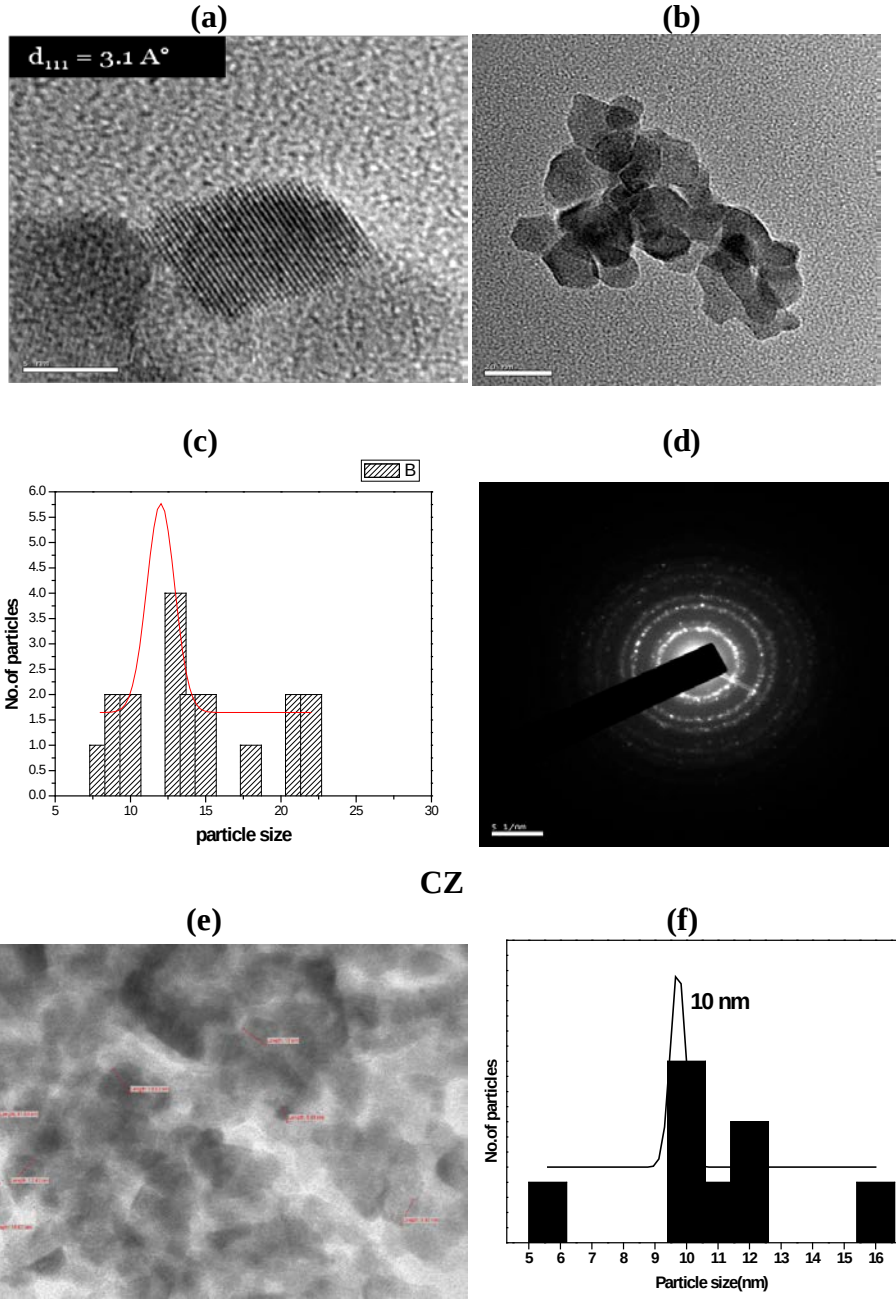

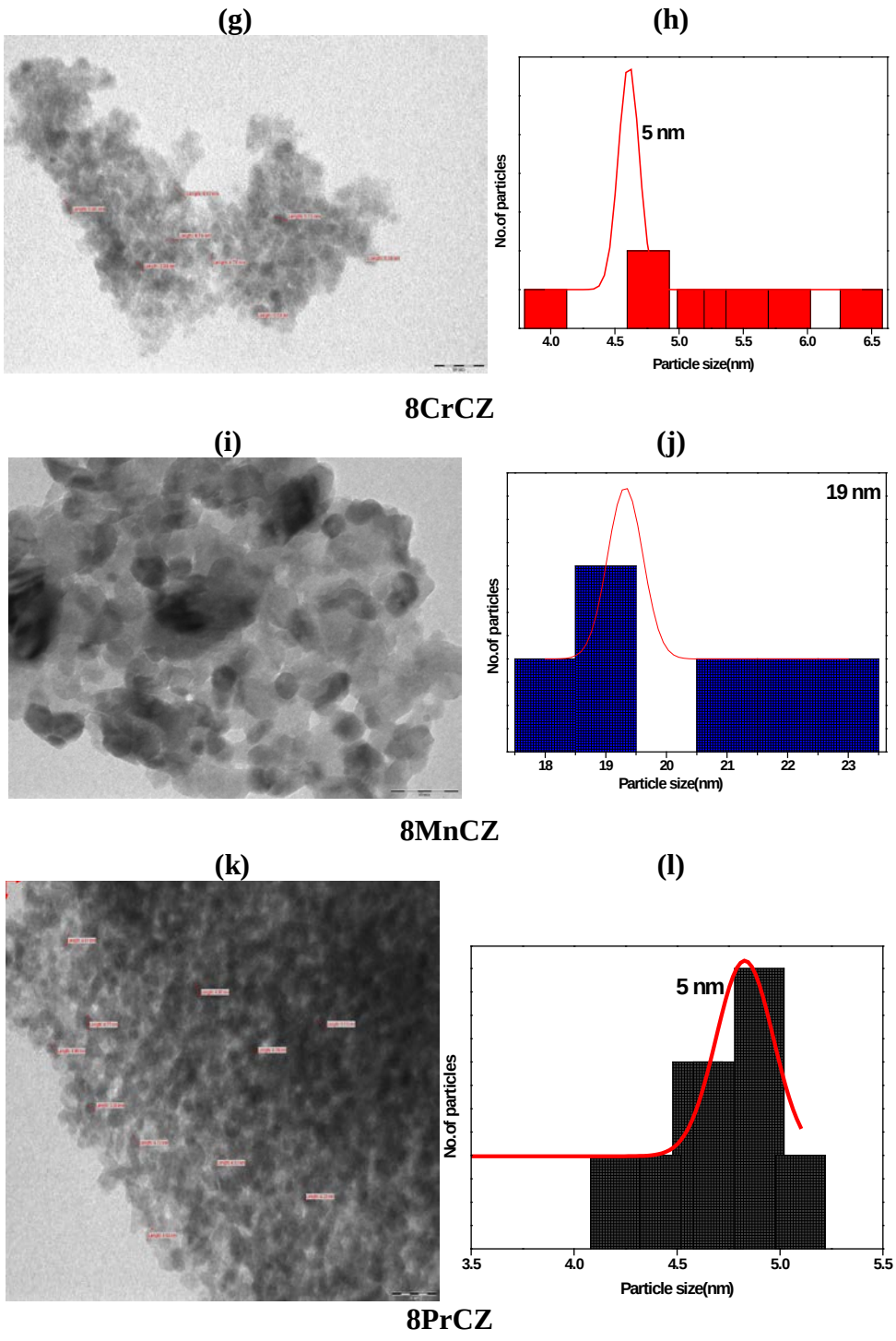

Fig. 3.15: Transmission electron micrographs and particle size histogram of pure and modified ceria-zirconia catalysts.

3.2.11. Temperature Programmed Reduction

The reducibility of the carrier of supported metal catalysts is a very important issue in association with its ability to generate oxygen vacancies and transfer the oxygen onto the metal particles. H_2-TPR experiments were performed to analyze the reducibility of the catalysts. TPR profiles are plotted in Fig.3.16. The quantification of H_2 consumption is estimated and summarized in Table 3.4.

TPR patterns of ceria-zirconia support are given in Fig.3.16 (a). It is reported in the literature that two peaks are observed in the TPR patterns of some ceria-based catalysts and are assigned as (i) the reduction of the most easily reducible surface oxygen of ceria species and (ii) the removal of oxygen from bulk ceria.[2] In the case of ceria-zirconia mixed oxides, researchers suggest that it is difficult to differentiate between the surface and bulk reduction as both reduction peaks appear together i.e., both reduction occurs concurrently.[24,38] For CZ sample, the temperature maxima for the reduction is around 521°C. In addition to this, there is a small hump observed at lower temperature region around 405°C. This can be attributed to the reduction of surface Ce^{4+} to Ce^{3+}.[11] In line with earlier findings as the Zr content increases (for C1Z2), one TPR peak at 516°C is observed. The H_2 consumption values calculated from the peak area under the reduction peaks over the complete temperature range for the CZ and C1Z2 samples are 1145 and 1187 μmol g^{-1} of the catalyst, respectively. This shows that the degree of reduction is enhanced to more extent when the Zr content is increased, as shown by higher H_2 consumption. This shows that redox properties of ceria-zirconia systems are improved by increasing Zr content.

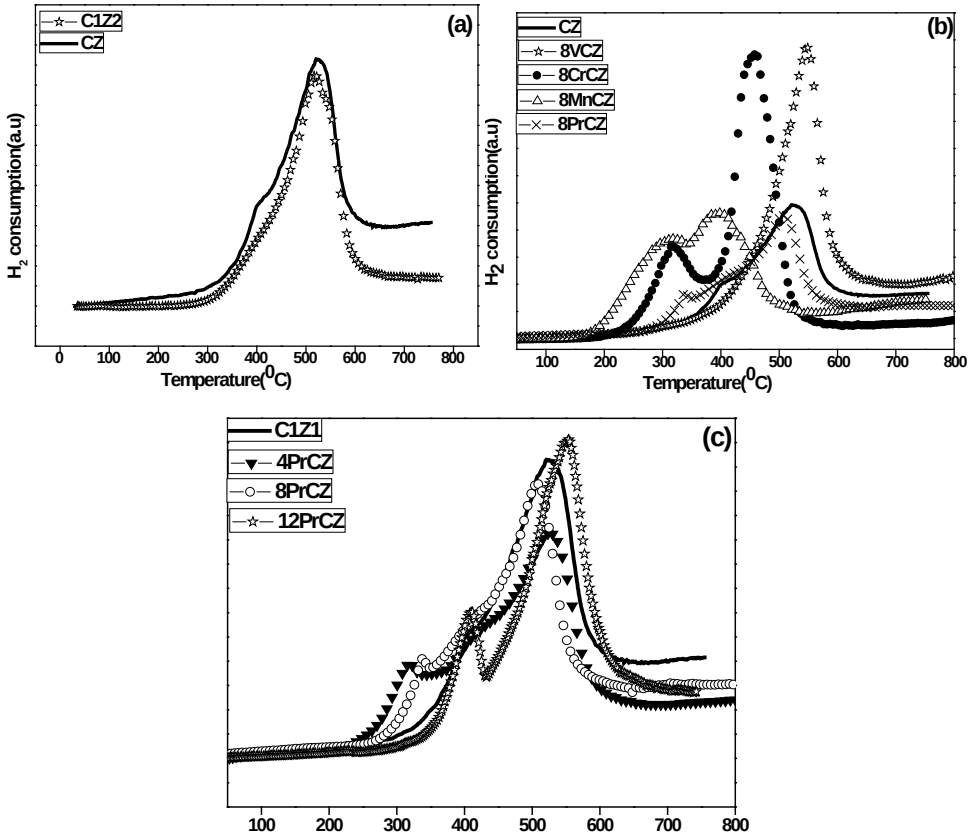

Fig. 3.16: H_2-TPR profile of modified and pure ceria-zirconia catalysts.

3.2.11.1. Modified Ceria-Zirconia Catalysts

The H_2-consumption profiles of metal modified ceria-zirconia obtained from TPR are compiled in Fig.3.16 (b) and (c).

i. Vanadium impregnated ceria-zirconia

TPR profile of vanadium modified ceria-zirconia mixed oxide is shown in Fig.3.16 (b). Addition of vanadium to the pure ceria-zirconia brought about increase in the intensity of peak, which is centered around 550°C. This is apparently due to the reduction of surface vanadium species

(V^{5+} to V^{3+}) and the reduction of surface cerium ions.[7] The reduction of pure V_2O_5 to V_2O_3 is evidenced between 600 and 790°C.[39] Nevertheless, the purity, the preparation method and the partial pressure of hydrogen can have major influence on the reduction level of vanadium oxide.

ii. Chromium impregnated ceria-zirconia

8CrCZ give rise to a major TPR peak at 460°C with shoulder peak around 318°C. The high-temperature peak can be attributed to the combined reduction of Cr^{6+} in the dispersed chromium oxide particles and oxygen removal of ceria, while the low-temperature peak can be attributed to the reduction of Cr^{6+} in the large crystals of chromia in the catalysts.[40] TPR patterns do not show any indication about Cr^{3+} oxidation state. The phase transformation of the high-oxidation state of Cr species [Cr(VI)] to low-oxidation-state Cr species [Cr(III)] starts from the surface region and then extends to the bulk. The presence of Cr^{3+} is more obviously detected by Raman spectroscopy. This is because Raman spectroscopy is more sensitive to the surface region, but the TPR technique usually gives bulk information of the sample.[41]

iii. Manganese impregnated ceria-zirconia

The reduction profile of manganese modified catalysts is complicated. TPR profile of 8MnCZ is characterized by two peaks at 312°C and 396°C. The assignment of the aforementioned peaks to different MnO_x species or to specific reduction steps is not straightforward, because reduction of ceria takes place concurrently. It is reported that peak reduction temperature for pure MnO_x is about 464°C.[19] The low-temperature peak is perhaps corresponds to the formation of the Mn_3O_4 phase and the high-temperature reduction is assigned to the surface oxygen removal of ceria i.e., reduction of

Ce^{4+} to Ce^{3+}. For the manganese modified sample, considerable decrease in the reduction temperature suggest the absence of crystallites or islands of the MnO_x phase in this sample.[42]

iv. Praseodymium impregnated ceria-zirconia

The TPR profiles of 4, 8 and 12 wt % Pr modified catalysts are shown in Fig.3.16 (c). For each sample, there are two reduction peaks. As the Pr content increases, the low temperature reduction peak shifts to a higher temperature, whereas the high temperature reduction peak shifts to lower temperature for 8PrCZ and then to higher temperature for 12PrCZ. It is also reported that as T_{max} increases, dispersion of the metal decreases. The crystallites formed may not have a strong interaction with the support oxide.

TPR behavior appears to be governed both by textural and structural properties of the samples. Thus a good correlation is observed between hydrogen consumption with surface area for metal modified ceria-zirconia catalysts (Fig.3.17). In conformity with literature reports, it appears a linear relationship between the surface area and hydrogen consumed in the TPR peak.[43, 44]

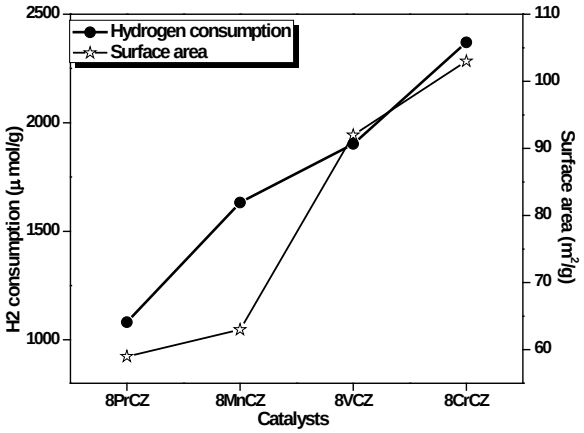

Fig. 3.17: Variation of the hydrogen consumption TPR peak as a function of BET surface area

Table 3.4. Peak temperatures and calculated H_2 consumption in the TPR of pure and modified samples

Catalysts	Peak temperature (°C)	Total H_2 consumed (µmol/g)
C1Z2	519	1187
CZ	405	1145
	521	
8VCZ	550	1902
8CrCZ	460	2370
	318	
8MnCZ	312	1632
	396	
4PrCZ	318	1132
	524	
8PrCZ	337	1082
	506	
12PrCZ	412	1178
	555	

3.2.12. Surface Acidity Measurement

3.2.12.1. Temperature Programmed Desorption of Ammonia

Acidity depends on the nature of the oxide, the charge and radius of the metal ions, nature of the metal-oxygen bond and the filling of the metal d-orbitals. In this method, to determine the amount and strength of the acid sites, the interaction of acid sites with basic probe molecule is studied.[45] Ammonia is an excellent probe molecule since it allows the distribution of both the protonic and cationic acid centers. The temperature programmed desorption of ammonia (NH_3-TPD) is used to characterize the acid site distribution and furthermore to obtain the quantitative amounts of the acid sites in the specified temperature range. The TPD of ammonia is performed to determine the total

amount of acidity of the catalysts. The acid site distribution pattern can be classified into weak (desorption at 100-400°C) and strong (above 400°C) acid sites.[46] The amount of ammonia desorbed below 100°C may contain some amount of physisorbed ammonia also. The sum of the areas under the peak at temperature less than 400°C is assumed to be the number of weak acid sites and the sum of the areas under the peak at temperature higher than 400°C is associated with the number of strong acid sites.

The TPD of NH_3 for ceria-zirconia mixed oxides is presented in Fig.3.18 (a). Table 3.5 gives the distribution of acid sites of metals modified and pure ceria-zirconia samples. The total concentration of acid sites was calculated as the amount of ammonia adsorbed per gram of the catalyst. All the catalysts exhibited a broad NH_3-TPD peak. The broad desorption pattern indicates a large distribution of acid sites of different strength. From Fig.3.18 (a) and Table 3.5, it is noticed that the contribution to the total acidity was higher at larger ZrO_2 contents. The observation was consistent with the earlier literature reports.[17,47] It is generally established that the surface acidity of ceria-zirconia mixed oxide is due to surface Ce^{4+} species, Zr^{4+} species and $OH^{\delta-}$ species. As the zirconium content increases, the total acidity increases. The zirconium ion radius is (0.84 Å) smaller than that of Ce ion (0.97 Å) and it is likely to exhibit acidic nature in solid solutions.[48,49]

3.2.12.1.1. Modified Ceria-Zirconia Catalysts

The TPD profiles of metal modified ceria-zirconia are shown in Fig.3.18 (b), (c), (d), (e). These desorption profiles show a different pattern signifying a marked increase in the acidic strength and its distribution in comparison to the ceria-zirconia support. This clearly indicates that

impregnated metal strongly influence the acidic properties of ceria–zirconia mixed oxides. This is speculated to the presence of surface M^{x+} ions.

i. Vanadium impregnated ceria-zirconia

For vanadium loaded series, a broad ammonia desorption profile in the range 170–310°C with highest desorption around 250°C can be noted. This is due to the presence of weak acid sites. In addition to this peak, high temperature desorption peak is also observed. The formation of strong acid sites may be responsible for the high temperature desorption peaks. As vanadium content increases, the total acidity also increases. At higher loading (12VCZ), the large amount of weak acid site may be due to the presence of crystalline V_2O_5.[11]

ii. Chromium impregnated ceria-zirconia

In the case of Cr modified samples, a single low temperature desorption peak is observed at about 260-280°C. The sample possesses only weak acid sites. It does not show acid sites in higher acidity region. The decrease of acidity with increasing Cr content is in agreement with literature report.[47]

iii. Manganese impregnated ceria-zirconia

TPD profile of 12MnCZ shows typical peaks at 230-260°C, 530°C and 690°C. The former peak can be related to the weak acidity present in the catalysts while the latter two peaks to strong acidity. It can be seen that weak acid site decrease with increasing Mn content (Fig. 3.18 (d) and Table 3.5). On the other hand, strong acid sites decreases first and then increases.

iv. Praseodymium impregnated ceria-zirconia

Addition of praseodymium enhanced the surface acidity. Intensity of the peak for Pr modified catalyst is rather high which indicates the presence of high

concentration of acid sites (Fig. 3.18 (e)). The strong acid sites may be due to the highly dispersed praseodymia.[11] Strength of the acid sites become stronger gradually with an increase in Pr loadings both in weak and strong acid region.

It can be concluded that metal loading modifies surface acidic properties of the ceria-zirconia support. The strength and position of ammonia desorption peak is influenced by the nature of the metal impregnated on the support oxide. Within each series as the metal content increases, even though there is a change in the total acidity, there is no steady increase in the acidity for all the metals. Among different metals, the acidity is roughly in the order: PrCZ>VCZ>MnCZ>CrCZ. It appears from the present study that the relatively strong acidity of V and Pr loaded ceria-zirconia catalysts may be due to relatively high oxidation state of the metal ion.

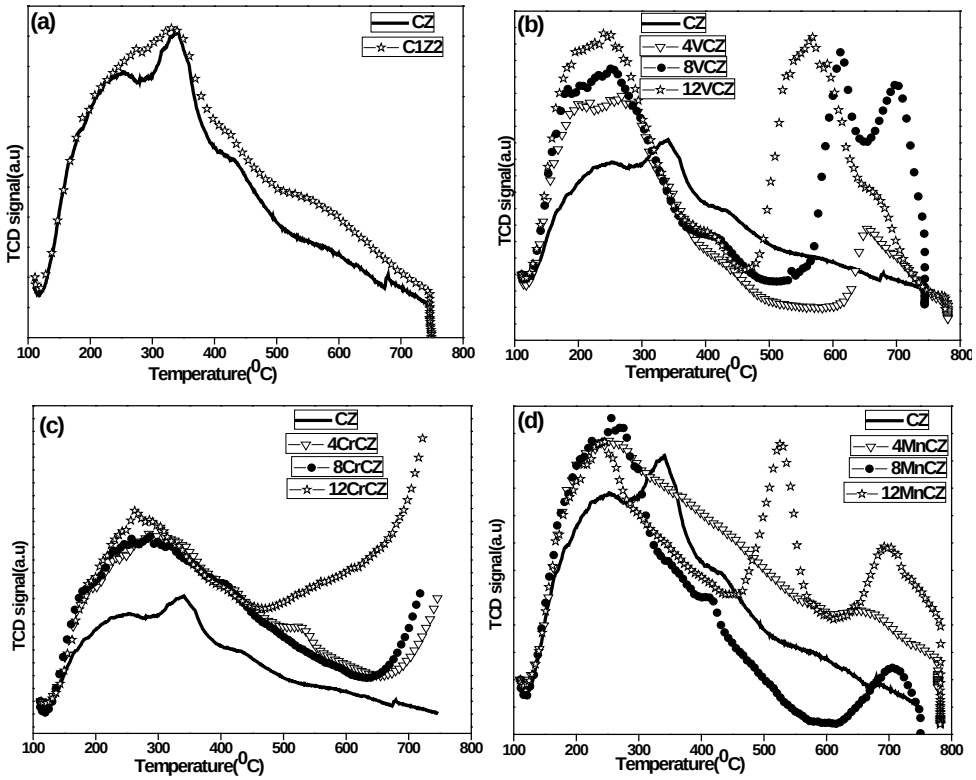

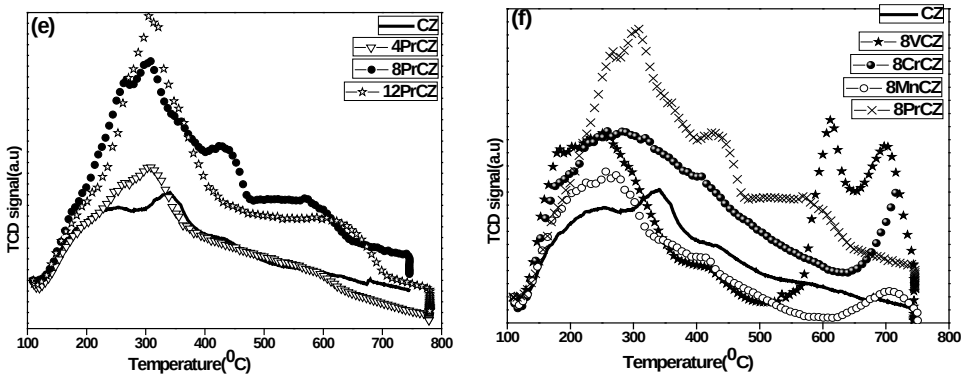

Fig. 3.18: Temperature programmed desorption of modified and pure ceria-zirconia catalysts.

Table 3.5. Acidity distribution of modified and pure ceria-zirconia catalysts.

Sample	Acidity Distribution (mmol/g)		
	Weak [(101-400℃)	Strong (Above 400℃)	Total Acidity
CZ	0.054	-	0.054
C1Z2	0.067	-	0.067
4VCZ	0.056	0.012	0.068
8VCZ	0.053	0.041	0.094
12VCZ	0.065	0.052	0.117
4CrCZ	0.084	-	0.084
8CrCZ	0.072	-	0.072
12CrCZ	0.048	-	0.048
4MnCZ	0.066	0.008	0.074
8MnCZ	0.055	0.005	0.060
12MnCZ	0.045	0.043	0.088
4PrCZ	0.056	0.021	0.077
8PrCZ	0.073	0.046	0.119
12PrCZ	0.106	0.042	0.148

3.2.12.2. Cumene Cracking Reaction-Test Reaction for Acidity

Model reactions allow not only to verify rapidly the suitability of a solid acid as a catalyst but also to characterize its acidity. It is well known that acidity of the mixed oxide support has a substantial effect on the activity of cumene hydrocracking.[50] Vapour phase cumene cracking is a model reaction for identifying the Lewis and Brønsted acid sites present in a catalyst. The major reactions taking place during the cracking of cumene are dehydrogenation to give α-methyl styrene over Lewis acid sites (LAS) and dealkylation to give benzene, ethylbenzene and propene over Brønsted acid sites (BAS). The cracking of cumene, producing benzene and propene, is generally attributed to the action of Bronsted acid sites, following a carbonium ion mechanism. Dealkylation and side chain cracking results in the formation of ethyl benzene and toluene while dehydrogenation of ethyl benzene gives styrene.[51]

A comparison of the amount of benzene and α-methyl styrene gives an idea about the BAS and LAS possessed by the catalyst. In the present work cumene conversion reaction was carried out in a vapour phase reactor. The procedure is given in Chapter 2 (section 2.3.12.2). α-methyl styrene and benzene were observed as the major products with small amounts of other dealkylated products. The cracking products are considered together as dealkylated products.

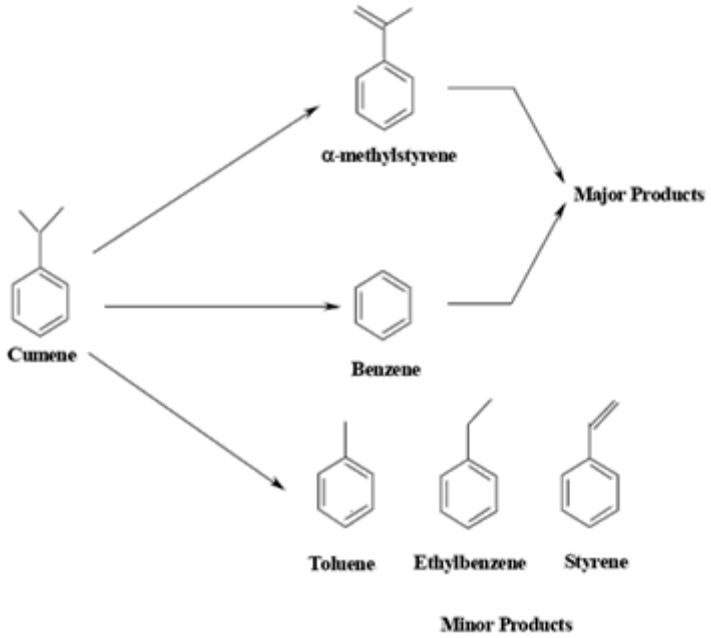

Scheme 3.1. Pathways of cumene cracking reaction.

It can be found that α-methyl styrene is the major product along with some de-alkylated products (Table 3.6). This shows the presence of both Lewis and Brönsted acid sites on the catalyst. Higher selectivity towards α-methyl styrene for the impregnated systems suggests the enhancement in Lewis acidity upon modification. In pure ceria-zirconia, the Lewis acidity markedly increased on adding ZrO_2. This is attributed to more number of surface Zr^{4+} ions. Therefore, the high acidity is found for the mixed oxide with the highest ZrO_2 content. For the transition metal impregnated catalysts, selectivity to α-methyl styrene was found to decrease with increase in metal content. Barton *et al*. have reported that an increase in Brønsted acidity with increasing tungsten oxide, WO_x, surface coverage appears to be related to the conversion of isolated tungstate groups into polytungstate clusters, which can delocalize protons among neighbouring WO_x species.[52] At low WO_x coverages, isolated tetrahedral tungstate groups are responsible for the enhanced Lewis acidity. So in our study

also, Lewis acidity is higher for low metal content which may be due to the presence of isolated metal oxide sites. Cluster of metal oxide species can cause the increase in Bronsted acidity i.e., reduction in Lewis acidity.

Table 3.6. Catalytic activity of modified and pure ceria-zirconia catalysts on cumene cracking reaction.

Sample	Cumene Conversion	Distribution of Products (%)		Lewis/Bronsted acidity
		α-Methyl styrene	Dealkylated products	
C2Z1	12.1	26.3	73.7	0.3
CZ	9.5	28.2	71.8	0.4
C1Z2	6.3	61.8	38.2	1.6
4VCZ	9.3	72.9	27.1	2.7
8VCZ	10.0	69.0	31.0	2.2
12VCZ	10.9	32.2	67.8	0.5
4CrCZ	16.8	73.7	26.3	2.8
8CrCZ	11.0	72.8	27.2	2.7
12CrCZ	10.0	37.7	62.3	0.6
4MnCZ	4.2	78.0	22.0	3.5
8MnCZ	4.4	77.7	22.3	3.4
12MnCZ	5.3	64.3	35.7	1.8
4PrCZ	4.8	70.5	29.5	2.4
8PrCZ	4.9	56.0	44.0	1.3
12PrCZ	9.0	53.4	46.6	1.1

3.3. Concluding Remarks

- The structural characteristics of modified and unmodified ceria-zirconia mixed oxide have been systematically investigated. These catalysts were synthesised via hydrothermal method and modified

with vanadium, chromium, manganese and praseodymium by wet impregnation method.

- Wide Angle XRD studies revealed the presence of cubic fluorite structure for ceria-zirconia mixed oxide. Reflections observed in the low angle XRD analysis was an indication of mesoporous nature of the prepared material.
- The prepared catalysts exhibited good BET surface area and mesoporosity was further confirmed by type IV isotherm which is typical of mesoporous material.
- Thermal stability of the prepared catalyst was evident from the thermogram.
- Raman spectroscopy measurements revealed the structure of metal oxides dispersed on the support.
- Oxidation states of the metal were suggested by XPS measurements.
- Surface morphology was studied from TEM images which confirm the presence of nano-meter sized particles of the prepared catalysts.
- Redox behaviour was evident from the TPR patterns.
- Acidity studies confirmed the enhancement of surface acidity upon modification with transition metals.

References

[1] S. Sato, K. Koizumi, F. Nozaki, J. Catal. 178 (1998) 264.

[2] S. Damyanova, B. Pawelec, K. Arishtirova, M.V.M. Huerta, J.L.G. Fierro, Applied Catalysis A: General 337 (2008) 86.

[3] F. Zhang, Chih-Hao Chen, C.J. Hanson, D.R. Robinson, P.I. Herman, Siu-Wai Chan, J. Am. Ceram. Soc. 89 (2006) 1028.

[4] K.J.P. Rose, Ph. D thesis, Studies on catalysis by mesoporous ceria modified with transition metals, Cochin University of Science And Technology (2012).

[5] M.K. Devaraju, X. Liu, K. Yusuke, S. Yin, T. Sato, Nanotechnology 20 (2009) 405.

[6] K.J. P. Rose, S. Sugunan, Bulletin of Chemical Reaction Engineering, Catalysis, 7 (2012) 158.

[7] S.S.R. Putluru, A. Riisager, R. Fehrmann, Catal. Lett 133 (2009) 370.

[8] T. Radhika, S. Sugunan, Catalysis Communications 8 (2007) 150.

[9] R.P. Viswanath, P. Wilson, Applied Catalysis A: General 201 (2000) 23.

[10] M. Salavati-Niasari, F. Davar, M. Mazaheri, Polyhedron 27 (2008) 3467.

[11] X. Gu, J. Ge, H. Zhang, A. Auroux, J. Shen, Thermochimica Acta 451 (2006) 84.

[12] K.J. P. Rose, S. Sugunan, International Journal of Scientific & Engineering Research 3 (2012)1.

[13] Q. Yu, X. Wu, C. Tang, L. Qi, B. Liu, F. Gao, K. Sun, L. Dong, Y. Chen, Journal of Colloid and Interface Science 354 (2011) 341.

[14] D. Ramimoghadam, M.Z.B. Hussein, Y. H. Taufiq-Yap, Int. J. Mol. Sci. 13 (2012) 1327.

[15] W. Man-juan, G. Ying-ying, Q. Li-ping, L. Jin-lin, X. Wen-yang, J. Cent. South Univ. Technol. 15 (2008) 796.

[16] M. Ocana, Colloid Polym Sci. 280 (2002) 274.

[17] G. R. Rao, H.R. Sahu, Proc. Indian Acad. Sci. (Chem. Sci.) 113 (2001) 651.

[18] L. Jian, Z. Zhen, X. Chunming, D. Aijun, J. Guiyuan, Journal of rare earths, 28 (2010) 198.

[19] B. Murugan, A.V. Ramaswamy, D. Srinivas, C.S. Gopinath, V. Ramaswamy, Chem. Mater. 17 (2005) 3983.

[20] M. B. Reddy, G. Thrimurthulu, L. Katta, J. Phys. Chem. C 113 (2009) 15882.

[21] I. Atribak, A. Bueno-López, A. García-García, Journal of Molecular Catalysis A: Chemical 300 (2009) 103.

[22] M.B. Reddy,P. Bharali, G. Thrimurthulu, P Saikia, L. Katta, S. Park, Catal Lett 123 (2008) 327.

[23] V.S. Escribano, E.F. Lopez, M. Panizza, C. Resini, J.M.G. Amores, G. Busca, Solid State Sciences 5 (2003) 1369.

[24] L. Katta, P. Sudarsanam, G. Thrimurthulu, M. B. Reddy, Applied Catalysis B: Environmental 101 (2010) 101.

[25] J. Matta, D. Courcot, E. Abi-Aad, A. Aboukais, Chem. Mater. 14 (2002) 4118.

[26] J. Mougin, T. L. Bihan, G. Lucazeau, Journal of Physics and Chemistry of Solids 62 (2001) 553.

[27] F. Farzaneh, M. Najafi, Journal of Sciences, Islamic Republic of Iran 22 (2011) 329.

[28] M.B. Weckhuysen, E.I. Wachs, J. Phys. Chem. 100 (1996) 14437.

[29] K. Kohler, J. Engweiler, H. Viebrock, A. Baiker, Langmuir 11 (1996) 3423.

[30] F. Buciuman, F. Patcas, R. Craciun, R.T.D. Zahn, Phys. Chem. Chem. Phys. 1 (1999) 185.

[31] M.B. Reddy, K.G. Reddy, H. L. Reddy, I. Ganesh, The Open Physical Chemistry Journal 3 (2009) 24.

[32] D. Cheng, M. Chong, F. Chen, X. Zhan, Catal Lett 120 (2008) 82.

[33] Q. Wu, J. Chen, J. Zhang, Fuel Processing Technology 89 (2008) 993.

[34] Bharali, Ph. D thesis, Design of novel nanosized ceria-based multicomponent composite oxides for catalytic applications, Osmania University (2009).

[35] X. Shi, S. Ji, K. Wang, Catal Lett 125 (2008) 331.

[36] D. Delimaris, T. Ioannides, Applied Catalysis B: Environmental 84 (2008) 303.

[37] A.M.E. Raj, S.G. Victoria, V.B. Jothy, C. Ravidhas, J. Wollschlager, M. Suendorf, M. Neumann, M. Jayachandran, C. Sanjeeviraja, Applied Surface Science 256 (2010) 2920.

[38] I. Atribak, A. Bueno-Lopez, A. Garcıa-Garcıa, Catalysis Communications 9 (2008) 250.

[39] E. Abi-Aad, J. Matta, D. Courcot, A. Aboukais, J Mater Sci. 41 (2006) 1827.

[40] L. Huiyun, Y. Yinghong, M. Changxi, X. Zaiku, H. Weiming, G. Zi, Chin J Catal, 27 (2006) 4.

[41] L. Xing, Q. Bi, Y. Wang, M. Guo, J. Lu, M. Luo, J. Raman Spectrosc. 42 (2011) 1095.

[42] M. Abecassis-Wolfovich, M.V. Landau, A. Brenner, M. Herskowitz, Ind. Eng. Chem. Res. 43 (2004) 5089.

[43] A. Frennet, J.M. Bastin, Catalysis and automotive pollution control III, Elsevier Science B.V. (1995) ISBN 0-444-82019-1

[44] V. Perrichon, A. Laachir, G. Bergeret, R. Frety, L. Tournayan, J Chem. Soc. Faraday Trans. 90 (1994) 773.

[45] R. Alcantara, L. Canoira, P.G. Joao, J.M. Santos, I. Vasques, Appl. Catal. A: Gen. 203 (2000) 259.

[46] S. Wang, X. Ma, J. Gong, X.Yang, H. Guo, G. Xu, Ind. Eng. Chem. Res. 43 (2004) 4027.

[47] J.I. Gutierrez-Ortiz, B.D. Rivas, R. Lopez-Fonseca, J.R. Gonzalez-Velasco, Journal of Thermal Analysis and Calorimetry 80 (2005) 225.

[48] K. Tomishige, H. Yasuda, Y. Yoshida, M. Nurunnabi, B. Li, K. Kunimori, Green Chem. 6 (2004) 206.

[49] B.1. Mishra, G.R. Rao, J. Mol Catal. A: Chem. 243 (2005) 204.

[50] S. M. Rana, S.K. Maity, J. Ancheyta, G. M. Dhar, T.S.R. P. Rao, Applied Catalysis A: General 258 (2004) 215.

[51] S.M. Bradely, R.A. Kydd, J. Catal. 141 (1993) 239.

[52] G. D. Barton, L. S. Soled, E. Iglesia, Topics in Catalysis 6 (1998) 87.

…..ꕥ…..

Chapter 4

TRANSESTERIFICATION OF DIETHYL MALONATE

Contents

Transesterification reaction with alcohols has been recognized as one of the most important unit reactions in organic synthesis. It provides essential synthons for a large number of applications in organic processes. In this chapter, transesterification of diethyl malonate with n-butanol has been carried out in liquid phase condition using modified ceria-zirconia as catalyst. Effect of various reaction parameters have been investigated thoroughly. Influence of acid strength of the catalyst on the catalytic properties has been taken into consideration for the better understanding of the reaction.

4.1. Prologue

Transesterification is one of the classic organic reactions that have the benefit of numerous laboratory uses and industrial applications. Transesterification is a process in which an ester is transformed into another one through interchange of the alkoxy moiety (Scheme 4.1).

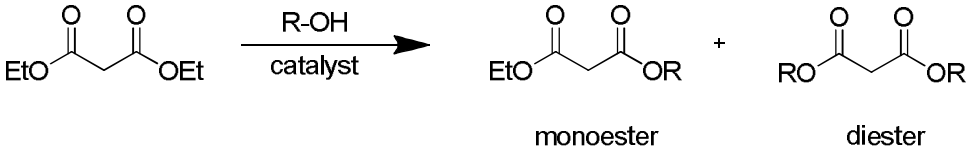

Scheme 4.1: Reaction scheme for the transesterification of dimethyl malonate with alcohol

Since the reaction is an equilibrium process, the transformation occurs essentially by simply mixing the two components.[1] However, it has long been

known that the reaction is accelerated by acid or base catalysts. Because of their versatility, the acid- or base-catalyzed reactions have been the subject of extensive investigation and the fundamental features were almost brought to light during 1950s and 1960s. The conventional catalysts which are readily available and highly active catalysts for this reaction come under homogeneous class. But the use of homogeneous catalysts requires neutralization, use of large amount of solvents and energy.[2] Besides, it is difficult to remove the catalyst from reaction products, thus leading to environmental problems such as generation of corrosive, toxic and hazardous wastes. Under this circumstance, researchers are endeavouring the use of heterogeneous catalysts for the transesterification reaction.[3]

Transesterification is nowadays a well studied reaction in association with the production of fuels and chemicals from renewable feed stocks. Transesterification of vegetable oil with alcohols has long been a preferred method for producing biodiesel. Vegetable oil, a natural product that is abundant in plants, is a combination of glycerol and different fatty acids. Biodiesel can be used as a blend with or as a total substitute for petroleum diesel. Biodiesel fuel produced during this transesterification process is already on the market in some countries such as those in North America, some European countries and in Japan. The major draw-back with this reaction is that by-products like diglyceride, monoglyceride and commercially important fatty esters poses problem during product purification and catalyst recovery.[4,5] Jitputti *et al.* studied the preparation of biodiesel *via* the transesterification of palm kernel oil and crude coconut oil using metal oxide catalysts such as ZrO_2, ZnO, SnO_2/SO_4^{2-}, BrO_2/SO_4^{2-}, KNO_3/KI zeolites and KNO_3/ZrO_2 and has shown that all of these materials show a potential to be used as heterogeneous catalysts for these reactions.[6]

Furthermore, transesterification is applicable in the paint industry for the curing of alkyl resin. It also plays an important role in polymerization.[7]

Transesterification is catalyzed by acidic or basic catalysts such as tertiary amine ion exchange resins, sodium chloroacetate, alkali alcoholates, Zr, Ti and Sn based homogeneous catalysts, acidic ion exchange resins bearing sulfonic acid and carboxylic acid functional group as well as enzymes. Reagents based on iodine include indium triodide, iodotrimethyl silane–iodine, and others.[2] Transesterification can be classified into three categories, *i.e.* heterogeneous, homogeneous and enzymatic catalyzed transesterification.[4] Tetrahydofurfuryl butyrate has been synthesized by transesterification between tetrahyrofurfuryl alcohol and ethyl butyrate catalyzed by enzyme lipase. The application of a dibutyltin oxide complex as a homogeneous catalyst for transesterification has been reported in the literature.[8] This catalyst was used for the preparation of diphenyl carbonate *via* transesterification of dimethyl carbonate with phenol. The homogeneous reactions are characterized by high reaction rates as well as selectivities, but the major disadvantage associated with such processes is the intricate recovery of the catalyst from the reaction mixture. Tin oxide modified mesoporous SBA-15 catalyst was evaluated for transesterification of diethyl malonate with a number of alcohols and good results were obtained.[2] During transesterification with *n*-butanol, 75.2% of diethyl malonate was converted in 24 hours with a selectivity of 98.8% over Sn incorporated mesoporous silica molecular sieve SBA-15. Recently Vijayasankar *et al*. reported that amorphous mesoporous iron aluminophosphates exhibited better catalytic activity in the transesterification of diethyl malonate and benzyl alcohol with higher yield and selectivity.[9] Total transester yield was found to be 79% over the

prepared FeAlPs. Very recently, Si MCM-41 supported heteropolytungstic acid (HPWA) was reported as a promising catalyst for the production of transesters in chemical industries.[3] They reported the transesterification of diethyl malonate (DEM) with n-butanol, under autogeneous conditions, yielded two trans-esterified products, butyl ethyl malonate (monoester) and dibutyl malonate (diester).

Strong acids catalyse the reaction by donating a proton to the carbonyl group, thus making it a more potent electrophile whereas bases catalyse the reaction by removing a proton from the alcohol, thus making it more nucleophilic. The acid catalyzed reaction follows usually the formation of a carbocation on the carbonyl carbon of an ester, which then facilitates nucleophilic attack by the nucleophile of the alcohol.[2,3]

As part of our studies on the development of modified ceria zirconia mixed oxide for catalytic applications, in the present chapter we report the catalytic activity of the prepared catalyst systems in the transesterification of diethyl malonate with *n*-butanol and correlated their structure and catalytic activity.

4.2. Effect of Reaction Parameters

The transesterification reaction was done in solvent-free conditions according to the procedure given in section 2.4.1. of chapter 2. The reaction yielded two trans-esterified products, butyl ethyl malonate (monoester) and dibutyl malonate (diester). Effective catalytic systems for the transesterification require not only optimizing the structural and chemical properties of the solid catalyst but also the proper choice of other reaction parameters such as temperature, catalyst amount, time, and DEM: *n*-butanol molar ratio etc.

4.2.1. Effect of Temperature

Effect of temperature in the transesterification of DEM with *n*-butanol was initially assayed with 8VCZ as the catalyst. The reaction was carried out in the temperature range of 80-110°C. (Fig.4.1) Temperature has a notable effect on the catalytic activity and selectivity towards the products. With reaction temperature, the rate increased to reach a good conversion of DEM at 110°C. At 80°C, 39% DEM conversion was observed whereas at 110°C, the conversion of DEM reached 71.2%. Among the products, the monoester is the predominant one at lower temperature. However, as the reaction temperature increases, selectivity towards the monoester decreases. The mono and diester selectivity is nearly comparable at 110°C. The formation of diester is a conservative reaction from the initially formed mono trans-ester. Therefore the rise in temperature facilitates the diester formation.

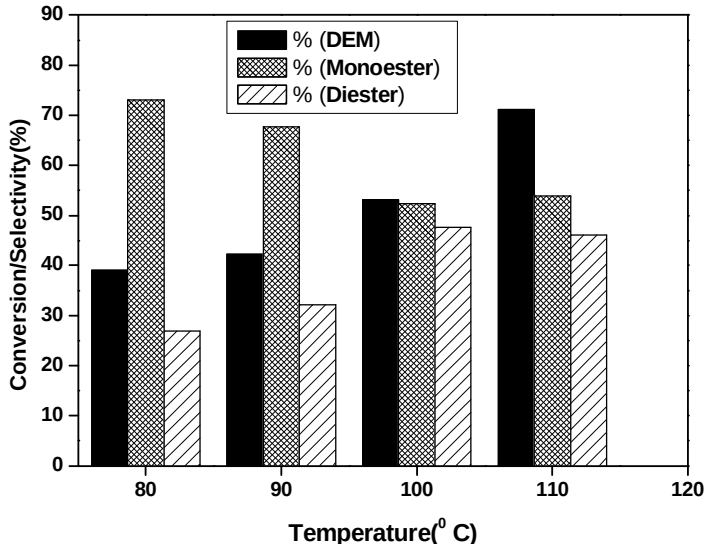

Fig. 4.1: Effect of temperature on the transesterification of DEM with *n*-butanol (Reaction conditions: 8VCZ - 0.15g, DEM: *n*-butanol - 1:5,Time-20hrs)

4.2.2. Effect of Catalyst Amount

The influence of catalyst amount was studied by taking different weight of the catalyst, 8VCZ, while keeping the other parameters constant.

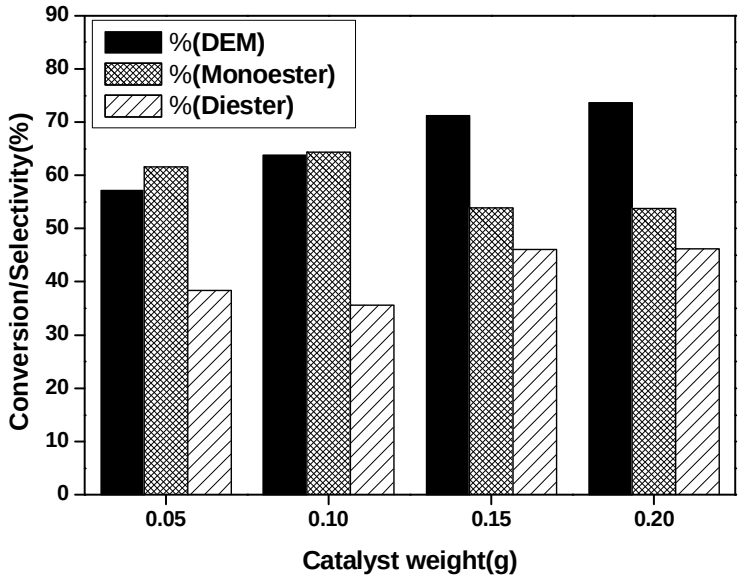

Fig. 4.2: Effect of catalyst weight on the transesterification of DEM with *n*-butanol (Reaction conditions: catalyst-8VCZ, Temperature-110°C, DEM: *n*-butanol- 1:5, Time-20hrs)

Fig.4.2 illustrates the dependence of catalyst weight on the transesterification of diethyl malonate. DEM conversion increases with increasing catalyst amount. As the catalyst amount increase from 0.05 to 0.15g the percentage conversion increases from 57 to 71%. Further increase of catalyst amount to 0.2g shows only marginal increase (2%) in conversion. Hence 0.15g is selected as the optimum catalyst amount for further studies. The selectivity for diester is found to increase with increase in the catalyst amount. The results of this study indicate that an appropriate conversion and selectivity is obtained even with the small amount of catalyst of 0.05g.

4.2.3. Effect of DEM: *n*-butanol Mole Ratio

It is reported that a large excess of alcohol is normally used in order to achieve a high yield of trans-ester.[2] Furthermore, from the economic point of view, the alcohol is more cost effective than the ester. Hence, the reaction can be performed in an excess of alcohol in the feed, which increases the conversion of DEM.

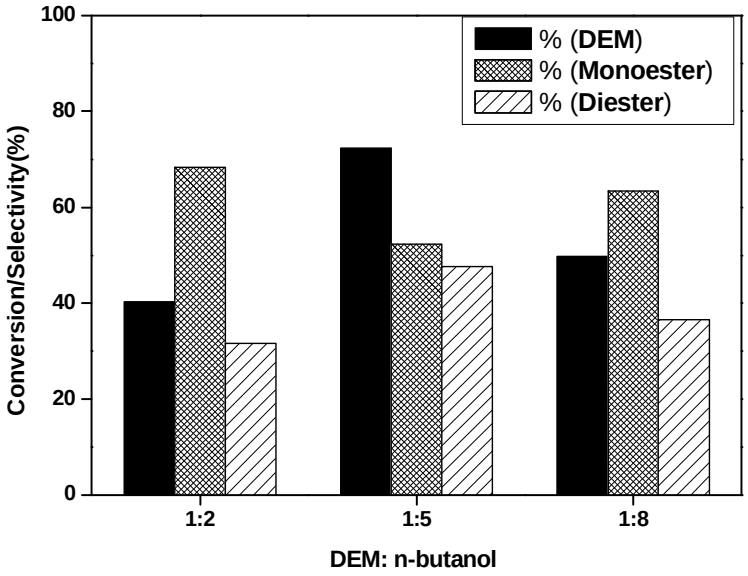

Fig. 4.3: Effect of DEM: *n*-butanol mole ratio on the transesterification of DEM with *n*-butanol (Reaction conditions: 8VCZ -0.15g, Temperature-110°C, Time-24h)

From Fig.4.3, it is clear that the mole ratio has a profound influence on the catalytic activity. The reaction was inspected over 8VCZ with mole ratios of 1:2, 1:5 and 1:8 (DEM: n-butanol) at 110°C. The percentage conversion increases with increase in alcohol concentration up to 1:5 mole ratio. The maximum conversion attained was 79.15% for the mole ratio of 1:5. Further increase in mole ratio caused a decrease in conversion. Ajaikumar *et al*. reported that decreased DEM conversion at higher alcohol content might be due to dilution in the availability of carbonyl groups of the

ester nearer to the Brønsted acid sites of the catalyst which reduced the formation of carbocation.[3] This might indeed be the case for the present study given that low conversion is observed at DEM: n-butanol ratio of 1:8.

4.2.4. Effect of Time

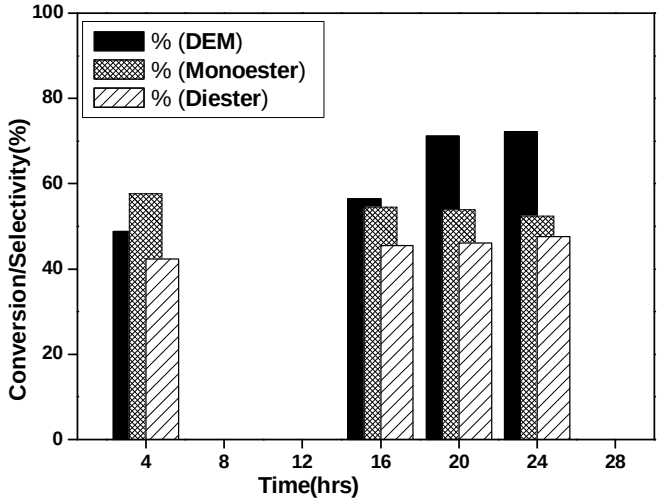

Fig. 4.4: Effect of time on the transesterification of DEM with *n*-butanol (Reaction conditions: 8VCZ -0.15g, Temperature-110°C, DEM: *n*-butanol - 1:5)

The results presented in Fig. 4.4 revealed the effect of reaction time on the conversion of diethyl malonate. Conversion of DEM increases with increase in reaction time. DEM conversion increased from 4th h (48.8 %) to 20th h (71.2 %) of reaction. After 20th hr of the reaction time it showed only marginal increase in conversion thereby the reaction time of 20th hr is the optimum time for the conversion of diethyl malonate in the case of modified ceria-zirconia catalyst. The studies show that the monoester conversion decreases slightly with increase in reaction time. Among the products, the distribution of trans-mono ester and diester show that the latter is being formed at the expense of monoester and points to a consecutive reaction scheme in the presence of the prepared catalyst.

4.2.5. Effect of Solvent

An appropriate solvent in liquid phase reaction should be inert, not reacting with reactants or deactivating the catalyst. The nature of solvent may have a profound effect on the activity of transesterification. Therefore, the reaction was carried out in presence of a polar solvent, dimethyl sulfoxide and a non-polar solvent, *o*-xylene.

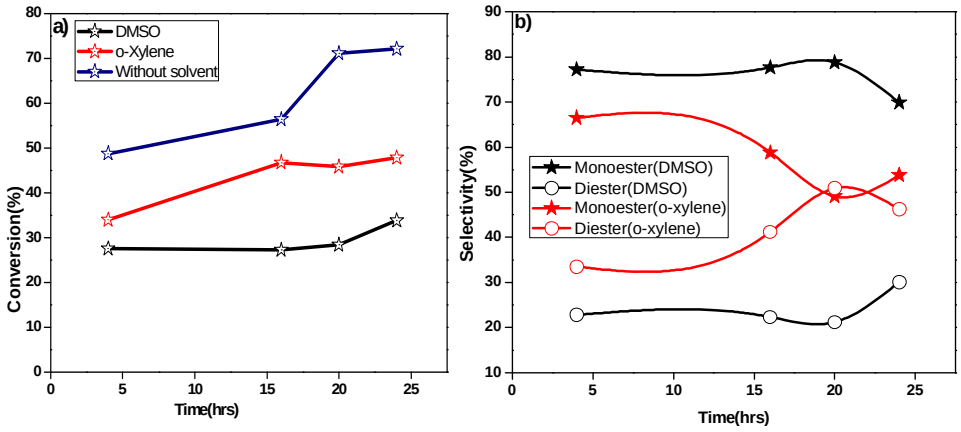

Fig. 4.5: Effect of solvents on the transesterification of DEM with n-butanol (a) conversion (b) selectivity (Reaction conditions: 8VCZ -0.15g, Temperature-110°C, DEM: *n*-butanol - 1:5, Solvent-10ml)

The influence of the solvents on the conversion of DEM over 8VCZ is presented in Fig. 4.5 (a). The presence of solvent causes lower activity in the tranesterification reaction. In DMSO, the activity is quite less. It can be seen from the figure that catalytic activity is improved by using *o*-xylene. DMSO, being a polar aprotic solvent, is more likely to adsorb on the catalyst surface and compete for sites with the substrate. Furthermore, one purpose of using a solvent is to reduce the kinematic viscosity of the reaction mixture. The better catalytic activity in presence of *o*-xylene is perhaps due to the fact that *o*-xylene has lower kinematic viscosity than DMSO. These results are in agreement with the observation of Ngaosuwan

et al.[10] They reported that high catalytic activities for transesterification of tricaprylin using hexane as solvent over tungstated zirconia is due to the non-polar and low kinematic viscosity inducing characteristics. They found that tetrahydrofuran (THF), in contrast, having a higher polarity, tended to reduce the activity for transesterification reaction. From Fig.4.5 (b), it can be seen that when DMSO was used as the solvent, the reaction is more selective towards monoester in spite of the lower conversion.

It is remarkable to mention that the catalytic activity of the solid catalysts was higher in solvent free condition than in the presence solvents such as dimethyl sulfoxide and o-xylene. The decrease in conversion under solvent conditions is attributed to the blocking of active sites by solvent molecules or may be explained by the diffusion competition of the solvent and the substrate.

4.3. Catalytic Activity of Prepared Catalysts

The applicability of the optimized protocol was examined by carrying out the reaction with all the prepared catalysts. The results are given in Table 4.1. When compared with modified catalysts, parent ceria-zirconia support demonstrates comparatively low level of conversion. It can be seen that the catalytic materials with different modified metal exhibits distinct variation in catalytic performance.

Table 4.1. Catalytic activities of different prepared catalysts (Reaction conditions: Catalyst-0.2g, Temperature-110°C, DEM: *n*-butanol - 1:5, Time-20 hrs)

Catalyst	Conversion of DEM (%)	Selectivity (%)	
		Monoester	Diester
C2Z1	38.6	58.5	41.5
CZ	37.7	62.0	38.0
C1Z2	37.5	57.7	42.3
4VCZ	60.5	54.9	45.1
8VCZ	73.6	53.8	46.2
12VCZ	88.4	48.3	51.7
4CrCZ	31.2	68.4	31.6
8CrCZ	33.3	68.5	31.5
12CrCZ	37.6	65.0	35.0
4MnCZ	43.2	59.5	40.5
8MnCZ	49.5	65.0	35.0
12MnCZ	53.4	62.6	37.4
4PrCZ	53.6	63.4	36.6
8PrCZ	55.1	54.9	45.1
12PrCZ	58.3	58.4	41.6

Among the catalysts, vanadium modified ceria-zirconia showed the most desired catalytic performances. The conversion of DEM increases with the increasing V content in the catalyst. 4VCZ gives 60.5% conversion of DEM and 54.9% selectivity for monoester. In case of 12% V loading the conversion increased to 88.4% with 48% selectivity for monoester. The selectivity for monoester is found to decrease with increase in the vanadium content. It can be noted from Table 4.1 that CrCZ exhibited the lowest activity for transesterification as compared with other

modified systems. As Cr content increases, the conversion marginally increases and reaches 37.6% with 12CrCZ. However, the selectivity to monoester is quite good. When the transesterification was conducted over Mn modified catalysts, it is observed that the conversion reaches as high as 53.4% (62.6% monoester selectivity) with 12MnCZ. Pr modified catalysts underwent smooth transesterification of DEM. 12PrCZ exhibits an activity of 58.3% with around 58% selectivity to monoester. It is interesting to note that the selectivity of monoester decreases with increase in the Pr content from 4% to 8% and then increases with further increase in metal content. Overall, vanadium modified ceria-zirconia catalysts showed more significant conversion of DEM than other catalysts.

4.4. Leaching Studies

In order to substantiate whether the ceria-zirconia support stabilizes the active vanadium species, hot filtration experiments were performed over vanadium modified support. For that, after 1h of the reaction, the catalyst was removed by filtration. The filtrate obtained was subjected to transesterification reaction for 4 hrs and then subjected to GC analysis. Results are presented in Fig. 4.6. There is no noticeable increase in conversion; in fact, the conversion remains practically constant within experimental error. At the same time, the selectivity towards monoester diminishes in the absence of the catalyst. Furthermore, elemental analysis of the filtrate, done by AAS, revealed the absence of vanadium element. The catalyst, which resists the leaching of vanadium species, reveals the true heterogeneous nature of the reaction with this catalyst. Hence, 8VCZ has better stability and well-isolated active sites and are promising heterogeneous catalysts for transesterification reaction.

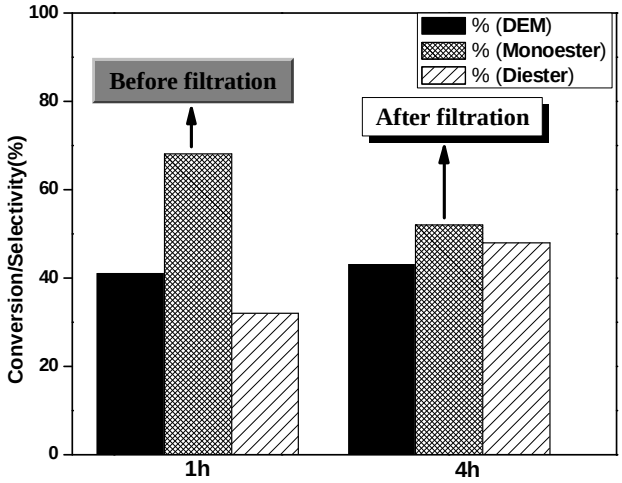

Fig. 4.6: Influence of metal leaching on the transesterification of DEM with n-butanol. (Reaction conditions: 8VCZ -0.1g, Temperature-110 °C, DEM: *n*-butanol - 1:5)

4.5. Recycle Studies

Recycling tests were performed over vanadium supported on ceria-zirconia catalyst, 8VCZ in order to evaluate whether the catalytic activity arise from stable catalytic materials. For this, the catalyst was recovered by filtration after the reaction, washed several times with acetone, dried and calcined at 400^0 C for 4hrs. Then the reaction was conducted with the recovered catalyst under the same reaction condition.

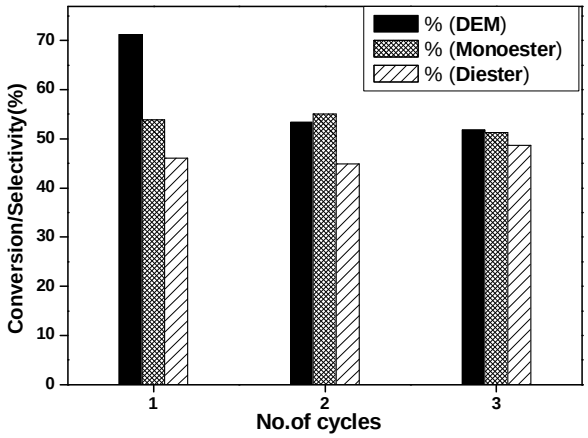

Fig. 4.7: Recycling studies performed over 8VCZ catalyst. (Reaction conditions: 8VCZ -0.15g, Temperature-110 °C, DEM: *n*-butanol - 1:5, Time-20 hrs)

Fig. 4.7 shows that during the first recycle (second run), DEM conversion decreased to 53%. The decrease in conversion during the second run may be due to the removal of trace amounts of metal species. The conversion remained more or less the same thereafter, in the third run. The product selectivity is more or less the same in all cases.

4.6. Discussion

A noteworthy feature of the present reaction is that almost all prepared materials catalyzed the transesterification reaction affording the corresponding products in fairly to excellent yields. The effect of metal impregnation on the activity of the reaction is also described by giving particular attention in correlating activity with the acidity. It is widely accepted that transesterification reaction is efficiently catalyzed by acid-base catalysts. Therefore, it is worth noting the acidity distribution from TPD of NH_3 (section 3.2.12. 1) in this context. Fig. 4.8 shows the correlation between acidity and catalytic performance of the prepared catalysts.

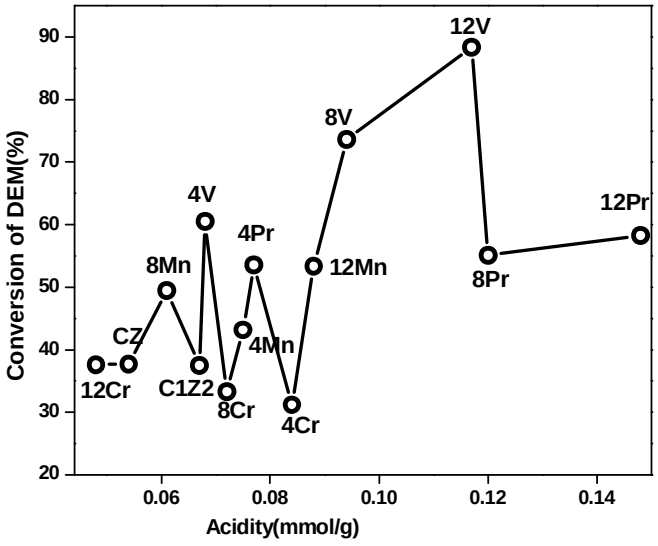

Fig. 4.8: Effect of acidity on the conversion for transesterification of diethyl malonate.

Acidity (mmol/g from NH_3-TPD) can be directly correlated with the catalytic activity. Among the catalysts tested, 12CrCZ and CZ with the least acidity exhibited the lowest catalytic efficiency. It is reported in the literature that if the catalyst has very weak acidity, the catalyst-substrate complex is speculated to be unstable.[11] As can be seen from the Fig. 4.8, below 0.08 mmol/g, the curve is in a zigzag manner. Cr modified catalysts lies in lower catalytic activity side of the curve. This may due to the fact that CrCZ's have only very weak acidity. Beyond 0.08 mmol/g, the transesterification activity increased with increasing acidity of the catalysts till it reaches 0.12 mmol/g. Notwithstanding the fact that 8Pr and 12Pr exhibit higher acidity, activity is lower. This may be due to the fact that if the catalyst is very acidic, the catalyst-substrate complex is too stable to undergo further reaction. Hence, catalysts with intermediate acidity contribute the highest catalytic activity. This indicates that the acidity of the catalyst plays a crucial role in determining the catalytic performance in this reaction.

It is clear that selectivity for monoester decreases with the acid strength. Ajaikumar *et al.* have reported that the monoester selectivity was higher at lower acid strength of the catalyst and the diester selectivity increased with an increase in acid strength.[3] Lewis acid catalysts are reported to be more active in transesterification [11, 12, 13]

4.7. Concluding Remarks

- The studies revealed that vanadium on ceria-zirconia mixed oxide is an efficient solid catalyst for transesterification of diethylmalonate with *n*-butanol in the absence of solvent.

- Various reaction parameters have considerable effects on the catalytic properties of the prepared materials. Use of solvents has diminished the conversion of DEM.
- The promising heterogeneous nature of the catalyst was well established.
- Considering the relationship between activity and acidity (from TPD), it is reasonable to infer that the acid sites on the catalyst surface have a vital influence on the catalytic activity.
- The obvious advantages of heterogeneous catalysis in terms of simple operation and recyclability of the catalyst are noteworthy.

References

[1] J. Otera, Chem.Rev. 93 (1993) 1449.

[2] S. Pallavi, V.A. Ramaswamy, K. Lazar, V. Ramaswamy, Applied Catalysis A: General 273 (2004) 239.

[3] S. Ajaikumar, M. Backiaraj, J.P. Mikkola, A. Pandurangan, J Porous Mater 20 (2013) 951.

[4] M.S. Sibiya, Catalytic transformation of propylene carbonate into dimethyl carbonate and propylene glycol, Master of Science thesis (2006).

[5] Y. Isono, H. Nabetani, M.J. Nakajima, Am. Oil Chem. Soc. 72 (1995) 887.

[6] J. Jitputti, B. Kitiyana, P. Ransunvigit, K. Bunyakiat, L. Attanatho, P. Jenvanitpanjakul, J. Chem. Eng. 116 (2006) 61.

[7] E.D. Ponde, H.V. Deshpande, J.V. Bulbule, A. Sudalai, S.A. Gajare, J. Org. Chem. 63 (1998) 1058.

[8] H. Lee, J.S. Kim, B.S. Ahn, K.W. Lee, S.H. Kim, Catal. Today 87 (2003) 139.

[9] A.V. Vijayasankar, N. Mahadevaiah, Y.S. Bhat, N. Nagaraju, J Porous Mater 18 (2011) 369.

[10] K. Ngaosuwan, X. Mo, G.J. Goodwin Jr, P. Praserthdam, Applied Catalysis A: General 380 (2010) 81.

[11] W. Shi, J. Zhao, X. Yuan, S. Wang, X. Wang, M. Huo, Chem. Eng. Technol. 35 (2012) 347.

[12] S. Wang, X. Ma, J. Gong, X. Yang, H. Guo, G. Xu, Ind. Eng. Chem. Res. 43 (2004) 4027.

[13] A.V. Biradar, S.B. Umbarkar, M.K. Dongare, Applied Catalysis A: General 285 (2005) 190.

…..ꕥ…..

Chapter 5

SIDE-CHAIN OXIDATION OF ETHYLBENZENE

Contents

Catalytic oxidation is indeed the single most important technology for the conversion of hydrocarbons to industrially important oxygenated derivatives. This chapter describes the studies on the catalytic activities of the prepared materials for the liquid phase oxidation of ethylbenzene with tert-butyl hydroperoxide oxidant. Influence of various reaction parameters such as temperature, time, substrate to oxidant ratio and solvent were studied. Heterogeneous nature of the chromium modified catalyst for the reaction was also analyzed. The observed results have been interpreted as due to the presence of catalytically active metal sites on the ceria-zirconia support.

5.1. Prologue

Oxygen, which is an inseparable participant of oxidation reactions, is the most available chemical element present on Earth. The biological circulation of oxygen consists of its absorption by the animal kingdom (breathing) and its evolution from the vegetable kingdom (photosynthesis). A balance between these two processes is maintained through an enormous number of fine redox reactions regulated by enzymes – sole catalysts perfected by nature for millions of years. Although man-made catalysts are not as ideal as enzymes, oxidation reactions are widely practiced in industry and are thoroughly studied in academic and industrial laboratories.[1] Oxidation catalysis is one of the most dynamic and fruitful areas of catalytic chemistry, which is definitely on the rise. Recent decades

show impressive progress in oxidation catalysis, resulting in many novel industrial technologies. However, this is a difficult and challenging field which cannot be selectively implemented via traditional approaches. The first examples of liquid phase catalytic oxygen transfer dates back to 1936. The so-called Milas reagents were formed by reaction of transition metal oxides with a solution of H_2O_2 in *tert*-butanol resulting in soluble inorganic peracids.[2] These catalysts were used for the vicinal dihydroxylation of olefins. From these basics, a great deal of effort has been put into the development of transition metal based catalysts, as homogeneous and heterogeneous, for various selective oxidation reactions.[3] Metal supported heterogeneous catalysts that can operate in combination with a satisfying oxidant in the liquid phase are advantageous because they are recoverable and have minimal environmental impact.[4–8]

Side-chain oxidation of alkyl aromatics using cleaner peroxide oxidants catalyzed by heterogeneous catalysts still attracts interests. Traditional laboratory procedures use stoichiometric oxidants such as permanganate and dichromate which are hazardous.[9] Hence, there has been an interest to develop eco-friendly catalysts for the oxidation of alkyl aromatics. Recently, there is much attention in using environmentally accepted oxidants rather than pollutant ones. The choice of oxidants depends mainly upon two factors viz., the nature of the corresponding by-product and the active-oxygen content besides the key properties like price and ease of handling. The former property is important in terms of environmental considerations, while the latter factor influences the overall productivity of the process. In this respect, molecular oxygen is a striking choice. Nevertheless, the free radical nature of the reaction restricts its applicability to a rather small number of molecules. Hence, for the

catalytic epoxidation and oxidation reactions of a wide variety of organic molecules, organic peroxides as well as hydrogen peroxide was used as single oxygen donors.[10] The presence of molecular oxygen or single oxygen atom donors such as *tert*-butyl hydroperoxide for the oxidation of alkanes to alcohols and ketones are shown to be important.[11–15] Selectivity control is a major concern in various chemical reactions and selective process are always superior to nonselective ones to purify the target compound for its use in further application. This can be done by minimizing the difficulties in the separation of the products from the reaction mixture. Thus the selectivity in oxidation catalysis has been thoroughly reviewed for conventional catalysts employed in oxidations.[16] Titanium substituted silicates have been thought to catalyze ring hydroxylation of arenes with H_2O_2, but vanadium,[17–24] tin[21–25]and chromium[7,27,28] substitution into a variety of zeolites and alumino phosphate molecular sieves have led to favored oxidation at the side-chain.

Ethylbenzene is available in the xylene stream of the petrochemical industry and its exploitation to more value added products is a promising one in chemical industry.[29] The oxidation products of ethylbenzene are widely employed as intermediates in organic, steroid and resin synthesis. Zeolite encapsulated Co(II), Ni(II) and Cu(II) complexes gave acetophenone as the only partial oxidation product during ethyl benzene oxidation with H_2O_2. Titanosilicates mainly catalyze ring hydroxylation of arenes with H_2O_2, whereas vanadium and chromium substituted zeolites and aluminophosphate molecular sieves have been known to favour side-chain oxidation selectively.

Numerous solid catalysts have been applied for the liquid-phase oxidation of ethylbenzene which possesses reasonable activity and

selectivity in the reaction.[30-35] This includes mesoporous Mn-MCM-41 materials[11], grafted Co (II) onto SBA-15 etc. Immobilized cobalt Schiff base complexes over SiO_2–Al_2O_3 were found to be recoverable and effective for the oxidation of ethylbenzene with TBHP under milder reaction conditions.[30] Besides, the reaction was carried out in solvent free condition. More recently, silica supported silver nanoparticles prepared by chemical reduction method have been reported for the preferential formation of the desired product, acetophenone with ethyl benzene conversion of around 38%.[31] Copper containing three dimensional amorphous mesoporous material, TUD-1, has been investigated as efficient heterogeneous catalysts for the ethylbenzene oxidation reaction using *tert*-butyl hydroperoxide giving pronounced acetophenone selectivity.[32] However, when H_2O_2 was used as an oxidant, acetophenone selectivity diminished with phenol as a major by-product. Recently, Macedo *et al.* have reported the liquid phase oxidation of ethylbenzene using *tert*-butyl hydroperoxide over cerium oxide nanorods in the presence of acetonitrile solvent.[33] At 55ºC, 1-phenylethyl-tert-butyl-peroxide (PhEtOOT) is the only reaction product until 51% conversion which is the first report for the formation of PhEtOOT by the catalytic oxidation of ethylbenzene using tert-butyl hydroperoxide. In the range 70–105ºC, PhEtOOT selectivity decreases with ethylbenzene conversion, while that to acetophenone increases.

The existing industrial production of acetophenone is through the oxidation of ethyl benzene with molecular oxygen using cobalt cycloalkane carboxylate or cobalt acetate as catalyst in acetic acid solvent.[36] This method suffers from its corrosive and environmentally aloof nature. One of the major drawbacks of using organometallic compounds in homogenous

solutions is the formation of μ-oxo dimers and other polymeric species which lead to irreversible catalyst deactivation. Hence it is highly desirable to develop an eco-friendly catalysts system for the oxidation of ethyl benzene selectively to acetophenone.

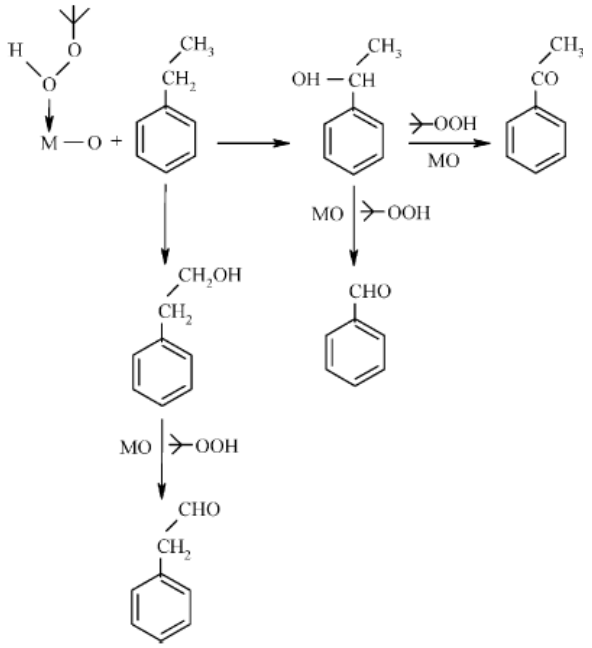

Scheme 5.1. Pathways of ethyl benzene oxidation (adapted from ref: 11)

The pathway of ethyl benzene oxidation is illustrated in the above reaction scheme. (Scheme.5.1) *t*-butylhydroperoxide is activated by coordinating with metal oxide.[11] The activated distant oxygen of coordinate *t*-butylhydroperoxide reacts with ethylbenzene to yield the products. 1-Phenylethanol is produced by the insertion of oxygen between carbon hydrogen bond of the methylene group. Abstraction of an alcoholic -OH hydrogen and the -CH hydrogen by the activated *t*-butylhydroperoxide oxygen yields acetophenone. Similar abstraction of -OH hydrogen of 1-phenylethanol by the activated *t*-butylhydroperoxide yields benzaldehyde by forming methane. By the suitable choice of catalyst, oxidant,

temperature and other reaction conditions, high conversions and prominently, selectivity in oxidation reaction could be obtained.

In the present study, based on these reports we have utilized modified ceria zirconia as catalysts in the oxidation of ethyl benzene using t-butyl hydroperoxide as oxidant in liquid phase condition. The aim was to understand the course of the reaction, which predominantly occurs through the activation of the primary or the secondary carbon atom of the ethyl substituent without aromatic ring hydroxylation. The mesoporous structure of the prepared catalysts enabled a better accessibility of active sites to substrate molecule which is reflected in high conversion of ethyl benzene and selectivity to acetophenone.

5.2. Effect of Reaction Parameters

The experiments were done and the products were analyzed by the procedure given in section 2.4.2. of chapter 2. The influence of different reaction parameters were analyzed in order to maximize the product yield and selectivity. Effect of reaction conditions for ethylbenzene oxidation with TBHP was initially assayed in non-optimized conditions with 8CrCZ as the catalyst.

5.2.1. Effect of Oxidant

The ethyl benzene (EB) oxidation was carried out using different oxidants such as hydrogen peroxide (H_2O_2), *tert*- butyl hydroperoxide (TBHP). The results are tabulated in Table 5.1. When the reaction was carried out in the presence of H_2O_2, EB conversion was found to be about 16% with a selectivity of acetophenone (AP) 38.7% and 1-phenyl ethanol (1-PE) 61.3%. However, under similar reaction condition TBHP oxidant displayed pronounced EB conversion of 54.5% with AP as the only product. Radhika *et*

al.[28] have reported that when ceria, possessing a cubic crystal structure, was used as catalyst in the oxidation of EB with H_2O_2 and acetonitrile as solvent, the reaction is sluggish giving 4% conversion after 6h, at 60ºC, and benzaldehyde (87%) and acetophenone (13%) were the products. In the case of H_2O_2, the poor catalytic results may be due to the relatively fast 'non-productive' decomposition of H_2O_2.[33] Therefore the rest of research was devoted on TBHP oxidant.

Table 5.1. Effect of oxidant on the ethylbenzene oxidation reaction. (Reaction conditions: 8CrCZ-0.1g, Acetonitrile-10 ml, Time-5hrs, Temperature: 60 °C, Ethylbenzene: oxidant ratio-1:2)

Oxidant	Conversion (%)	Selectivity of acetophenone (%)
H_2O_2	16	38.7
TBHP	54.5	100

5.2.2. Effect of Temperature

The effect of temperature on the rate and selectivity of ethyl benzene oxidation with TBHP over 8CrCZ catalyst is depicted in Fig. 5.1. Oxidation of ethyl benzene in acetonitrile solvent produced acetophenone as the major product. Five temperatures have been tested and found that both the EB conversion and AP selectivity increase with increase of temperature from 40 °C to 80 °C. This is due to the higher activation of *t*-butyl hydro peroxide at 80 °C. A further increase in temperature caused decrease in the selectivity. From 80 °C to 90 °C, the conversion was increased by about 4 wt %, but the selectivity to acetophenone was decreasing which is due to the formation of side product namely 1-phenyl ethanol. Therefore 80 °C was optimized for further studies.